JOURNAL OF MECHANICAL ENGINEERING

STROJNIŠKI VESTNIK

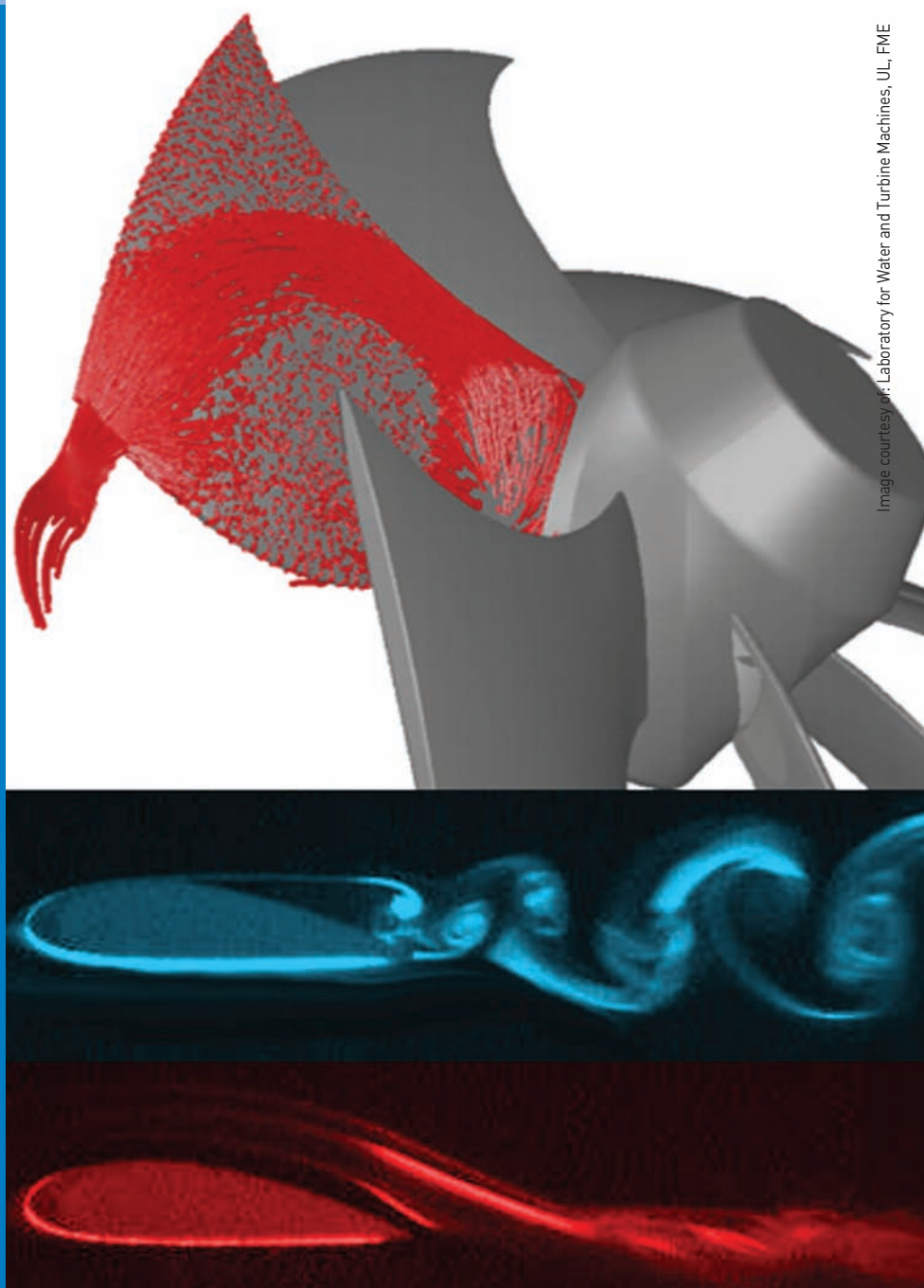

Image courtesy of: Laboratory for Water and Turbine Machines, UL, FME

no. 3
year 2008
volume 54

Contents

Strojniški vestnik - Journal of Mechanical Engineering
volume 54, (2008), number 3
Ljubljana, March 2008
ISSN 0039-2480

Published monthly

Editorial

It is my privilege to write this page introducing 3rd issue of the Journal of Mechanical Engineering, 2008. In doing so, I shall not describe the contents and other characteristics of these contributions, but I intend to touch the delicate field of Mechanical Engineering study reform, called the Bologna curriculum, which already runs at the Maribor Faculty since 2007, while the Ljubljana Faculty is lagging behind and shall start it this autumn of 2008. Last year the vice deans of the two faculties have been asked to describe their programmes in detail, but no reply has reached our editorial office yet. Due to this reason, I only wish to describe my own experience with the first year students of Bologna course in Maribor, in particular with Mechanics course in the fall term (from end of November, 2007 till January, 2008).

Students in Maribor had a 8 weeks of contact lectures and tutorials, doing also guided seminary home work. This included 1st paper on cross-sections (centre of gravity, moments of inertia) by using polygonal formulae, a 2nd paper in thick walled compounded cylinders, and 3rd paper on trusses with forces and deflections. This home work represented 20 evaluation marks.

In addition they wrote two partial exams on Mechanics yielding 40 evaluation marks. By then the oral examination has been carried out, bringing up-to 40 of evaluation marks. A total of over 90 would mean an A excellent score, while over 60 means E pass score. In practice only 1 (one) student achieved 20+40+25 = B score, and none the A score yet.

The following table gives data on particular results (only of 1st and 2nd steps, while 3rd step is still unfinished by most of the students). From the total of 27 participating students, the results are at the moment:

Written part
- 76 to 100 % = 2 students,
- 51 to 75 % = 11 students,
- 26 to 50 % = 10 students,
- Up-to 25 % = 4 students.

Home work
- 51 to 100 % = 24 students,
- Up-to 50 % = 3 students.

Final score (February to May, 2008)
- B = 1 student,
- C = 1 student,
- D = 4 students,
- E = 6 students.

The next written and oral examinations will take place in June and September, 2008.

From the above data, some experience may be drawn for the next generation, studying 1st year in 2008/2009. First of all 8 lectures per week for 8 weeks, should be changed to 4 lectures per week for the duration of the total autumn term (October to January), as it used to be in previous years. In addition the seminary home work should be replaced by guided team work on faculty premises and with equal means for all participants.

Prof. Dr. Andro Alujevic, Editor

Strojniški vestnik - Journal of Mechanical Engineering 54(2008)3, 159-169
UDC 533.662.3
Paper received: 25.5.2007
Paper accepted: 28.9.2007

Influence of Blade Deformation on Integral Characteristic of Axial Flow Fan

Matjaž Eberlinc*,[1] - Matevž Dular[1] - Brane Širok[1] - Bojan Lapanja[2]
[1]University of Ljubljana, Faculty of Mechanical Engineering, Slovenia
[2]Hidria Institute Klima, Godovič, Slovenia

Axial flow fan blades deform during operation due to the various forces that act on them. That is why, we can ask ourselves about the influence of the blade deformation on the integral and local characteristics. In the paper, we present a study of influence of axial flow fan blade deformation. The paper deals with measurements of the blade deformation at the known integral working conditions. Results - deformations of fan blade tip were used for numerical study of the influence of the changed blade form on the fan's aerodynamic characteristic. Fan integral characteristics were measured in accordance with the ISO-DIS 5801:2006 standard and were carried out on the wind tunnel of the Hidria Institute Klima, Godovič. Other measurements of the blade deformation were done on the measuring station on the Faculty of Mechanical Engineering, University of Ljubljana, with the help of computer aided visualization. Deformations were measured in three working points, which were defined with fan integral parameters.

Results of the measurements helped to determine modified form of the blade, which was then used for the numerical simulation for the same fan integral parameters. The study of deformation influence, based on the numerical simulation, was carried out.

Keywords: axial flow fan, blade deformation, visualization

0 INTRODUCTION

With the development of fans, more often numerical supported CFD methods are used, which can enable predictions of machine's integral characteristic and local flow properties. Method used here is based on the exact defined geometry of the flow tract, which was given on the basic precedent selection and boundary conditions, which were set on the machines basic nominal properties. Blade geometry of the rotor, which presents the essential element of the flow tract is constant and during simulation is not treated as deformation body. In real working conditions on the axial flow fan blade and axial flow pump blade, distinctive transformation can appear, which mainly reflects the changes of the profile angle on the tip position of the blade. This feature can typically influence the machine's actual characteristic. Because deformations are generally not considered in CFD analysis, there poses a question of the assessment of the deformation influence on the integral and local level of the analysis.

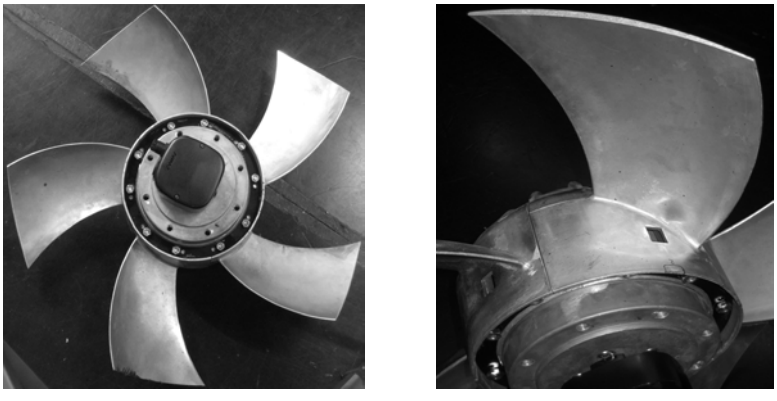

Fig. 1. *Axial flow fan ∅630 mm with five profiled blades* [1]

*Corr. Author's Address: University of Ljubljana, Faculty of Mechanical Engineering, Aškerčeva 6, SI-1000 Ljubljana, Slovenia, matjaz.eberlinc@fs.uni-lj.si

As an example we present in this paper the influence of blade deformation on the integral and local characteristic of axial flow fan ∅630 mm with five profiled blades, which is shown in Figure 1 [1].

Blade is effected by centrifugal and pressure force while working in steady working point. Centrifugal force occurs in reaction to a centripetal acceleration, acting on a mass and is equal in magnitude to the centripetal force, directed away from the center of rotation (Fig. 2), pressure force is a result of flow conditions in flow cross section of the rotor axial cascade. Resultant of the pressure forces is divided into axial and circumferential component. Axial force is estimated on the basis of pressure difference in and out of the fan rotor and is a result of the working point. On the other hand, circumferential component is estimated with moment on fans axle [2]. Nevertheless, it has to be pointed out that the integral analysis mentioned above, does not give the handling of resultant pressure force, which prevents from estimating load state on the points of blade fastening. In such a manner, we have to take into account that fan blades are exposed due to pressure fluctuations, as a consequence of turbulent flow. Pressure disturbances are a distinctive generator of blade oscillation around its poise position.

The aim of this paper is to determine the influence of deformation on axial flow fan integral characteristic. On the other hand, when we are looking from local prospective, this paper is mainly directed to determine changes of flow properties and static pressure distributions on the blade surface as a consequence of blade geometry change during operation. Fig. 3 presents procedure of determining the influence of blade deformation on axial flow fan aerodynamic characteristic. Measurements were divided into three stages. In the first stage, measurements of axial flow fan integral characteristic, carried out at the Hidria Institute Klima, Godovič are presented. The purpose of these measurements is mainly, to determine fan's optimum working point. Selection of fan's working points was made, where in continuation of the study, deformation measurements and numerical CFD simulation of fan's aerodynamic characteristics were carried out [5] to [7].

In the second stage, in the selected working point, blade deformation measurements on the measuring station on the Faculty of Mechanical Engineering, University of Ljubljana, were carried out. Computer aided visualization was used, to determine the deformation of fan blades tip [3]. Analysis mainly aimed to estimate absolute deviation of measuring points in meridian surface of flow field, which enabled to detect deformations of blade tip, regarding reference point, located on

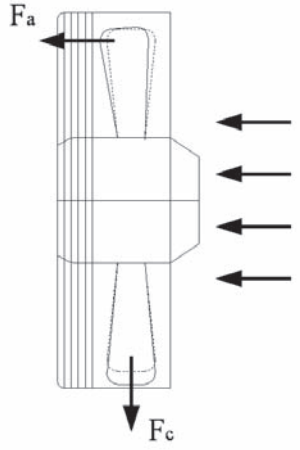

Fig. 2. *Deformations, due to axial and centrifugal forces*

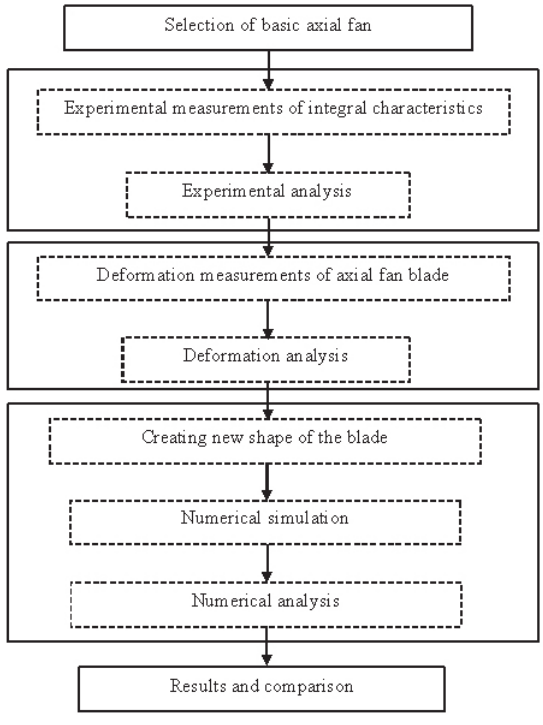

Fig. 3. *Procedure for determining the influence of blade deformation on axial flow fan integral characteristic*

the fan casing. Data obtained, subsequently enabled the statistic assessments of deformation conditions on the observed blade. Assessment of oscillating amplitude depends on maximum standard deviations of time-averaged deviation. On the secondary axis the corresponding standardized visualization of time averaged blade deformation and fluctuations of blade tip around its poise position enabled evaluation of blade geometry changes on the field, which is of highest importance for fan operation.

1 INTEGRAL CHARACTERISTIC MEASURMENTS

Measurements were performed at the equivalent working conditions and equivalent working points, to achieve the desired comparisons with the results. Figure 4 shows the integral characteristic of axial flow fan ∅630 mm with five profiled blades, which was measured at the Hidria Institute Klima, Godovič [1]. Point A in Figure 4, at which deformation measurements were carried out, is given in the diagram. In point A, a difference in static pressure Δp_s was defined, which was used to determine the reference parameter in wind tunnel (Fig. 5). Pressure difference was measured with differential pressure transmitter Endress + Hauser Deltabar S PMD75, with measuring uncertainty of 0,05 %.

2 MEASUREMENTS AND ANALYSIS OF DEFORMATIONS WITH COMPUTER AIDED VISUALIZATION

In the Laboratory for water and turbine machines at the Faculty of Mechanical Engineering, University of Ljubljana, deformations with computer aided visualization were measured [2]. Experiment was carried out on the measuring station, which is shown in Fig. 5. Measurements were performed in accordance with recommendations written in standard ISO 5151:1994 [8]. Working conditions were set with integral parameters:

- axial flow fan motor rotations per minute: n = 1344 rpm,
- fan static pressure difference: Δp_s = 241 Pa,
- air density: ρ = 1.15 kg/m^3.

Fan static pressure difference and rotor rotating velocity were measured. On the basis of this data it was possible to set the desired fan working point. Camera Dragonly Express IEEE-1394 with objective Pentax Precision Co. B25140, 25 mm was used for image capturing. The camera was triggered with inductive sensor, which was in front of fan rotor. Triggering enabled to set the desired repetition of the blade's location, when the blade was crossing by the hole on the fans casing, regarding the selected reference point, which is also located on the fans casing – point T_0 on Figure 6 a).

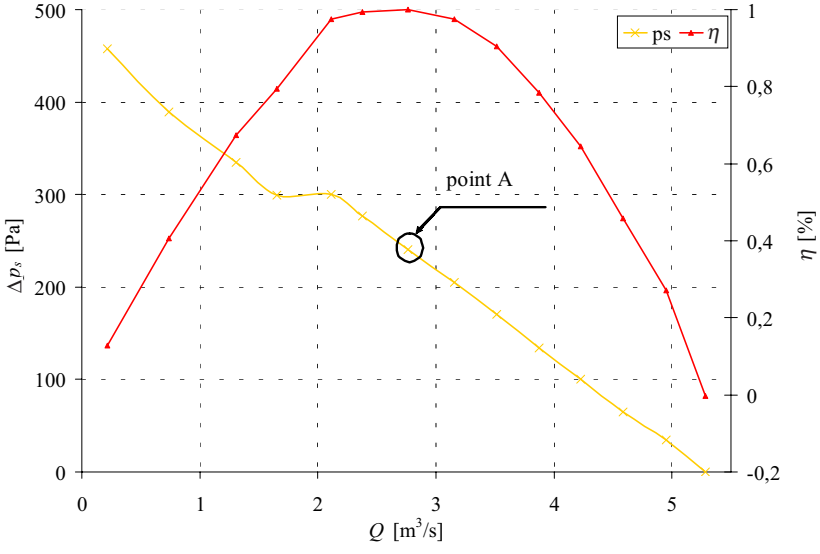

Fig. 4. *Axial flow fan integral characteristic* [1]

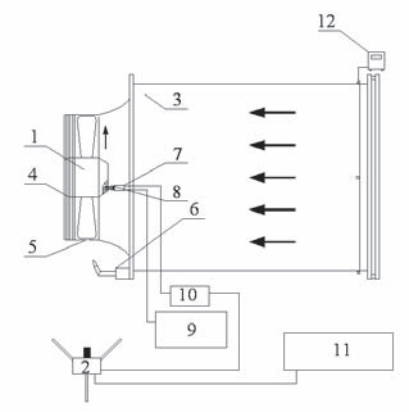

1 - axial fan
2 - camera Dragonfly Express IEEE-1934
3 - wind tunnel
4 - axial fan grid
5 - measuring port
6 - extra light
7 - inductive sensor
8 - M6 screw
9 - system power supply Agilent
10 - voltage transmitter
11 - computer
12 - differential pressure transmitter

Fig. 5. *Measuring station scheme of axial flow fan blade deformation measurement*

Digital images were made with triggering of the camera in the selected time period, which belong to the chosen blade position. Software package LabView was used for controlled capturing of digital images. Images were processed with the help of Matlab software package. For every discussed example, 150 successive images were used, which is satisfactory for statistic estimation – time averaged blade deformation and appurtenant standard deviation of fluctuation around mean value.

Three measuring points (T_1, T_2 in T_3) on the blade tip were selected, enabling the estimation of rotating deviations of the selected measuring points, with respect to reference point T_0 (Fig. 6 a).

Figure 6 b presents the relation between the reference point T_0 on the fan casing and measuring points T_1, T_2 and T_3 on the blade tip. Starting point of Cartesian coordinate system (Fig. 6 b) was reference point T_0. Measuring points on the blade tip T_i (i = 1, 2, 3) were, regarding the selected coordinate system, given by coordinates x_i and y_i.

Measurement uncertainty is mainly accumulated due to assessment of influence on high-speed camera time deviation, while triggering and capturing digital images of the blade. Plain estimation of measurement uncertainty is while determining selected fan working points, which is conditioned mainly with determining the rotating velocity and is accordance with ISO/WD 5801

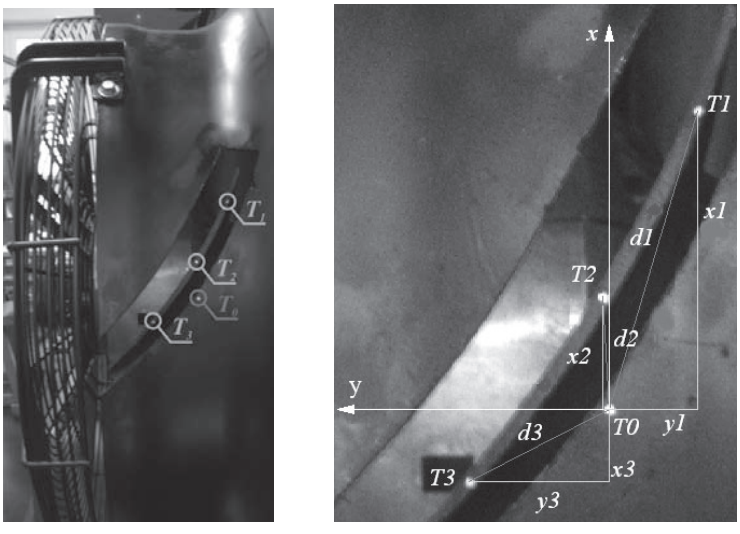

(a) (b)

Fig. 6. a) *Axial flow fan blade measuring position;* b) *Scheme presentation of selecting the points for analysis, made by software package AutoCad*

standard estimated with u_n = 0,2 %, measuring pressure difference on the fan u_p = 1,4 % and determining air density in flow, which is, if every procedure is in accordance with the standard, equal to u_ρ = 0,4 %. Measurement uncertainty of visualization method of blade deformation measurements can be divided only on the basis of each step of the presented method. It results from circumferential velocity of the blade tip, fans rotor diameter and frequency of capturing the inductive sensor signals, which triggered digital camera. The highest possible absolute measurement uncertainty is 0.038°, which does not, at the expected maximum blade deformations be approximately 3°, exceed the relative measurement uncertainty of u_v = 1,3 %.

Algorithms for recognizing the digital image samples – measuring points and calculation of measuring points position were elaborated in software package MatLab. Algorithm was aimed to recognize single measuring point on the blade tip and in continuation determining center of a measuring point, which gave the momentarily measuring point coordinate, regarding the starting – reference point T_0. Considering the fact that digitalization was carried out by 8-bit divisibility, where the value of the variable $E_p(i,j,t)$ in Eq. (1), which represents the value of the grey intensity (i, j) in period of time t, is in range:

$$E_p(i, j, t) \in \{0, ..., 255\} \qquad (1).$$

Indices i and j of element E digital image, present the position of the cell. In observed field in formed cell – size of the window (di, dj), where di in dj presents the size of the window.

For every separate image in the sequence of blade tip digital image, scalar value function $f(i,j)$ was calculated, obtained by:

$$f(i, j) = \frac{1}{di}\frac{1}{dj}\sum_{i_p=1}^{di}\sum_{j_p=1}^{dj} E_p\left(i_c + i_p, j_c + j_p\right) \quad (2),$$

where i_c and j_c are coordinates of the selected window. Value of grey intensity E_p in point (i,j) has boundary values from 0 (black colour) to 255 (white colour). In the observed area the function $f(i,j)$ is changed significantly from crossing black field to white field, which belongs to each measuring point T_0, T_1, T_2 and T_3.

To set the edges of measuring points, gradient value of $f(i,j)$ is calculated in the next step, where maximum scalar value allows determining of the edge of measuring point. Procedure of determining the contour of measuring point is the same in all observed measuring points T_1, T_2 *in* T_3 and reference point T_0. In the final stage, center of a contour for the selected measuring T_1, T_2 *in* T_3 and reference point T_0 is calculated.

Position, as well as distance between measuring points on the blade tip and reference point T_0 on the fan casing are time-varying. From the analysis of time successive digital images, the evaluation of fluctuation deviation of measuring points can be carried out, which enables the assessment of average deformation of tip position and assessment of fluctuation intensity of momentary deviations of observed measuring points regarding the time-averaged deformation image.

In this paper, on the basis of presented algorithms, blade tip main deviation values and standard deviation regarding the main deformation values, which are presented in the following chapter, were calculated.

3 EXPERIMENTAL RESULTS

At working conditions, given with point A in fan integral characteristic, shown in Figure 4, sequences of digital images were saved. Figure 7 shows the qualitative comparison of fan rotor at standstill (n = 0 rpm) and at the known rotating

Fig. 7. *Comparison of position of the axial flow fan blade in two working points (n = 0 and 1344 rpm)*

velocity (n = 1344 rpm) in working point A (Fig. 4). For easier demonstration of the blade deviation, the blade image in two different working points was joint with the help of software package MatLab into one image, shown in Fig. 7. Blade deviation along the blade tip is clearly seen. Distinctive blade deformation is visible, which is reflected in deviation, as well as blade tip distortion.

Quantitative analysis is based on methodology of determining the position of measuring points regarding the reference point T_0, as it was presented in chapter 1. In first stage the length between measuring and reference point was set. Length between points T_1, T_2, T_3 and point T_0 was calculated in two working points of the fan (n = 0 and 1344 rpm), as presented in Figure 6. Time-averaged deviation and standard deviation is given in standard form:

$$x^* = \frac{x}{R_o}\cdot 100\%, y^* = \frac{y}{R_o}\cdot 100\%, d^* = \frac{d}{R_o}\cdot 100\%$$
$$\sigma_x^* = \frac{\sigma_x}{R_o}\cdot 100\%, \sigma_y^* = \frac{\sigma_y}{R_o}\cdot 100\%, \sigma_d^* = \frac{\sigma_d}{R_o}\cdot 100\% \quad (3),$$

where R_0 is fan radius.

In Figure 8 standardized deviations of measuring points on axial flow fan blade tip are presented. On the basic axis time-averaged deviation x^*, y^* in d^* for measuring points T_1, T_2 and T_3 are given. On the secondary axis the corresponding standardized standard deviations σ^*_x,σ^*_y, σ^*_d are given.

Similar deviations in all directions of coordinate system were perceived with the fan – Figure 6 b). In the direction of x axis, deviation of blades tip towards the outlet of flow is perceived. On the inlet edge of the blade tip smaller deviation are seen, similar as on the outlet edge of the blade tip. This occurrence influences on the change of blade angle of attack and indirectly on the fan integral characteristic. In the direction of y axis (Fig. 6b), deviations are minimal, which is the result of blade shape. Collective deviation is combined from deviations of above-mentioned directions, shown in Figure 8.

4 NUMERICAL SIMULATION OF THE FLOW

Fluid flow through the fan was treated in a steady condition. Simulations in five working points were done. In one series of simulations, blade deformation was considered; in other series it was not (determining blade deformation geometry is presented in 4.1). Software package Fluent 6.1.22 was used, where system of Reynolds average Navier-Stokes equations were computed. Mass conservation equation (Eq. 4) and momentum conservation equation (Eq. 5) along with equations of k-ω SST turbulence model (Eq. 6 and 7) are forming a closed system of equations [4]:

$$\frac{\partial \rho}{\partial t} + \frac{\partial\left(\rho \bar{u}_j\right)}{x_j} = 0 \quad (4),$$

$$\frac{\partial\left(\rho \bar{u}_i\right)}{\partial t} + \frac{\partial\left(\rho \bar{u}_j \bar{u}_i\right)}{\partial x_j} = -\frac{\partial \bar{p}}{\partial x_i} + \frac{\partial}{\partial x_j}\left[\mu\left(\frac{\partial \bar{u}_i}{\partial x_j} + \frac{\partial \bar{u}_j}{\partial x_i}\right) - \rho\overline{u_i' u_j'}\right] \quad (5),$$

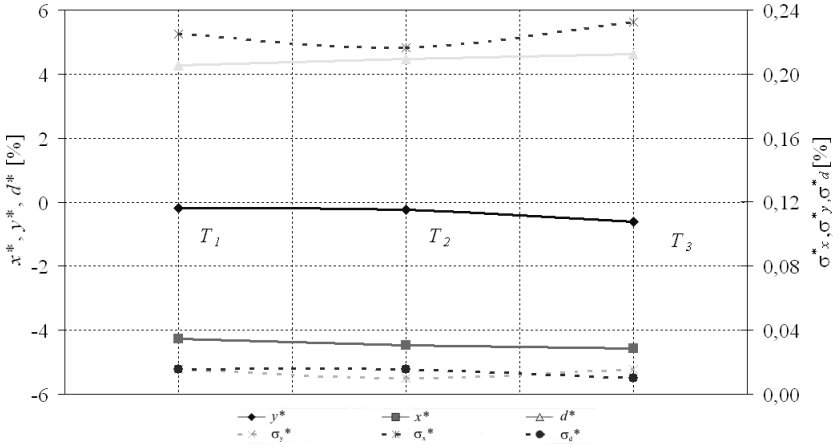

Fig. 8. *Deviation and standard deviation for three measuring points in two working points (n = 0 and 1344 rpm)*

$$\frac{\partial(\rho k)}{\partial t}+\frac{\partial\left(\rho k\bar{u}_j\right)}{\partial x_j}=\frac{\partial}{\partial x_j}\left[\Gamma_k\frac{\partial k}{\partial x_j}\right]+\tilde{G}_k-Y_k \quad (6),$$

$$\frac{\partial(\rho\omega)}{\partial t}+\frac{\partial(\rho\omega\bar{u}_i)}{\partial x_j}=\frac{\partial}{\partial x_j}\left[\Gamma_\omega\frac{\partial\omega}{\partial x_j}\right]+G_\omega-Y_\omega+D_\omega \quad (7),$$

where $\tilde{G}_k$ is the turbulence source, due to of velocity gradient, G_ω is the source of ω. Γ_k and Γ_ω are the effective diffusivity k and ω. Y_k and Y_ω are dissipations of k and ω, due to of turbulence, D_ω is the diffusive term.

4.1 Geometry and Mesh

With measurements (chapter 3) the blade deformation of blade tip was determined. To be able to set the deformed blade geometry, following procedure was adopted:

- that blades (at fixing area on the motor) are not deforming,
- deformations are increasing linearly from the root to the tip of the blade,
- blade deformation in fans different working points does not significantly change.

Comparison between blade original and deformed geometry is shown in Figure 9.

Meshes of original and deformed blade were topologically equivalent. Computational domain was discretized with structural mesh. To reduce the calculating time, only one interblade area (1/5 total area) was calculated, on borders a periodic boundary condition was regulated. Influence of the mesh was examined only at optimum flow and for the case of original – not deformed blade. Finally, the mesh with approximately 400.000 nodes was used, which was on the channel walls and along

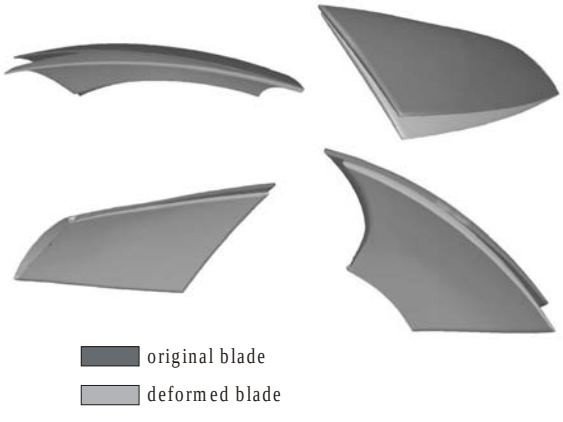

Fig. 9. *View of original and deformed blade*

the fan blade refined - y^+ was between 30 and 80. With this kind of mesh density we evaluated the error of discretization to 0,5 %. Geometry, as well as deformed blade mesh, was equivalent for all working points - it was adopted, that for every single working point of the axial flow fan, deformation does not change significantly.

4.2 Convergence Criterion

Convergence criterion was set, regarding the pressure development on the inlet and velocity on the outlet from the computational domain. Parameters were always converging, when the residuals sum of transport equation in the entire computational domain was less then 1×10^{-3}. Finally, for convergence criterion, the situation was used, when the residuals decreased below 1×10^{-4}, for which approximately 350 iterations were needed. Iteration error was estimated to 0,05 %.

4.3 Calculating Condition

- Flow: for turbulence k-ω SST turbulence model was used;
- Boundary conditions: on the channel walls, fan blade and rotor no slip boundary condition was assumed;
- On the inlet air flow was defined ($\cong$ 1.31, 2.11, 2.76, 3.52, 4.22 m^3/s);
- On the outlet pressure was defined (0.1013 MPa);
- Fan rotating velocity was constant (1344 rpm), fan rotating was described by rotating reference frame model.

Air density was 1.225 kg/m^3, dynamic viscosity was 1.79×10^{-5} Pas. The results from numerical simulation are presented in chapter 5.

5 RESULTS

Results from prediction of flow fields for original and deformed – modified form of the blade in various working points of the machine, final numerical predictions and axial flow fan integral characteristic measurements are presented.

5.1 Numerically Predicted Blade Pressure Distribution

Pressure distributions in three different working points of the fan (1.31, 2.76, 4.22 m^3/s)

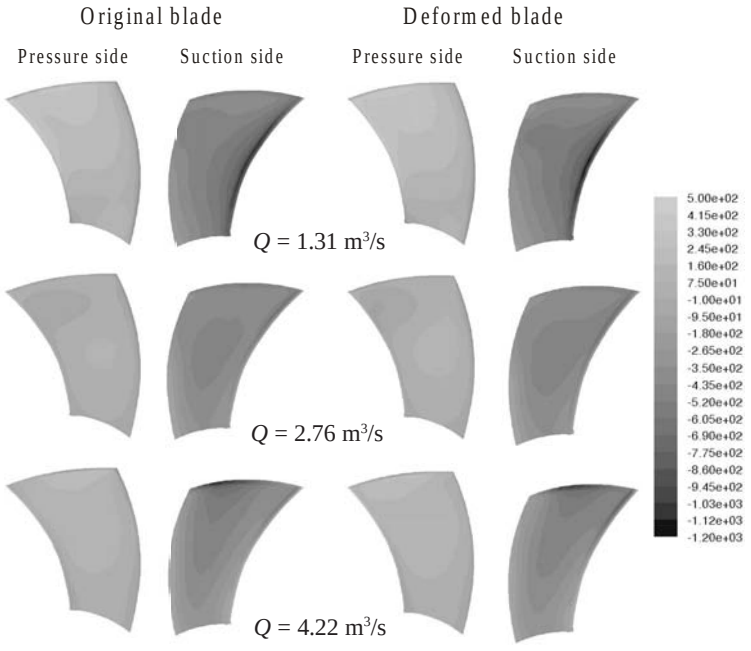

Fig. 10. *Pressure distribution for original blade geometry and deformed blade geometry*

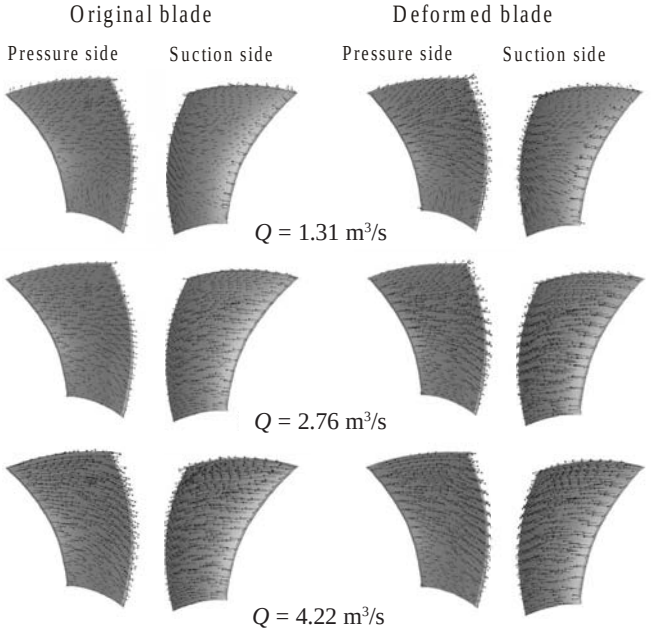

Fig. 11. *Relative velocity vectors on pressure and suction side of original and deformed blade for fan three working points*

are presented in Figure 10. Presented pressure distributions on the pressure and suction side for case of original blade geometry (left) and for case of deformed blade geometry (right).

Pressure distribution on blade is similar for both, the original and deformed blade. At lower flow (Q = 1.31 m³/s) it can be noticed, that pressure on suction side of the deformed blade is slightly lower, which effects the intensive separation of flow at this location. The reason for this is a larger blade angle of attack, because of deformation. Near the optimum (Q = 2.76 m³/s) changes are less distinctive, pressure

on suction side of deformed blade is slightly lower that in the case of original blade. In working point 4.22 m³/s, pressure conditions on blade are not distinctive. Pressure on the trailing edge on the section side of the deformed blade is slightly higher in comparison to the pressure on the same place of the original blade. The difference is the result of better flow conditions for the deformed blade, because the angle of attack is larger (optimum moves to the higher volume flow).

Despite the deformations, conditions on the blade pressure side remain mostly the same, and changes are negligible.

5.2 Numerically Predicted Velocity on the Blade

Figure 11 shows relative velocity vector on pressure and suction side of original and deformed blade in fan's three different working points (Q = 1.31, 2.76, 4.22 m³/s).

It can be noticed, that in case of smaller volume flow (Q = 1.31 m³/s), the flow on the deformed blade is less settled. On the blade tip on suction side, a large vortex can be seen, which is smaller in case of original blade. The cause for detaching of flow on this side and this working point is a larger angle of attack of the blade, which is even larger, because of deformation. We can also see a larger disorder of flow on the pressure side of the deformed blade. It seems that vectors point from the middle side of the blade in direction towards the tip and root of the blade. The reason is that flow cannot follow increased curvature of blade and hits into it, instead of flowing around it.

Near the optimum point (Q = 2.76 m³/s) the differences in flow field are less distinctive. On the suction side of the deformed blade, on the top, near the trailing edge, a field of lower velocity is seen, which can be assigned to separating of flow on this place (the reason again being larger blade angle of attack). Similar (but less obvious) as in the case of a smaller volume flow, hitting of the flow against the pressure side of the deformed blade can be seen.

At higher volume rate (Q = 4.22 m³/s) differences are not visible.

5.3 Velocity on Blade Tip

In Figure 12 relative velocity vectors are shown on the section 15 mm from the tip of the

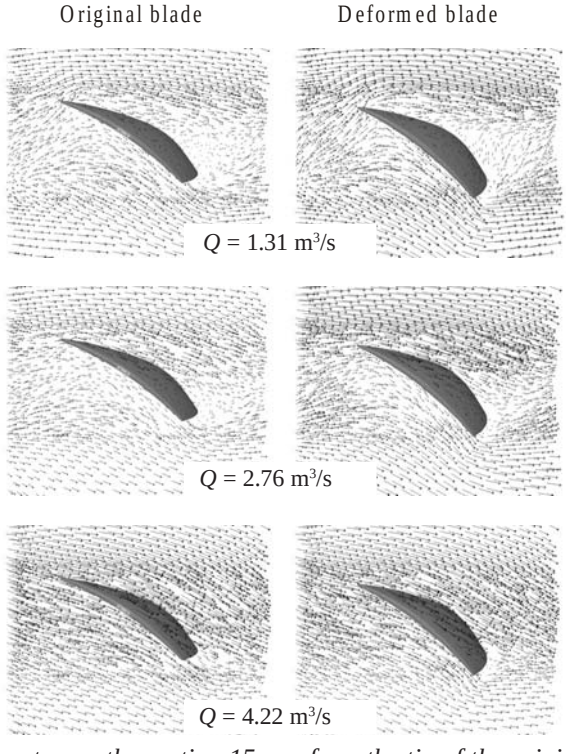

Fig. 12. *Relative velocity vector on the section 15 mm from the tip of the original and deformed blade in fan's three working points*

original and deformed blade in fan's three working points (Q = 1.31, 2.76, 4.22 m^3/s).

Images show velocity conditions at the most critical place (at the tip of the blade). Separating of flow on this place causes the efficiency and power drop and generation of aerodynamic noise.

At the lower and optimal flow (Q = 2.76 m^3/s) the separating of flow is obviously larger in case of deformed blade, which is the result of inappropriate (larger) blade angle of attack. In case of higher volume flow (Q = 4.22 m^3/s) the aggressiveness of separating between the blades is comparable, which is the result of shifting the optimum towards higher volume flow, because of blade deformation.

5.4 Predictions and Measurements of Integral Characteristics

Figure 13 shows measured and numerical (for original and deformed geometry) integral characteristic of standardized efficiency and pressure increase in dependence of volume flow.

Numerical model with original blade geometry agrees with measurement results near the optimum working point, otherwise deviations are higher. It is different with the results obtained from numerical model with the deformed blade geometry, which match with experimental results in wider range. Higher deviation can be seen at lower volume flow, which is probably the result of overestimated prediction of flow separation of trailing edge of the blade and incorrect estimation of blade deformation (for every case, measured deformation in optimum working point was considered – in chapter 3).

Suitableness consideration of actual (deformed) shape of the blade is obvious, because there is an option for better prediction of actual flow field and easier optimization of blade geometry.

6 CONCLUSION

This paper presented the influence of blade deformation on fan integral and local characteristic. With computer aided visualization blade tip deformations were defined. Measurement results were used to determine the variable blade formation, which was in continuation used for numerical modeling for the same fan integral working parameters. Considering to use actual (deformed) shape of the blade would be suitable in this case, because it enables better prediction of actual flow field and easier optimization of blade geometry.

Acknowledgement

Research was founded by European fund for regional development in project frame entitled *Research of Slovenian industry innovative environment for air-conditioning, heating and*

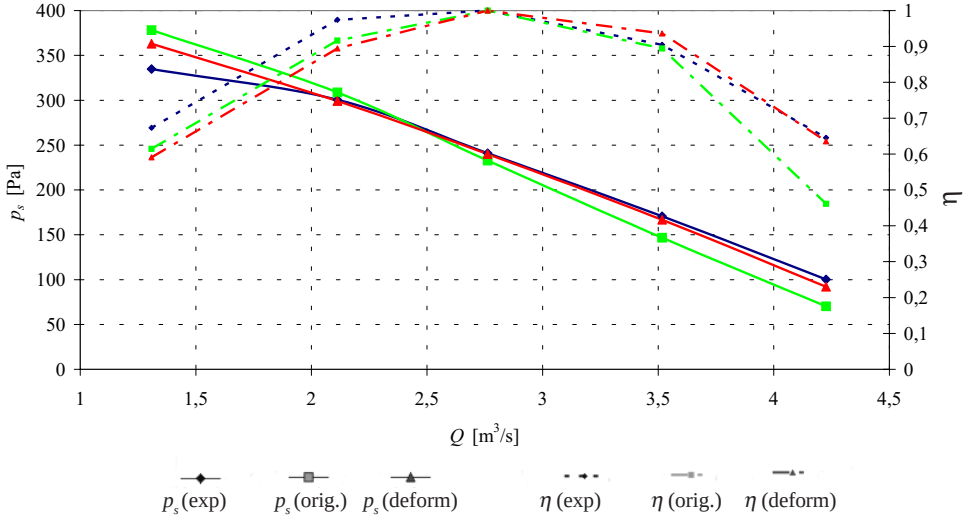

Fig. 13. *Comparison between the experimental results and numerical model for cases of original and deformed geometry*

cooling; Research of elements of power saving and environmental friendly CHC systems.

7 REFERENCES

[1] Pivk, S., Magajne, A., Tominec, U. *Measurements of integral properties of axial flow fan with 630 mm radius*. Sp. Idrija: Hidria Rotomatika, d.o.o., July 2006. (In Slovenian).

[2] Wallis, R. A. *Axial flow fans and ducts*. John Wiley & sons, 1983.

[3] Eberlinc, M., Hočevar, M., Pivk, S., Širok, B. Visualization method for measuring the deformation of axial-flow fan blades, *Ventil*, 13, 2007, no. 2, p. 94-101.

[4] Ferziger, J.H., Perić, M. *Computational Methods for Fluid Dynamics*, 3rd Edition. Springer, 2002

[5] Širok, B., Bajcar, T., Dular, M. Reverse flow phenomenon in a rotating diffuser. *J. flow vis. image process*, 2002, vol. 9, no. 2/3, p. 193-210.

[6] Širok, B., Hočevar, M., Zupan, S., Prebil, I. Study of radial rotor and bearing arrangement dynamic properties of the combat vehicles M 84 and 72 cooling system fan. *Stroj. vestn. - J. Mech. E.*, 1999, vol. 45, no. 11, p. 432-441.

[7] Širok, B., Potočar, E., Novak, M. Analysis of the flow kinematics behind a pulsating adaptive airfoil using computer-aided visualisation. *Stroj. vestn. - J. Mech. E.*, 2000, vol. 46, no. 6, p. 330-341.

[8] ISO 5151:1994: *Non-ducted air conditioners and heat pumps - Testing and rating for performance*

[9] ISO 5801:2006: *Industrial fans*

Strojniški vestnik - Journal of Mechanical Engineering 54(2008)3, 170-178
UDC 533.661
Paper received: 4.10.2006
Paper accepted: 19.12.2007

Improved Solution Approach for Aerodynamics Loads of Helicopter Rotor Blade in Forward Flight

Aleksandar Bengin[1] - Časlav Mitrović[1] - Dragan Cvetković*[,2] - Dragoljub Bekrić[1] - Slavko Pešić[1]
[1]University of Belgrade, Faculty of Mechanical Engineering, Serbia
[2]University "Singidunum" Belgrade, Faculty of Business Information Science, Serbia

This paper presents the numerical model developed for rotor blade aerodynamics loads calculation. The model is unsteady and fully three-dimensional. Helicopter blade is assumed to be rigid, and its motion during rotation is modeled in the manner that rotor presents a model of rotor of helicopter Aerospatiale SA 341 "Gazelle" (the blade is attached to the hub by flap, pitch and pseudo lead-lag hinges). Flow field around the blade is observed in succession of several azimuth locations. Flow field around helicopter rotor is modeled as fully three-dimensional, unsteady and potential. Blade aerodynamics is modeled using a lifting surface model. Rotor wake is generated from the straight elements of constant vorticity, released from the trailing edge, at fixed azimuth angles. These vortices represent both trailed and shed wake components, and are allowed to freely convect along local velocity vectors. Wake is modeled as free one, and its shape at certain moment can be calculated from simple kinematics laws applied on collocation points of the wake. Wake distortion is calculated only in the rotor near-field, i.e. in finite number of rotor revolutions. Vortex elements are modeled with vortex core. The radius of the vortex core is assumed independent of time, and it depends on circulation gradient at the point of vortex element released from the blade.

Keywords: unsteady aerodynamics, helicopter rotor blade, potential flow, lifting surface theory

0 INTRODUCTION

One of the most important challenges in helicopter aerodynamics is the accurate prediction of rotor loads, especially in forward flight.

Helicopter rotor aerodynamic flow field is very complex, and it is characterized by remarkably unsteady behavior. The most significant unsteadiness appears during the forward flight. In that case, the progressive motion of helicopter coupled with rotary motion of rotor blades causes drastic variations of local velocity vectors over the blades, where the advancing or retreating blade position is of great significance. In first case, the local tip transonic flow generates, while in second, speed reversal appears.

In addition, in forward flight, blades encounter wakes generated by forerunning blades and so encounter non-uniform inflow. The wake passing by the blade induces high velocities close to it causes changes in lifting force. Besides that, in horizontal flight blades constantly change pitch, i.e. angle of attack at different azimuths. Such angle of attack variations are very rapid, so that dynamic stall occurs, especially in case of retreating blades [1] and [2].

Various methods have been used to represent the rotor and its wake. The rotor blades have been represented by actuator disc, blade elements, a lifting line, lifting surface, or a finite difference and finite elements method. Lifting surface theory allows for a more realistic and general representation of the blade than lifting line theory, and has been shown to be more accurate as well [2] to [4]. Finite difference or finite element methods must be used to introduce transonic effect. Also, they offer the potential to predict blade drag [5]. However, the major drawback of finite elements and finite difference methods are their long computation times.

1 DYNAMICS

In this paper the rotor of helicopter SA 341 “Gazelle” is modeled, at which the blades are attached to the hub by flap, pitch and pseudo lead-lag hinges.

Blade motion in lead-lag plane is limited by dynamic damper, which permits very small

*Corr. Author’s Address: University "Singidunum", Faculty of Business Information Science, Danijelova St. 32, 11000 Belgrade, Serbia, dcvetkovic@singidunum.ac.yu

maximum blade deflection. Due to such small angular freedom of motion, we can assume that there is no led-lag motion at all.

Pitch hinge is placed between flap hinge and pseudo lead-lag hinge. In derivation of the equations of motion [6] and [7], the following was assumed:

- the rotor does not vibrate, and its rotation velocity Ω is constant,
- the blade is considered absolutely rigid.

According to the above mentioned, the following frames have been selected for use:

- fixed frame F, with *x*-axis in the direction of flight, and *z*-axis oriented upwards;
- frame H, connected with the rotor and rotates together with it; it is obtained by rotating the F frame for a certain azimuth angle ψ; keeping the common *z*-axis;
- frame P, connected to the flapping hinge, so that the *y*-axis is oriented along the blade; its origin is displaced from the rotating axis for the value e_β, while it is rotated for the angle β with respect to the frame H;
- frame B, connected to the blade, displaced for the value e_θ from the origin of P, and tilted for the value θ (pitch angle) with respect to the P.

With assumptions mentioned above, equation of blade flapping motion is [7]:

$$B\ddot{\beta} + \Omega^2 \left(B\cos\beta + m_b e_\beta x_g R \right) \sin\beta = M_A$$

where B is moment of inertia about P_x, m_b mass of the blade, x_g position of blade center of gravity in P frame, and M_A is aerodynamic moment.

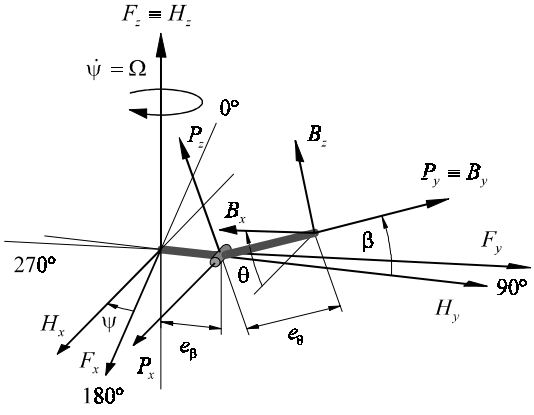

Fig. 1. *Coordinate systems*

2 AERODYNAMICS

2.1 Analytical Model

The flow field is assumed to be potential (inviscid and irrotational) and incompressible. In that case, velocity potential satisfies the Laplace equation:

$$\Delta\Phi = 0$$

The equation is the same, both for steady and unsteady flows. Owing to that, methods for steady cases can be applied for the solution of unsteady flow problems, as well. Unsteadiness is introduced by unsteady boundary condition:

$$\left(\vec{V} - \vec{V}_T\right) \cdot \vec{n} = 0$$

of the Kelvin theorem:

$$\frac{d\tilde{\Gamma}}{dt} = 0$$

and the unsteady form of the Bernoulli equation:

$$\frac{p - p_\infty}{\frac{1}{2}\rho_\infty} = V_\infty^2 - V^2 - 2\frac{\partial\Phi}{\partial t}$$

In order to define the aerodynamic characteristics of blades, two models should be established: blade model and wake model.

The blade is modeled as a thin lifting surface, which enables a complete 3D modeling around helicopter blades. Lifting surface model is more accurate in the treatment of the 3D effects at low angle of attack, and with some extensions, compressible flow effects. It is very suitable for modeling any blade geometry (symmetrical or non-symmetrical airfoils, various blade shape, blade tips i.e.), since they do not need airfoil experimental data. Unfortunately, it cannot deal with viscous flows, and thus is no more accurate than lifting line theory at high angle of attack.

Numerical modeling of the wake must be done very carefully due to it's high influence on the lift force generation. The free-wake model, which is applied in this paper, is one of the most advanced, since it can cover all relevant problems connected with the wake influence.

2.2 Unsteady Kutta Condition

In case of inviscid problems, it is necessary to satisfy Kutta condition at the trailing edge [8] to [10].

Based on unsteady Bernoulli equation, the pressure coefficient for unsteady flow is defined as:

$$C_P = \frac{p - p_\infty}{1/2 \rho_\infty V_\infty^2} = 1 - \frac{V^2}{V_\infty^2} - \frac{2}{V_\infty^2}\frac{\partial \Phi}{\partial t}$$

According to that, the difference between upper and lower surface pressure coefficients is:

$$\Delta C_P = C_{P_U} - C_{P_L} = -\frac{V_U^2 - V_L^2}{V_\infty^2} - \frac{2}{V_\infty^2}\frac{\partial}{\partial t}(\Phi_U - \Phi_L) \quad (1),$$

where subscripts *U* and *L* denote upper and lower surface values.

In case of the thin lifting surface, with the assumption that spanwise velocity components are small, the potential difference can be written as an integral from leading edge to a certain point *M* at the surface:

$$\Phi_U - \Phi_L = \int_{LE}^{M} \left(V_{U_T} - V_{L_T}\right) dl$$

where the tangential velocity difference is the local bound vortex distribution:

$$\gamma = \left(V_{U_T} - V_{L_T}\right)$$

Final equation defining the potential difference is:

$$\Phi_U - \Phi_L = \int_{LE}^{M} \gamma dl \quad (2).$$

If we assume that spanwise velocities are small, the difference of velocity squares can be calculated as:

$$V_U^2 - V_L^2 \approx 2 V_\infty \gamma \quad (3).$$

By substituting (3) and (2) in (1), the following equation is obtained:

$$\Delta C_P = -\frac{2}{V_\infty^2}\left(V_\infty \gamma + \frac{\partial}{\partial t}\int_{LE}^{M} \gamma dl\right)$$

The Kutta condition can be expressed as the uniqueness of pressure coefficients at the trailing edge, which, mathematically expressed, takes the form:

$$\Delta C_p = -\frac{2}{V_\infty^2}\left(V_\infty \gamma_{TE} + \frac{\partial}{\partial t}\int_{LE}^{TE} \gamma dl\right) = 0$$

Since it is impossible to be $V_\infty = \infty$, the relation within the parentheses must be equal to zero:

$$V_\infty \gamma_{TE} + \frac{\partial}{\partial t}\int_{LE}^{TE} \gamma dl = 0 \quad (4).$$

The integral in the upper equation is, in fact, the contour circulation, which covers the lifting surface:

$$\tilde{\Gamma} = \int_{LE}^{TE} \gamma dl$$

so, the equation (4) can be written as:

$$V_\infty \gamma_{TE} + \frac{\partial \tilde{\Gamma}}{\partial t} = 0$$

The expression for unsteady Kutta condition comes out directly as [11] and [12]:

$$\frac{\partial \tilde{\Gamma}}{\partial t} = -V_\infty \gamma_{TE}$$

If the right hand-side part is substituted with (3) written for the trailing edge, we obtain:

$$\frac{\partial \tilde{\Gamma}}{\partial t} = -\frac{V_{U_{TE}}^2 - V_{L_{TE}}^2}{2} = -\left(V_{U_{TE}} - V_{L_{TE}}\right)\frac{V_{U_{TE}} + V_{L_{TE}}}{2}$$

From this equation, it can be clearly seen that the variation of the lifting surface circulation in time can be compensated by releasing vortices of magnitude $\left(V_{U_{TE}} - V_{L_{TE}}\right)$ at the velocity $\left(V_{U_{TE}} + V_{L_{TE}}\right)/2$.

3 DISCRETIZATION AND NUMERICAL SOLUTION PROCEDURE

The method for the solution of this problem is based on the coupling of the dynamic equations of blade motion with the equations of aerodynamics. It is not possible to obtain an analytical solution of this problem, so discretization and numerical approach must be accepted.

Discretization in time is done by observing the flow around the blade in a series of positions that it takes at certain times $t_k (k = 0,1,2...)$, which are spaced by finite time intervals Δt at different azimuths.

Discretization of the thin lifting surface is done by using the panel approach [12] and [13]. By this method, the lifting surface is divided in a finite number of quadrilateral surfaces – panels. Vorticity distribution is discretized in a finite number of concentrated, closed quadrilateral linear vortices, whose number is equal to the number of panels, in such a way that one side of the linear vortex is placed at the first quarter chord of the panel, and represents the bound vortex of the corresponding panel. The opposite side of the vortex is always placed at the trailing edge, while the other two sides are parallel to the flow. The wake is represented by quadrilateral vortex in the

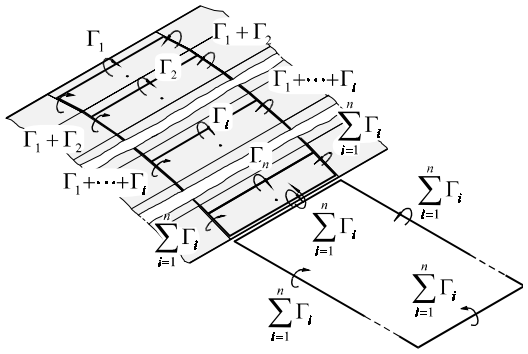

Fig. 2. *The steady panel scheme*

airflow behind the lifting surface. One side of it is connected to the trailing edge, while the opposite one is at the infinity. The other two sides (trailing vortices), which actually represent the wake, are placed parallel to the airflow. The vorticity of the quadrilateral vortex is equal to the sum of the vorticities of all bound vortices of the panels that correspond a certain lifting surface chord, but opposite in direction. Then the trailing edge vorticity is equal to zero.

Model established in such a manner corresponds to the steady flow case. On the other hand, it can be very easily spread in order to include the unsteady effects.

3.1 Vortex Releasing Model

The variation of the lifting surface position in time induces variation of circulation around the lifting surface as well. According to the Kelvin theorem, this variation in circulation must also induce the variation around the wake. According to the unsteady Kutta condition, this can be achieved by successive releasing of the vortices in the airflow [13].

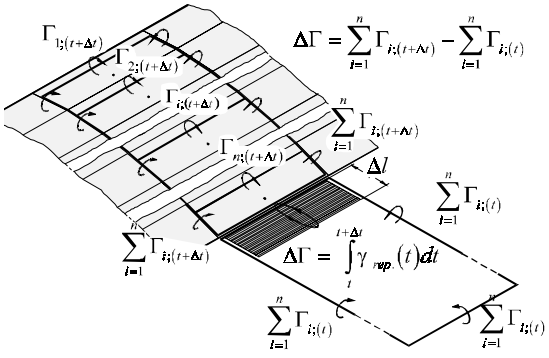

Fig. 3. *Vortex releasing*

Suppose that the lifting surface has been at rest until the moment t, when it started with the relative motion with respect to the undisturbed airflow. The vortex releasing, as a way of circulation balancing, is done continuously, and in such a way a vortex surface of intensity $\gamma(t)$ is formed.

At the next moment $t + \Delta t$, the flow model will look like in Fig. 3. The circulation of the vortex element joined to the trailing edges equal to the difference in circulations at moments $t + \Delta t$ and t. We will discretize the vortex "tail" by replacing it with the quadrilateral vortex loop, whose one side is at the trailing edge, and the opposite side is at the finite distance from the trailing edge (shed vortex). By this, we can obtain the final model for unsteady case.

3.2 Discretization of Wake

The established vortex-releasing model is appropriate for the wake modeling using the "free wake" approach [13] to [15].

During the time, by continuous releasing of the quadrilateral vortex loops, the vortex lattice formed of linear trailed and shed vortices is created. The collocation points of the vortex lattice are node points. The wake distortion is achieved by altering the positions of the collocation points in time, by application of a rather simple kinematics relation:

$$\vec{r}_i\left(t+\Delta t\right)=\vec{r}_i\left(t\right)+\vec{V}_i\left(t\right)\Delta t$$

The velocities of the collocation points are obtained as sums of the undisturbed flow velocity and velocities induced by other vortex elements of the flow field.

Induced velocities are calculated using the Biot-Savart law. In order to avoid the problems of

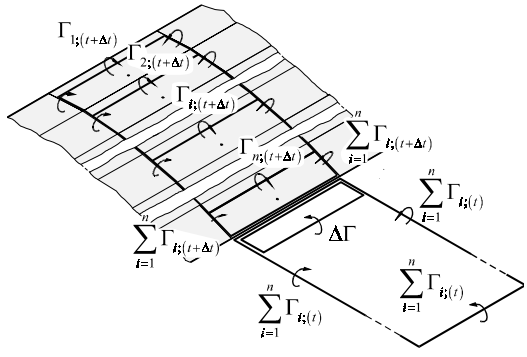

Fig. 4. *Unsteady panel scheme*

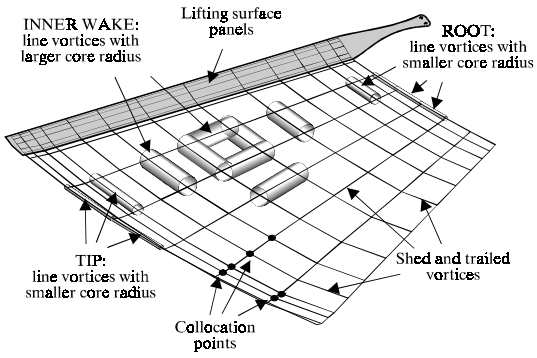

Fig. 5. *Discretized wake*

velocity singularities, line vortex elements are modeled with viscous core. The existence of the vortex core has remarkable influence in blade-wake interactions, since in this way large velocity irregularities on the blade close to the wake are avoided. Thus, using appropriate core model is important for accurate predictions of the wake development. Distributed core model is used since it is more realistic [1].

The core radius varies with the gradient of the bound circulation at the position where vortex is released, from the value $r_c = 0.00275R$ (where R is the rotor diameter) for the elements at the end of the wake (high gradient positions), to the values $r_c = 0.05R$ inside the wake (low gradients) [16].

The wake influence at large distances from the blade is negligible, so it is possible to neglect the wake distortion at a sufficient distance from the rotor. The area in which distortion is relevant depends on the helicopter flight regime, and it can be determined by the advance ratio μ [1]:

$$m = \frac{0.4}{\mu}$$

where m is the number of revolutions for which it is necessary to calculate the wake distortion. After that, the wake shape is "frozen" in achieved state, and it moves through the flow field keeping it for the rest of the time (velocity of collocation points is equal to the flow field velocity).

The "frozen" part of the wake still influences the adjacent area in which it is still being distorted. After some distance, even the influence of the "frozen" part becomes negligible, and then it is eliminated from the model. Decision of elimination row of shed and trail vortex elements from "frozen" part of the wake is made when the intensity of velocities they induced on blade panels becomes smaller than prescribed value close to zero. In this way, a discretized wake model, consistent with the panel model of the lifting surface and vortex releasing is obtained.

3.3 Discretization in Time of Unsteady Kutta Condition

Let us consider the unsteady Kutta condition from the aspect of the assumed discretized model. The condition can be written as:

$$V_\infty \gamma_{TE} + \frac{\partial \tilde{\Gamma}}{\partial t} = 0 \qquad (5).$$

In case of transition to the discretized time domain, it is necessary to substitute the partial derivative with the finite difference form:

$$\frac{\partial \tilde{\Gamma}}{\partial t} = \frac{\tilde{\Gamma}(t+\Delta t) - \tilde{\Gamma}(t)}{\Delta t} = \frac{\Delta \tilde{\Gamma}}{\Delta t}$$

By substituting this equation in (5), we obtain:

$$V_\infty \gamma_{TE} + \frac{\tilde{\Gamma}(t+\Delta t) - \tilde{\Gamma}(t)}{\Delta t} = 0 \qquad (6).$$

In case of numerical solutions, it is customary to satisfy Kutta condition in vicinity of the trailing edge. According to that, the intensity of the distributed vorticity at the trailing edge γ_{TE} is treated as equal to the intensity of the distributed vorticity at the trailing edge panel γ_n. The intensity of the distributed vorticity is constant at every panel, so it can be written:

$$\gamma_{TE} = \gamma_n = \frac{\Gamma_n}{l_n}$$

where γ_n is intensity of the distributed vorticity at the trailing edge panel, and l_n is the panel cord length. Substituting this equation in (6), we have:

$$V_\infty \frac{\Gamma_n}{l_n} + \frac{\tilde{\Gamma}(t+\Delta t) - \tilde{\Gamma}(t)}{\Delta t} = 0$$

i.e. the difference of circulations around the lifting surface at the moments $t + \Delta t$ and t can be calculated by:

$$\tilde{\Gamma}(t+\Delta t) - \tilde{\Gamma}(t) = -V_\infty \frac{\Gamma_n}{l_n} \Delta t$$

4 DEFINITION OF EQUATION SET

The boundary condition of impermeability of the lifting surface should be satisfied at any moment of time, $t_k (k = 0,1,2...)$ in a finite number of points of lifting surface:

$$\left(\vec{V}_i - \vec{V}_{Ti}\right)\cdot\vec{n}_i = 0; \quad i = 1,2,\ldots,N$$

Points at which this condition must be satisfied are called the control points. One of them is placed on each panel, at the three-quarter chord panel positions. By this, at every moment of time, the number of lifting surface impermeability conditions is equal to the number of unknown values of circulations of bound vortices.

The equations of motion of the lifting surface are known, as well as the velocities $\vec{V}_{Ti}$ of all characteristic points, and their normals $\vec{n}_i$ as well.

At each flow field point, velocity can be divided to the free stream velocity and perturbation velocity:

$$\vec{V}_i = \vec{V}_\infty + \vec{w}_i$$

The perturbation velocity is induced by lifting surface and wake vortex elements. Boundary condition of impermeability of the lifting surface can be written at any moment of time as:

$$\left(\vec{V}_\infty + \left(\vec{w}_i\right)_B + \left(\vec{w}_i\right)_S + \left(\vec{w}_i\right)_W - \vec{V}_{Ti}\right)\cdot\vec{n}_i = 0 \qquad (7),$$

where perturbation velocities are:
$\left(\vec{w}_i\right)_B$ – induced by bound vortices,
$\left(\vec{w}_i\right)_S$ – induced by shed vortices,
$\left(\vec{w}_i\right)_W$ – induced by wake vortices.

At every moment, the wake shape and circulations of its vortex lines are known, and so the wake-induced velocity at every flow field point is known as well. On the other hand, the circulations of the bound vortices are unknowns (their positions are defined by the lifting surface shape).

Therefore, equation (7) can be rewritten in the form where unknowns are on the left side, and knowns are on the right side of the equation (fact is that second term on the left side has an unknown and a known part, as will be shown later):

$$\left(\vec{w}_i\right)_B\cdot\vec{n}_i + \left(\vec{w}_i\right)_S\cdot\vec{n}_i = \left(\vec{V}_{Ti} - \vec{V}_\infty\right)\cdot\vec{n}_i - \left(\vec{w}_i\right)_W\cdot\vec{n}_i \quad (8).$$

Let us consider one column of the *n* panels on the lifting surface which spreads itself chordwise, from the leading edge to the trailing edge of the blade (Fig. 6) and shed vortex *AD* with circulation $\Delta\tilde{\Gamma}$.

Perturbation velocity in the first term on the left side of the equation (8) can be calculated as sum of the velocities induced by bound vortices:

$$\left(\vec{w}_i\right)_B = \sum_{j=1}^{n}\left(\vec{w}_{i,j}\right)_B$$

where $\left(\vec{w}_{i,j}\right)_B$ is velocity induced by *j*-th bound vortex.

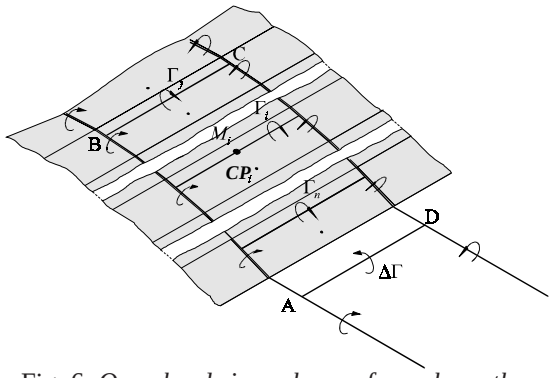

Fig. 6. *One chordwise column of panels on the lifting surface and shed vortex*

This velocity is calculated as sum of velocities induced by all of the line vortices that make horseshoe vortex *ABCD*. While circulation is constant along one horseshoe, and induced velocity is calculated by Biot-Savart law, it is possible to be written:

$$\left(\vec{w}_{i,j}\right)_B = \frac{\Gamma_j}{4\pi}\left(\sum_{ABCD}\vec{G}\right)_{i,j}$$

where $\left(\sum_{ABCD}\vec{G}\right)_{i,j}$ is vector depending only on blade geometry, i.e. position of *i*-th control point and shape of *j*-th horseshoe vortex. Finally, we may obtain:

$$\left(\vec{w}_i\right)_B = \sum_{j=1}^{n}\frac{\Gamma_j}{4\pi}\left(\sum_{ABCD}\vec{G}\right)_{i,j}$$

On the similar way, it is possible to express other induced velocities as product of circulation and vector depending only of geometry:

$$\left(\vec{w}_i\right)_S = \frac{\Delta\tilde{\Gamma}}{4\pi}\vec{G}_S \text{ , and } \left(\vec{w}_i\right)_W = \sum_{p=1}^{M}\frac{\Gamma_p}{4\pi}\left(\vec{G}_W\right)_p$$

According here developed vortex releasing method, $\Delta\tilde{\Gamma}$ can be expressed as:

$$\Delta\tilde{\Gamma} = \tilde{\Gamma}(t) - \tilde{\Gamma}(t-\Delta t) = \sum_{j=1}^{n}\Gamma_j(t) - \sum_{j=1}^{n}\Gamma_j(t-\Delta t)$$

By substituting above expressions for induced velocities in equation (8), and using necessary time notifications we may obtain:

$$\left(\sum_{j=1}^{n}\Gamma_j(t)\left(\sum_{ABCD}\vec{G}\right)_{i,j}\right)\cdot\vec{n}_i + \left(\sum_{j=1}^{n}\Gamma_j(t) - \sum_{j=1}^{n}\Gamma_j(t-\Delta t)\right)\vec{G}_S\cdot\vec{n}_i =$$
$$= 4\pi\left(\vec{V}_{Ti} - \vec{V}_\infty\right)\cdot\vec{n}_i - \left(\sum_{p=1}^{M}\Gamma_p\left(\vec{G}_W\right)_p\right)\cdot\vec{n}_i$$

Circulation of bound vortices Γ_j are known from the calculations made in previous moment of time (t - Δt), so second term on the left side of equation above can be divided in known and unknown part at the time t.

Finally, the boundary condition for the i-th control point can be written as:

$$\sum_{j=1}^{n} a_{i,j}\Gamma_j(t) = b_i$$

where:

$$a_{i,j} = \left(\left(\sum_{ABCD} \vec{G} \right)_{i,j} + \vec{G}_S \right) \cdot \vec{n}_i$$

$$b_i = 4\pi\left(\vec{V}_T - \vec{V}_\infty\right)\cdot\vec{n}_i - \left(\sum_{p=1}^{M} \Gamma_p \left(\vec{G}_W\right)_p \right)\cdot\vec{n}_i + \left(\sum_{j=1}^{n} \Gamma_j\left(t-\Delta t\right) \right)\vec{G}_S \cdot \vec{n}_i$$

In this way, by writing equations for all control points, the equation set of the unknown bound circulations in the certain panel column at the time t is obtained.

Along with this equation set, the Kutta condition must be satisfied:

$$\sum_{j=1}^{n-1} \Gamma_j(t) + \Gamma_n(t)\left(1 + V_\infty \frac{\Delta t}{l_n}\right) = \sum_{j=1}^{n} \Gamma_j\left(t-\Delta t\right) \quad (9).$$

By adding the Kutta conditions to the equation set, an over-determined equation set is obtained.

Each blade consist of many cord-wise panel columns, and if we notate total number of them over all the blades as m, then total number of panels will be $n.m$, as well must be number of boundary conditions of impermeability. Number of the Kutta conditions in the form (9) must be m. Thus, there are $n{\cdot}m + m$ equations, and $n{\cdot}m$ unknown bound circulations. Over-determined equation set, obtained in this way, can be reduced to the determined system by the method of least squares. After that, it can be solved by some of the usual approaches, by which the unknown values of circulations Γ_j at the time t are obtained.

5 DETERMINATION OF THE AERODYNAMIC FORCE

After unknown circulations are obtained, velocity at every point of the flow field is known, and we can use them for the determination of aerodynamic forces that act on the blade. The calculation aerodynamic force is necessary for the defining of the blade position at the next moment of time. The total aerodynamic force is calculated as the sum of forces acting on all panels:

$$\vec{F} = \sum_{i=1}^{N} \vec{F}_i$$

Aerodynamic force acting on a single panel can be defined by introducing the Kutta condition in a vector form (Fig 6):

$$\vec{F}_i = \rho\vec{V}_\infty \times \Gamma_{i(ef.)}\overrightarrow{BC}$$

where $\overrightarrow{BC}$ is bound circulation vector and effective circulation can be defined by using:

$$\Gamma_{i(ef.)} = \Gamma_i + \frac{1}{V_\infty}\frac{\partial}{\partial t}\int_{LE}^{M_i} \gamma dl$$

The integral should be calculated from the leading edge to the quarter-chord position of the i-th panel:

$$\Gamma_{i(ef.)} = \Gamma_i + \frac{1}{V_\infty}\frac{\partial}{\partial t}\left(\sum_{k=1}^{i-1} \Gamma_k + \frac{\Gamma_i}{4} \right)$$

After determination of aerodynamic forces, moment of aerodynamic forces M_A, necessary for blade flapping equation, can be calculated as sum of moments acting on flapping hinge.

6 RESULTS AND DISCUSSION

Presented method for blade air-loads calculation has been implemented in a computer code. Forward flight application is presented for SA 341 "Gazelle" helicopter at moderate forward speed condition (advance ratio μ is 0.35). The rotor has three blades with constant NACA 0012 cross-sections, and the blade has a linear twist of -6°20'. In presented case, blade is modeled with 13 non-uniformly spanwise spaced panels (more panels at the tips), and 6 chordwise panels non-uniformly spaced (more panels near leading and trailing edges). Azimuthal step size of 10° and appropriate time discretization for calculations is used.

By analysing the drawings of the blade wakes (Figs. 7 and 8), it can be concluded that model applied in this paper gives reasonable simulation of actual wake behavior, specially in the domain of wake boundaries, where wake roll-up occurs (although it is slightly underestimated compared with existing experimental data). In

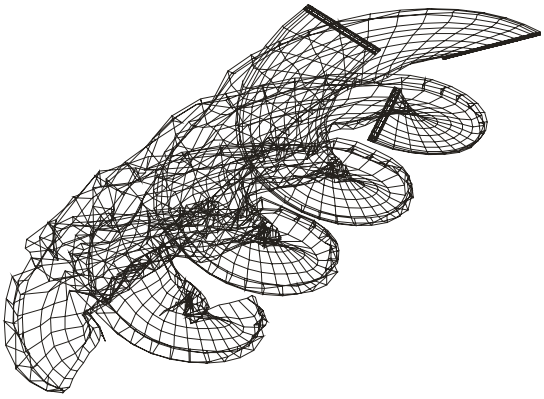

Fig. 7. *Calculated free wake geometry; μ = 0.35 (3D view)*

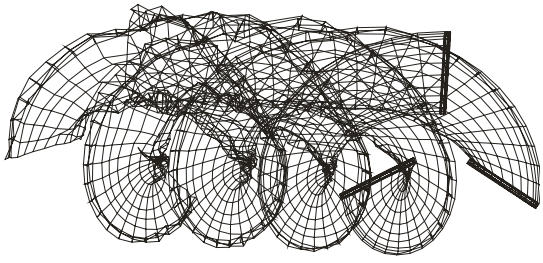

Fig. 8. *Calculated free wake geometry; μ = 0.35 (top view)*

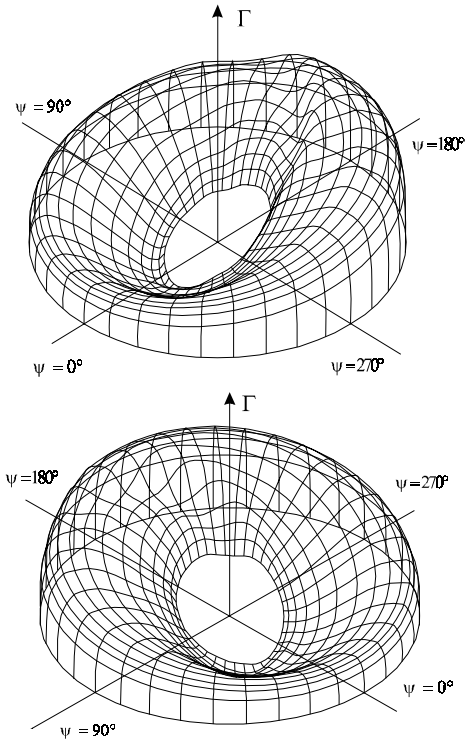

Fig. 9. *Circulation distribution on the rotor disk; μ =0.35 (different points of view)*

addition, larger wake distortion in the domains of the forerunning blades or their wakes is noticeable.

The program results (Figs. 9, 10 and 11), show the difference in circulation distributions at different azimuths, as well as the disturbances caused when blades are passing the wakes of other blades, and the characteristic reversal flow domains.

Range of azimuth where circulation is negative can be seen much clearly on the Figures 9 and 10.

Effects of the vortex-blade interaction are in the disturbing circulation and section lift distributions at the certain azimuth angles and span positions when blade passing the wakes of other blades. It is shown on the Figures 11 and 12.

On the Figure 13 is presented blade flapping angle distribution after achieving its periodical form.

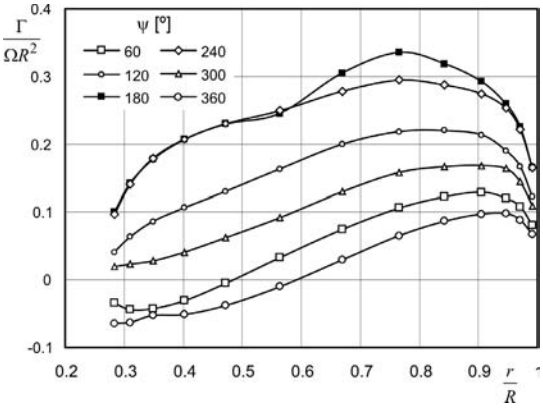

Fig. 10. *Rotor blade spanwise circulation distribution at different azimuth positions; μ =0.35*

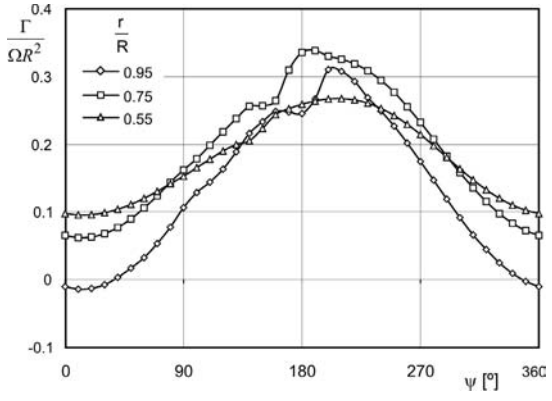

Fig. 11. *Rotor blade azimuth circulation distribution at different radial positions; μ =0.35*

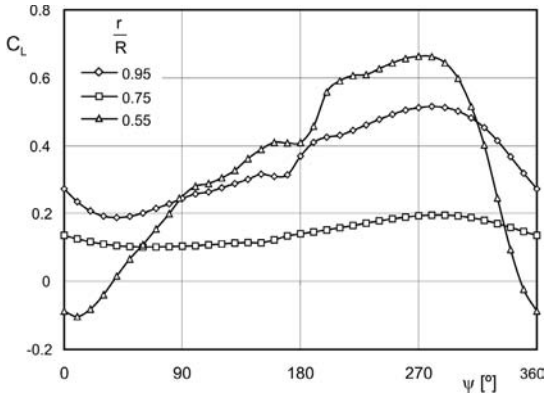

Fig. 12. *Blade section lift coefitient azimuth distribution at different radial positions; μ =0.35*

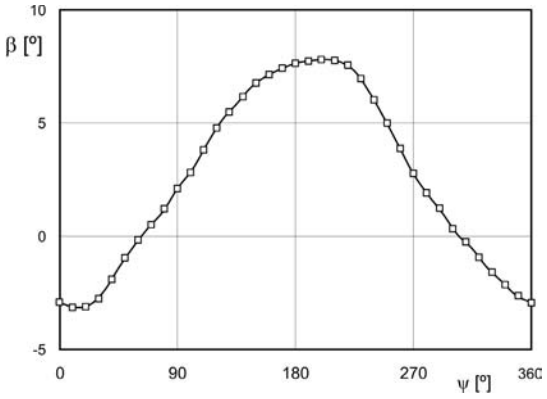

Fig. 13. *Blade flapping angle; μ=0.35*

7 CONCLUSION

A solution for potential, incompressible helicopter main rotor flow field has been developed, and preliminary validations were done.

Obtained results can define suggestions for the future solution improvement. Firstly, by incorporating the transonic flow calculations, the advancing blade tip simulation would be more appropriate. Secondly, viscous interaction should be included as well, which would improve the wake roll-up simulation. The viscous vortex core simulation in time would improve the results concerning the wake vanishing effects far enough from the blade. Finally, introduction of the curvilinear vortex elements would give better results from the aspect of wake self-induction.

With these enhancements, this solution should prove to be a useful and efficient tool to the rotorcraft performance evaluation.

8 REFERENCES

[1] Johnson,W. *Helicopter theory*. Princeton, New Jersey: Princeton University Press, 1980.

[2] Johnson, W. Airloads and wake models for a comprehensive helicopter analysis, *Vertica*, 1990, vol. 14, no. 3, p. 225-300.

[3] McCroskey, W. J. Some current research in unsteady fluid dynamics. *Journal of Fluids Engineering*, March 1977, p. 8-38.

[4] Mello, O., Rand, O. Unsteady, frequency-domain analysis of helicopter non-rotating lifting surfaces, *Journal of the American Helicopter Society*, 1991, p. 70-81.

[5] Chattot, J. J. *Calculation of three-dimensional unsteady transonic flows past helicopter blades*, NASA TP-1721, 1980.

[6] Kießling, F. Computer aided derivation of equations of motion for rotary wing aeroelastic problems, *ICAS 1982*, ICAS Proceeding-82-2.1.3, p. 67-77.

[7] Bramwell, A. R. S., Done, G., Balmford, D. *Bramwell's helicopter dynamics*, 2nd Ed. Oxford: Butterworth-Heinemann, 2001.

[8] Colin, O. Unsteady thin - airfoil theory for subsonic flow. *AIAA Journa*l, vol. 11, no. 2, 1973, p. 205-209.

[9] Basu, B. C., Hancock, G. J. The unsteady motion of a two-dimensional aerofoil in incompressible inviscid flow. *Journal of Fluid Mechanic*, 1978, vol. 87, part 1, p. 159-178.

[10] Sears, W. R. Unsteady motion of airfoils with boundary layer separation. *AIAA Journal*, vol. 14, no. 2, 1976, p. 216-220.

[11] Ardonceau, P. Unsteady pressure distribution over a pitching airfoil. *AIAA Journal*, vol. 27, no. 5, 1989, p. 660-662.

[12] Geissler, W. Nonlinear unsteady potential flow calculations for three-dimensional oscillating wings. *AIAA Journal*, vol. 16, no. 11, 1978, p. 1168-1174.

[13] Katz, J., Plotkin, K. *Low-speed aerodynamics – from wing theory to panel methods*, Int. Ed., New York: McGraw-Hill, 1991.

[14] Bliss D., Miller W. Efficient free wake calculations using analytical/numerical matching. *Journal of the American Helicopter Society*, 1993, pp. 43-52.

[15] Torok M., Berezin, C. Aerodynamic and wake methodology evaluation using model UH-60A experimental data. *Journal of the American Helicopter Society*, 1994, p. 21-29.

[16] Torok M., Chopra, I. A coupled rotor aeroelastic analysis utilising non-linear aerodynamics and refined wake modeling. *Vertica*, 1989, vol. 13, no. 2, p. 87-106.

Strojniški vestnik - Journal of Mechanical Engineering 54(2008)3, 179-188
UDC 681.5
Paper received: 10.5.2007
Paper accepted: 19.12.2007

Application of Neural Networks in Evaluation of Technological Time

Goran Šimunović* - Tomislav Šarić - Roberto Lujić
University of Osijek, Mechanical Engineering Faculty in Slavonski Brod, Croatia

The traditional approach to the process planning mostly based on experience of technologists, requires a lot of accumulated knowledge, is inflexible and time consuming. The application of artificial intelligence methods can support and greatly improve this approach. This paper describes the results obtained by investigating the application of neural networks in evaluating the manufacturing parameters and, indirectly, technological time of the seam tube polishing. Various structures of a back-propagation neural network have been analysed and the optimum one with the minimum RMS (Root Mean Square) error selected. The obtained model was integrated into the ERP system (Enterprise Resource Planning system) of a manufacturing company. The more precise evaluations of technological time obtained by the ERP system model complete the previously defined manufacturing operations and form the basis for production planning and times of delivery control. The work of technologists is thus made easier and the production preparation technological time made shorter.

Keywords: process planning, artificial intelligence, neural networks

0 INTRODUCTION

The fulfilment of the basic requirements modern enterprises are faced with, such as a product optimum quality, low production costs, holding to the agreed times of delivery and a more rational material and information management in a production system, cannot be imagined without new scientific approaches in production preparation. The level of knowledge and organisation in production preparation sectors has a considerable impact upon the final characteristics of a product and an indirect effect on production costs and the times of delivery. Integration of computers i.e. computer systems into the preparation, manufacturing and managing process has exerted a great influence on increasing the level of automation, productivity and flexibility in manufacturing companies. In this way the human involvement in production has been significantly reduced while at the same time the human factor's importance in production preparation has remained exceptionally great. By the application of the systems based on artificial intelligence attempts are made to integrate and make commonly accessible the accumulated individual knowledge and experience of the people working in the production preparation sectors. Some authors today deal with the way of collecting the technological knowledge, its presentation and application to intelligent systems. They use the acquired expert knowledge in the Computer Aided Process Planning (CAPP) system for the identification (classification) of work pieces, selection of a manufacturing process, machines and machining parameters in order to shorten the time and minimize the errors in the process planning of the machining process [1] to [3] and some other processes like forging [4].

The technological knowledge is necessary for determination of the basic material, sequence of manufacturing operations, selection of tools etc. The problem of optimization in the mentioned activities is quite important in manufacturing industries. One of the up-to-date techniques in the optimization procedure is the application of genetic algorithms (GA). This optimization technique, which is more efficient than the traditional ones (geometric programming, dynamic programming, etc.) is described and implemented in the works of many authors [5] to [8]. The authors [5] and [6] use genetic algorithms in the optimization of cutting parameters in turning processes. They consider a great number of constraints such as cutting force, machine power, tool reliability, cutting zone temperature etc. in order to shorten the time and reduce the operating costs. Attempts are made to

*Corr. Author's Address: University of Osijek, Mechanical Engineering Faculty in Slavonski Brod, Trg I. Brlić-Mažuranić 2, HR-35000 Slavonski Brod, Croatia, goran.simunovic@sfsb.hr

achieve the same goals by a continuous improvement of cutting conditions i.e. by the development and application of an on-line intelligent system for the monitoring and optimization of cutting conditions based on genetic algorithms [7] to [9]. The authors [10] and [11] also deal with the optimization of machining parameters but by the application of the modified GA with the self-organizing adaptive penalty (SOAP) strategy i.e. by the application of parallel GA and simulated annealing (SA). Besides the GA the neural networks (NN) [12] to [15] are also often combined in the procedures of the machining parameters optimization. Thus for the selection of optimal machining parameters, based on experimental data, when the analytical and empirical mathematical models are not available, Genetically Optimized Neural Network System (GONNS) [13] is proposed. In this paper the NN represents the relationship between the cutting conditions and machining-related variables, and Genetic Algorithm (GA) obtains the optimum operational condition. The paper [14] presents the use of neural network and genetic algorithm for modelling and optimal selection of input parameters of abrasive flow machining process. For a multi-criteria optimization of the cutting parameters in a turning process the hybrid analytical-neural network approach [15] and [16] is also proposed. Neural networks are also used for evaluation of the machined surface roughness [17] i.e. of the tool wear in the machining process [18]. The authors [17] and [18] compare the results obtained by the application of neural networks with the results obtained by analytical models. It is also possible to use neural networks for intelligent tool path generation for the milling of free surfaces [19] and [20]. In their work the authors take the required surface quality as a primary technological requirement for free surface milling programming. Therefore the application of artificial intelligence for the solution of specific manufacturing problems is in most cases justified in the conclusions of all the mentioned works. In multi-dimensional problems in which the mathematical dependence of input and output variables is difficult or almost impossible to set up, the application of neural networks is certainly significant. Nevertheless, no matter what the main objective of the application of neural networks, there are few authors only who speak about improvement in terms of the previously trained network integration into a corresponding data base within which the results the network gives might be repeatedly used. It is exactly the problem of predicting technological time by the application of neural networks and integration of a trained network into the ERP system that the present paper deals with.

1 THE PROBLEM AND INVESTIGATING GOAL DEFINITION

There are two phases in the production of stainless steel seam tubes: rolling phase and grinding and polishing phase. In the initial phase a stainless steel band of diverse width and thickness, depending on the required external diameter of the tube, is rolled over a number of vertical and horizontal rollers and formed into a tube. Then the edges of the rolled tube are heated and prepared for the TIG welding in a protective chamber. This is followed by the grinding of the raised edges of the weld and calibrating of the tube according to the required tolerance of external diameter and the required oval shaping. After the weld is tested by a non-destructive method and occasional technological trials, the tube is rough ground, marked, cut to the specified length and taken to a store for the semi-manufactured products. A planned minimum quantity of the tubes of various dimensions is kept in the store.

In most cases (about 95%) these stainless steel seam tubes need additional grinding and polishing. The scheme of the grinding and polishing line is given in Figure 1. Depending on the customers' orders the tubes are taken from the storage place and the second phase (grinding and polishing) follows. Passage through abrasive belts and polishing heads and rotation around axis give the required cleanliness and polish to the external surface. If the required quality is to be reached the worn out abrasive belts should be replaced in time. If this is not the case the tubes will be sent back for additional treatment (II or III phase of polishing) which results not only in the loss of time but in the increase of the working order costs too. Machining parameters and the time necessary for the second phase of production are mostly assessed based on experience. The machining time can be calculated on the basis of the polishing rate and the polishing rate depends on a great number of other parameters of influence.

It is almost impossible to establish a mathematical model of the polishing rate due to a number of influential parameters, which will be described later. Therefore, one of the goals of this paper, which deals with the evaluation of technological parameters and indirectly of technological time of the seam tube polishing, is to develop a processing model based on the application of neural networks. The developed model will be integrated into the existing ERP system of the company Đuro Đaković Welded Vessels Ltd. The values of input variables in the model will be based on the ERP system real data and the results the model gives should form the basis for a more precise assessment of delivery times and production planning. The integration of the model into the ERP system should upgrade the activities in the technological preparation of production and the jobs connected with production planning and make the data the model gives generally accessible and useful for the company as a whole.

Neural networks are selected for establishing the model because the knowledge about the problem is available in the form of a set of discrete values of the state vector element and the process output values. Real data for setting up the model have been collected over a longer period of time in the company Đuro Đaković Welded Vessels Ltd. in the production of stainless steel seam tubes.

2 EVALUATION OF THE MACHINING PARAMETERS BY THE APPLICATION OF THE BACK-PROPAGATION NETWORK

2.1 Selection of the Type of Neural Network – General Model

The observed research belongs to the problems dealing with continuous input and output values i.e. problems connected with prediction, thus the back-propagation network is applied. Figure 2 shows the structure of a back-propagation network with one hidden layer (there can be more hidden layers), while the structure of an artificial neuron is shown in Figure 3.

During the process of learning the aim is to enable fast convergence and reduce global error given by:

$$E = 0,5 \cdot \sum \left(d_k - x_k \right)^2 \qquad (1).$$

In this type of network global error propagates backwards through the network all the way to the input layer. During the backward pass all weighted connections are adjusted in accordance with the desired neural network output values. Increase or decrease of the actual values of the weights $w_{ij}^{[s]}$ affects the decrease of global error.

By the application of the gradient descent rules the increase in the network weighted connections $\Delta w_{ji}^{[s]}$ can be given as:

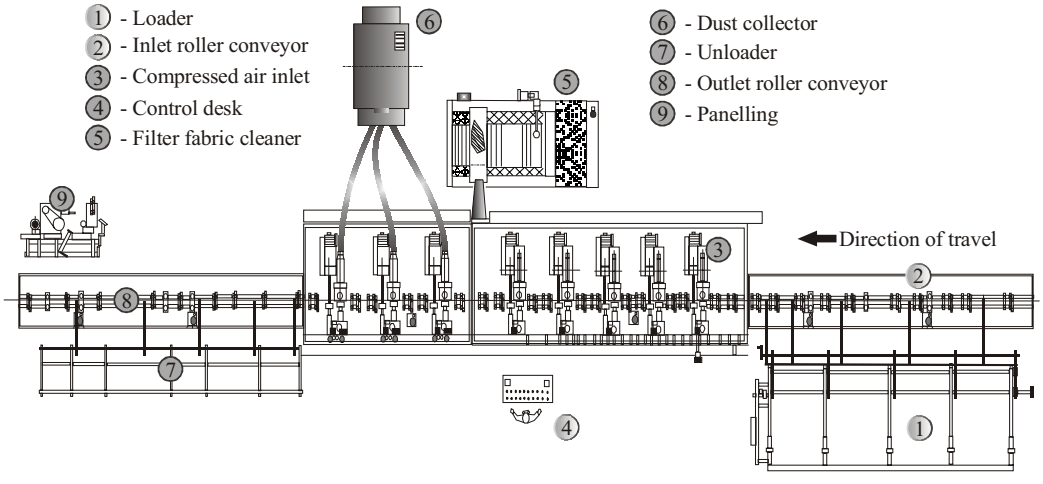

Fig.1. *Scheme of the polishing and grinding line*

$$\Delta w_{ji}^{[s]} = -\alpha \cdot \left(\frac{\partial E}{\partial w_{ji}^{[s]}} \right) \quad (2),$$

where α is the learning coefficient.

Derivations given above can be calculated as:

$$\frac{\partial E}{\partial w_{ji}^{[s]}} = \left(\frac{\partial E}{\partial I_j^{[s]}} \right) \cdot \left(\frac{\partial I_j^{[s]}}{\partial w_j^{[s]}} \right) = -e_j^{[s]} \cdot x_i^{[s-1]} \quad (3).$$

The value of the weighted connections increase in the network $\Delta w_{ji}^{[s]}$ is now:

$$\Delta w_{ji}^{[s]} = \alpha \cdot e_j^{[s]} \cdot x_i^{[s-1]} \quad (4),$$

where α is the learning coefficient, $x_j^{[s]}$ represents output state of the j -th of this neuron in the s-th layer, and the parameter $e_j^{[s]}$ that represents the error and propagates backwards through all the layers of the network is defined as:

$$e_j^{[s]} = \frac{-\partial E}{\partial I_j^{[s]}} \quad (5).$$

The learning coefficient should be kept law to avoid divergence although this could result in a very slow learning. This situation is solved by including a momentum term into expression (4):

$$\Delta w_{ji}^{[s]} = \alpha \cdot e_j^{[s]} \cdot x_i^{[s-1]} + momentum \cdot \Delta w_{ji}^{[s]} \quad (6) .$$

The weights in the network can be updated for each learning vector separately or else cumulatively, which considerably speeds up the rate of learning (convergence).

Therefore the objective of the learning process in a neural network is to achieve the lowest possible level of error between the outputs obtained by training the network and the actual (desired) results. This is realized by adjusting the weights of the neurons, and by accepting the objective function, defined below through the minimization of the mean square error.

General form vector of the model applicable for a neural network input is as follows:

$$X_i = \{x_{i1}, x_{i2}, x_{i3}, ..., x_{in}\} \Rightarrow$$
$$\Rightarrow Y_o = \{y_{o1}, y_{o2}, y_{o3}, ..., y_{on}\} \quad (7),$$

where vector $X_i = \{x_{i1}, x_{i2}, x_{i3}, ..., x_{in}\}$ represents input variables, and vector $Y_o = \{y_{o1}, y_{o2}, y_{o3}, ..., y_{on}\}$ output variables.

2.2 Application of the Back-Propagation Network in Evaluations of Machining Parameters

In the given problem the model vector has one output variable – the rate of polishing. The technological time is calculated from the rate of polishing. Input variables are: kind of material, tube external diameter, wall thickness, oval shaping of the tube after the first phase of production, gradation of the belts used for grinding or polishing adjusted on machine (conveyor), condition of belts (time of usage), pressure of belts, required and performed roughness of the surface, length of tubes and polishing phase (Table 1).

The RMS error (Root Mean Square error) is taken as a criterion for network validation. It is defined as:

$$RMS = \sqrt{MS} = \sqrt{\frac{\sum_{n=1}^{N} (d_n - y_n)^2}{N}} \quad (8),$$

where:

MS Mean Square error,

N Number of pairs of the training set input-output

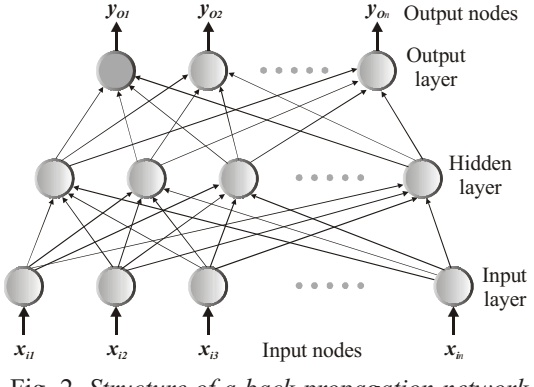

Fig. 2. *Structure of a back-propagation network*

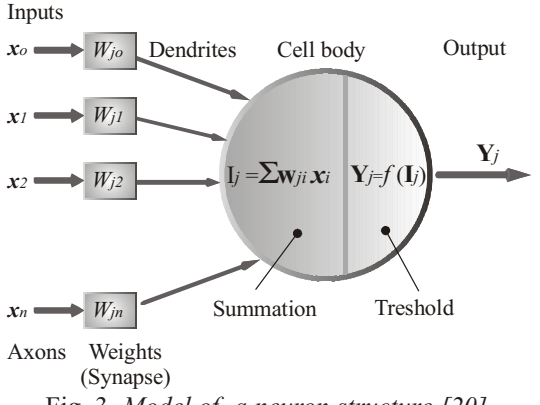

Fig. 3. *Model of a neuron structure [20]*

values,

y_n Neural network n-th output,

d_n Desired value of a neural network n-th output.

The Delta rule is applied for network training. This rule is also called Widrow/Hoff rule or the minimum mean square rule which has become one of the basic rules in the training process of most neural networks.

In expression (9) the formula for the Delta rule is given:

$$\Delta w_{ji} = \alpha \cdot y_{cj} \cdot \varepsilon_i \qquad (9),$$

where is the value of the difference in the weights of neuron *j* and neuron *i* realized in two steps (*k*-th and *k*-1), mathematically described by:

$$\Delta w_{ji} = \Delta w_{ji}^{k} - \Delta w_{ji}^{k-1} \qquad (10),$$

α is the rate (coefficient) of learning, y_{cj} is the output value of neuron *j* calculated according to transfer function, ε_i is the error given as:

$$\varepsilon_i = y_{ci} - y_{di} \qquad (11),$$

where y_{dj} is the actual (desired) output. The error given by the expression (11) returns to the network only rarely, other forms of error are used instead depending on the kind of network.

For most actual problems various rates of learning are used for various layers with a low rate of learning for the output layer. It is usual for the rate of learning to be set at a value anywhere in the interval between 0.05 and 0.5, the value decreasing during the learning process. While using the Delta rule algorithm the used data are to be selected from the training set at a random basis. Otherwise frequent oscillations and errors in the convergence of results can be expected.

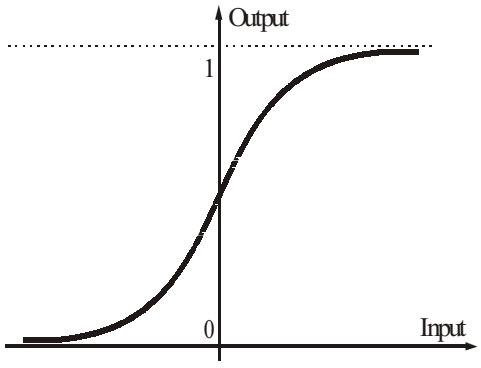

Fig. 4. *Graph of a Sigmoid transfer function*

The transfer function used in this paper is the Sigmoid function calculated according to expression:

$$Output_i = \frac{1}{1 + e^{-G \cdot input_i}} \qquad (12),$$

where *G* – is the function increment. It is calculated as *G=1/T*. *T* is the function threshold. This function is often used when neural networks are created or investigated. The graph of the function is continuously monotonous and is shown in Figure 4. As it can be seen the values of this transfer function are in the [0,1] interval range.

2.3 Obtained Results

The study of the application of the back-propagation network was carried out for a defined data model. By alternating the attributes diverse architectures of neural networks were studied. The attributes of the network that gives minimum RMS error are shown in Table 2. This network architecture generated the network output with

Table 1. *Variables with a value range for the proposed model*

No	Variable	Minimum value	Maximum value
1.	Kind of material	1	4
2.	Tube external diameter [mm]	10	50
3.	Wall thickness [mm]	0.5	2.5
4.	Tube oval shaping after first phase of production [μm]	0.04	0.1
5.	Gradation of belts for grinding or polishing	80	700
6.	Condition of belts (time of usage) [min]	0	1200
7.	Pressure of belts	0.8	2.5
8.	Required roughness [μm]	8	12
9.	Performed roughness [μm]	10	14
10.	Length of tube [mm]	1000	6000
11.	Phase of polishing	1	3

Table 2. *Attributes of neural network with minimum RMS error*

No.	Attributes	Accepted denotation
1.	Input number of neurons	11
2.	Output number of neurons	1
3.	Number of hidden neurons	6
4.	Learning rule	Delta
5.	Transfer function	Sigmoid
6.	Epoch Size	11
7.	Maximum number of training epochs	75000
8.	Number of training epochs between tests	215
9.	Attempts	45
10.	Learning Rate	0.21; 0.095; 0.1; 1.0
11.	Momentum	0.2; 0.05; 0.1; 0.8
12.	RMSE in learning phase	0. 0301
13.	RMSE in validation phase	0. 0482
14.	Correlation Coefficient	0.9870

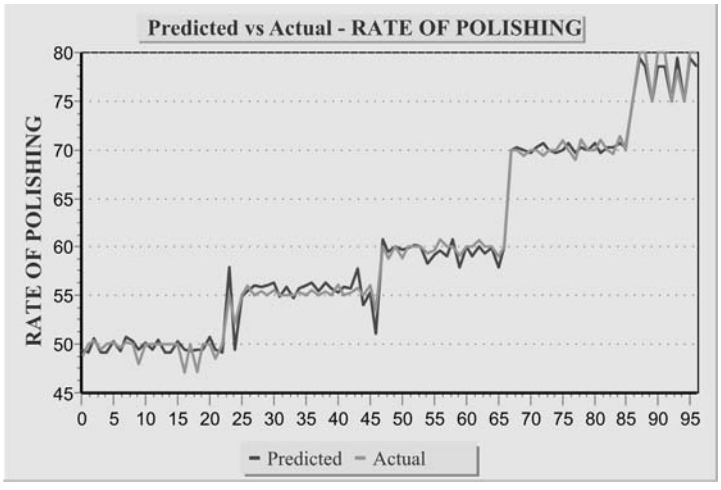

Fig. 5. *Presentation of actual and predicted values given by NN for the rate of polishing*

3.01% rate of RMS error in the training phase and 4.82 % in the validation phase.

Therefore the neural network whose attributes are given in Table 2 approximates best to experimental results. The graph in Figure 5 shows the results obtained by this network structure with regard to experimental results.

Subsequently an investigation into the importance of particular variables for a neural network model was also performed aimed at the possibility of reducing their number. As compared to the defined neural network structure with minimum rate of error (Table 2) a process was developed in which a reduced data model containing 10 input variables and 1 output one was observed. The network was trained with the reduced data model and the given results were analyzed subsequently. The results, shown in Table 3, point to a higher RMS error for each step (with the model reduced by one variable) compared with the initial model.

Therefore the conclusion is that leaving any of the variables out of the model would lead to an increase in error. In an extended model reduction process the dependence of polishing rate on two variables was also studied (Figs. 6 and 7).

3 INTEGRATION OF A PREDICTION MODEL BASED ON NEURAL NETWORKS INTO A TECHNOLOGICAL SUBSYSTEM

The company in which the study was carried out had an ERP (Enterprise Resource Planning) system integrated previously. The structure and

Table 3. *Importance of variables in the model*

No	Variables	RMS	Difference
0.	All model variables	0.0301	0.0000
1.	Kind of material	0.1216	-0.0915
2.	Tube external diameter [mm]	0.0819	-0.0518
3.	Wall thickness [mm]	0.0912	-0.0611
4.	Tube oval shaping after first phase of production [μm]	0.2230	-0.1929
5.	Gradation of belts for grinding or polishing	0.3377	-0.3076
6.	Condition of belts (time of usage) [min]	0.1484	-0.1183
7.	Pressure of belts	0.0867	-0.0566
8.	Required roughness [μm]	0.0473	-0.0172
9.	Performed roughness [μm]	0.0675	-0.0374
10.	Length of tubes [mm]	0.1241	-0.0940
11.	Phase of polishing	0.0672	-0.0372

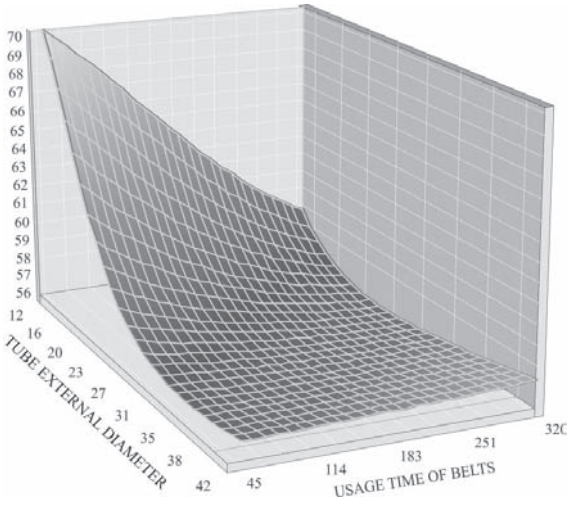

Fig. 6. *Rate of polishing dependence on tube external diameter and usage time of belts*

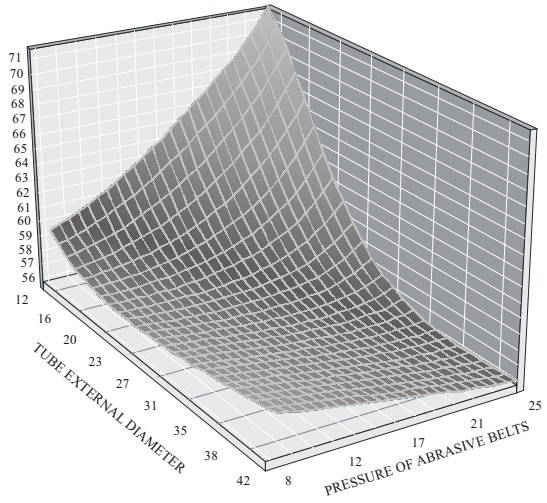

Fig. 7. *Rate of polishing dependence on tube external diameter and pressure of abrasive belts*

components of the ERP system are shown in Figure 8.

By implementing the ERP system the organization level of the preparation, manufacturing and service jobs has raised, quality of management has improved and control of the processes of preparation and production has become easier. Stocks of materials, production costs, costs of quality deviation (scrap, refinish), costs of customer complaints, costs of penalties due to delays in delivery have all been reduced. Production cycle time and production preparation time have been cut, number of required documents and amount of manual work needed for data entering and copying has become smaller. The time necessary to repair damages and machine breakdowns has been reduced. The ERP system technological subsystem DEPTO makes it possible to enter and define materials, raw materials, work-pieces, assembly blocks and products, product components with standards for raw materials, materials and finished parts. It also enables the definition of manufacturing processes, material ratings, technological times per operation resulting from experience, connection and inspection of drawings of parts, assembly blocks and products and print-out of technological documentation.

Determination of the feasible times of delivery based on offers and later also on orders in the Selling and Calculation subsystem – PROKA is mainly experientially based. The system users only rarely carry out multi-criteria analyses. A major factor in determining the times of delivery is the technological time. The overall time of a

manufacturing process can be calculated from the ERP technological subsystem previously defined technological parameters, including the rate of polishing. However, this theoretical, empirical value of the polishing rate based on the condition of the tubes, machine and equipment, changes. That is why the obtained model based on the application of neural networks has been integrated into the existing ERP system of the company Đuro Đaković Welded Vessels Ltd. The model is directly integrated into the DEPTO subsystem.

Therefore, one of the goals of the prediction model integration into the ERP system is to more precisely predict the rate of polishing, thus the time of machining and feasible times of delivery, on the basis of the system obtained model actual data. Such precise predictions of the rate and time of polishing that the previously obtained model gives, are essential in the planning and scheduling of production and particularly of the production plan revision.

Based on the system data and application of the prediction model it is also possible to make a correction of the empirical (theoretical) rate of polishing at the moment of the preparation of technological documentation and perform launching with the real technological times.

A month long application of the integrated model has proven efficient as it gives the actually needed times of polishing (Fig. 9). The necessary data that represent the input into the obtained model are collected from the following subsystems and modules (Fig. 10): Commerce and Sales, Definition of Products and Technology, Supply and Inventory, Maintenance of Production Facilities, Common Data Base, Production Monitoring, and Production Planning and Scheduling.

4 CONCLUSION

This paper outlines the results of the application of neural networks in evaluating the technological parameters and technological time of seam tube polishing. The prediction model based on neural networks gives the results with a less than 10% error. Although high, this is a limit to the model acceptability. Namely, the research showed that the young and less experienced engineers commit a 10% error in process planning when determining the rate of machining and technological time.

By integrating the model into the ERP system the process planning of the seam tube polishing has become easier and the time needed

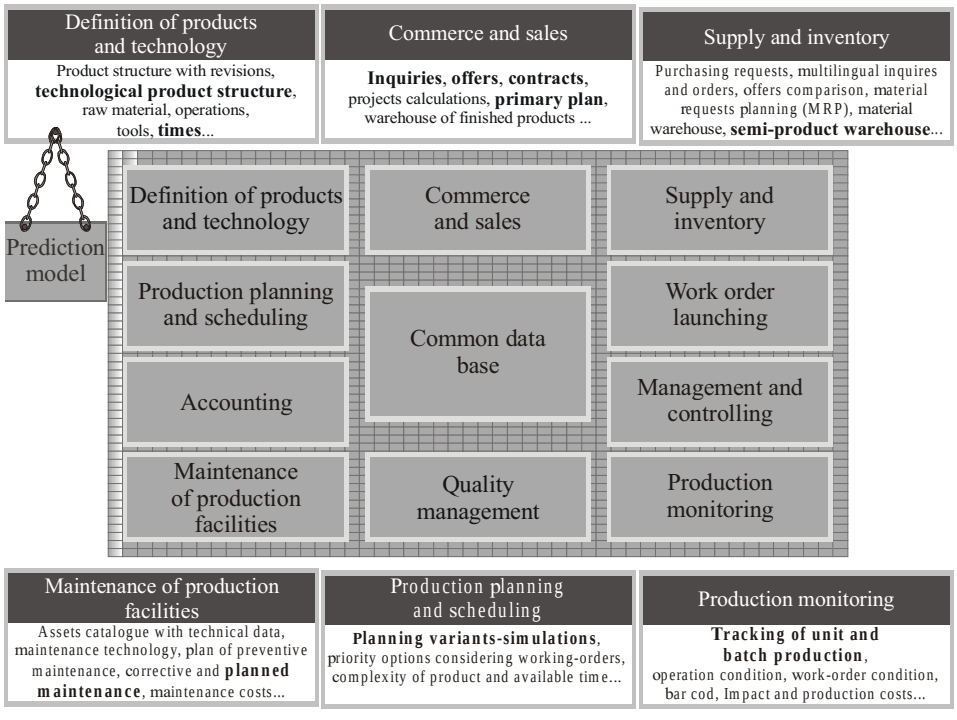

Fig. 8. *The ERP system structure*

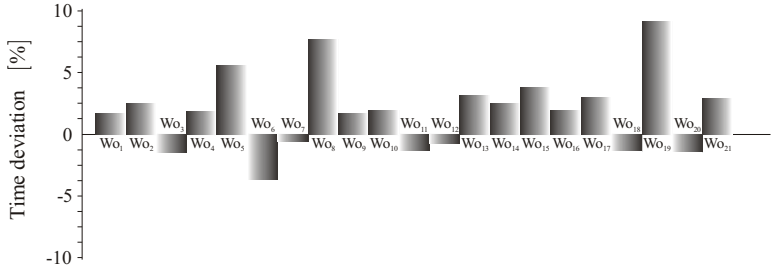

Fig. 9. *Deviation of the actual from scheduled time by a work order*

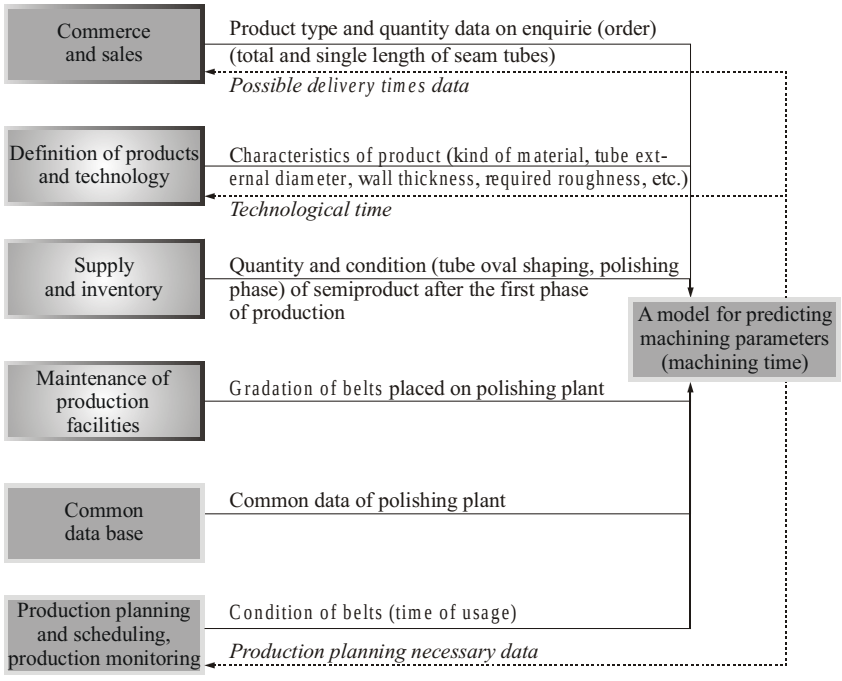

Fig. 10. *Neural network model integration into the ERP system*

for technological preparation of production has been reduced.

Monitoring of the application of the model within the ERP system showed that with the more precise predictions of the rate of polishing and of the values of technological times the model facilitates the activities of production planning and scheduling and of defining the times of delivery.

The research will continue and its aim will be to proceed with the collecting of real data in the production of polished seam tubes and to enlarge the amount of sample data. It is to be expected that after learning and training the network will give better results i.e. smaller error and that the time deviation of actual versus planned time by a working order will be reduced. The aim is also to perform optimization of machining parameters after proposing the rate of polishing. The optimization procedure will incorporate genetic algorithms (GA) so that the combined application of NN and GA should result in obtaining optimum machining parameters considering the ERP system data and condition of the semi products and equipment in the plant.

Acknowledgements

This research forms part of the project "Development of the ERP system for a digital enterprise" financed by the Ministry of Science, Education and Sports of the Republic of Croatia. Our acknowledgment alo goes to Mr Zdenko Frid, manager of the plant for production of stainless steel seam tubes in the company Đuro Đaković Welded Vessels Ltd.

5 REFERENCES

[1] Grabowik, C., Knosala, R. The method of knowledge representation for a CAPP system. *Journal of Materials Processing Technology,* 133(1-2):90-98, 2003.

[2] Wang, K.S. An integrated intelligent process planning system (IIPPS) for machining. *Journal of Intelligent Manufacturing,* 9(6):503-514, 1998.

[3] Park, K.S., Kim, S.H. Artificial Intelligence Approaches To Determination of CNC Machining Parameters In Manufacturing - A Review. *Artificial Intelligence in Engineering,* 12(1-2):127-134, 1998.

[4] Kim, C., Park, C.W. Development of an expert system for cold forging of axisymmetric product - Horizontal split and optimal design of multi-former die set. *International Journal of Advanced Manufacturing Technology,* 29(5):459-474, 2006.

[5] Singh, G., Choudhary, A.K., Karunakaran, K.P., Tiwari, M.K.) An evolutionary approach for multi-pass turning operations. *Proceedings of the Institution of Mechanical Engineers Part B-Journal of Engineering Manufacture,* 220(2):145-162, 2006.

[6] Sardinas, R.Q., Santana, M.R., Brindis, E.A. Genetic algorithm-based multi-objective optimization of cutting parameters in turning processes. *Engineering Applications of Artificial Intelligence,* 19(2):127-133, 2006.

[7] Cus, F., Balic, J. Optimization of cutting process by GA approach. *Robotics And Computer-Integrated Manufacturing,* 19(1-2):113-121, 2003.

[8] Cus, F., Milfelner, M., Balic, J. An intelligent system for monitoring and optimization of ball-end milling process. *Journal of Materials Processing Technology,* 175(1-3):90-97,2006.

[9] Balic, J. Intelligent CAD/CAM systems for CNC programming - an overview. *Advances in Production Engineering & Management (APEM) journal*, 1 (1):13-22, 2006.

[10] Ahmad, N., Tanaka, T., Saito, Y. Cutting parameters optimization and constraints investigation for turning process by GA with self-organizing adaptive penalty strategy. *JSME International Journal Series C-Mechanical Systems Machine Elements & Manufacturing*, 49(2):293-300, 2006.

[11] Wang, Z.G., Rahman, M., Wong, Y.S., Sun, J. Optimization of multi-pass milling using parallel genetic algorithm and parallel genetic simulated annealing. *International Journal of Machine Tools & Manufacture*, 45(15):1726-1734, 2005.

[12] Tansel, I.N., Ozcelik, B., Bao, W.Y., Chen, P., Rincon, D., Yang, S.Y., Yenilmez, A. Selection of optimal cutting conditions by using GONNS. *International Journal of Machine Tools & Manufacture*, 46(1):26-35, 2006.

[13] Jain, R.K., Jain, V.K. Optimum selection of machining conditions in abrasive flow machining using neural network. *Journal of Materials Processing Technology,* 108(1):62-67, 2000.

[14] Zuperl, U., Cus, F., Mursec, B., Ploj, T. A hybrid analytical-neural network approach to the determination of optimal cutting conditions. *Journal of Materials Processing Technology,* 157-58 (Special Issue SI):82-90, 2004.

[15] Zuperl, U., Cus, F. Optimization of cutting conditions during cutting by using neural networks. *Robotics And Computer-Integrated Manufacturing*, 19(1-2):189-199, 2003.

[16] Sanjay, C., Jyothi, C. A study of surface roughness in drilling using mathematical analysis and neural networks. *International Journal of Advanced Manufacturing Technology,* 29(9-10):846-852, 2006.

[17] Ozel, T., Karpat, Y. Predictive modelling of surface roughness and tool wear in hard turning using regression and neural networks. *International Journal of Machine Tools & Manufacture*, 45(4-5):467-479, 2005.

[18] Balic, J., Korosec, M. Intelligent tool path generation for milling of free surfaces using neural networks. *International Journal of Machine Tools & Manufacture,* 42(10):1171-1179, 2002.

[19] Balic J. *Intelligent manufacturing systems.* Univesity of Maribor, Faculty of Mechanical Engineering, Maribor, 2004. (In Slovenian).

[20] Novaković, B., Majetić, D., Široki, M. *Artificial neural networks*, University of Zagreb, Faculty of Mechanical Engineering and Naval Architecture, Zagreb, 2004. (in Croatian).

Strojniški vestnik - Journal of Mechanical Engineering 54(2008)3, 189-206
UDK - UDC 621.8
Paper received: 5.2.2008
Paper accepted: 12.3.2008

The Performance and Mechanisms of DLC-Coated Surfaces in Contact with Steel in Boundary-Lubrication Conditions - a Review

Igor Velkavrh - Mitjan Kalin* - Jožef Vižintin
University of Ljubljana, Faculty of Mechanical Engineering, Slovenia

The importance of hard coatings in mechanical applications has been increasing rapidly for more than 20 years. The development of novel coatings, such as improved ceramic, diamond-like-carbon and advanced nano-composites, has promoted scientific research in the field of tribology and surface engineering, and at the same time it has focussed attention on micro- and nano-technologies. Diamond-like-carbon (DLC) coatings are becoming one of the most promising types of hard coatings. Their main advantages are low friction, good anti-wear properties, and adhesive protection. However, due to their low surface energy their reactivity with conventional oils and additives is limited and remains unsatisfactory. For a qualitative step-change that would improve the performance and allow effective optimising and tailoring of boundary-lubricated DLC contacts for various mechanical systems it is necessary to understand the mechanisms of why, how, under which conditions, and with which types of DLC coatings and lubricants the actual boundary lubrication is possible. As a result of ten years of research in this field, a lot of data have been reported; however, due to the different types of coatings, lubricants and additives used in these studies, the results are often difficult to compare and are sometimes contradictory. As a result of the recent heavy demand from many industries to apply DLC coatings to lubricated systems, a much better understanding of these phenomena and their overall performance is required. Therefore, if we wish to see a more effective continuation of the research and a better understanding of the scattered results, an overview of the current state of the art of lubricated DLC contacts is needed. In this paper we analyse the performance and suggested boundary-lubrication mechanisms of DLC/steel contacts from already-published studies and we summarise our present understanding of the boundary lubrication in DLC/steel contacts, which complements our recent analyses of DLC/DLC contacts.

Keywords: diamond-like carbon coatings, boundary lubrication, base oil, additives, nanotribology

0 INTRODUCTION

The extensive research on diamond-like-carbon (DLC) coatings in the past ten years has made it possible for such coatings to become one of the most valuable and promising types of protective low-friction coatings for a variety of mechanical applications. During this period the improvements in the deposition parameters, the understanding of the coatings' structure and related properties, the operating contact conditions, and the wear and friction behaviours [1] to [7] were substantially improved.

Diamond-like-carbon materials can have different structures of sp^2- and sp^3-bonded carbon atoms, containing a substantial amount of hydrogen or almost none [8] to [10]. Figure 1 shows a ternary phase diagram of the sp^2, sp^3, and hydrogen contents of various forms of diamond-like carbon. With respect to their chemical structure, we can differentiate between "pure", i.e., non-doped-DLC coatings and "modified", i.e., doped-DLC coatings. Non-doped coatings consist of C and/or H atoms only, while the doped ones contain additional metal (Ti, W, Mo, etc.) or non-metal (Si, N, F, etc.) elements. DLC coatings can be further divided in two major groups, based on their hydrogen content: (i) non-hydrogenated DLC coatings that include amorphous (a-C) and tetragonal (ta-C) DLC coatings with a negligible hydrogen content, and (ii) hydrogenated DLC coatings that include amorphous (a-C:H) and tetragonal (ta-C:H) DLC coatings containing a substantial amount of hydrogen [11].

*Corr. Author's Address: University of Ljubljana, Faculty of Mechanical Engineering, Aškerčeva 6, SI-1000 Ljubljana, Slovenia, mitjan.kalin@ctd.uni-lj.si

Because there is such a wide variety of different DLC coatings, their physical and chemical properties can also be very different, which implies that DLC coatings are nowadays being used in various fields of industry, for example, automotive, aerospace, electronics, optics, as well as for medical equipment and many others. As a consequence many studies on the tribological performance of DLC for use in different mechanical applications can be found in literature, for example, for automotive valve-train applications [12] and [13], bearings [14] and [15], gears [16] and [17], piston rings [18] and [19], cam followers [20], spark-ignited, direct-injection fuel systems [21], cutting and forming tools [22] and [23], hydraulic systems [24], etc. For medical purposes, studies were performed primarily for the use of DLC in orthopaedic applications [25] and [26], while for applications in the computer industry, this is mostly related to the head-disk interface [27] to [30].

In the automotive industry, which is a strongly performance-driven field, there is an increased demand for the use of DLC coatings in various contacts and systems, and these are typically lubricated [31] to [33]. Due to an ever-growing demand to reduce oil consumption and thus the amount of oil in mechanical systems, but also because of the increased severity of the contact conditions, many of these systems need to operate under boundary- and starved-lubrication conditions [34] to [36]. Therefore, to achieve the appropriate performance under such conditions, some interactions between the coatings, the oils and the additives are necessary for long-term, low-friction and low-wear operation. However, DLC coatings

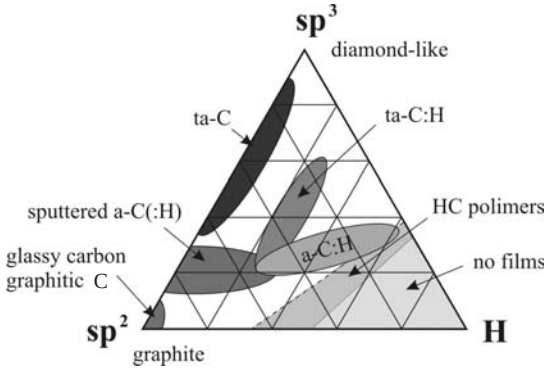

Fig. 1. *Ternary phase diagram of sp2, sp3, and hydrogen contents of various forms of diamond-like carbon*

are known as "inert" coatings with a low surface energy [37] and [38], and are therefore considered not to react with various oil additives and/or attract polar groups from the additives and the oil, which are the conventional mechanisms for the lubrication of steels and other metals [39] to [41]. Indeed, due to the early stage of research in this area, the chemical evidence and a definitive general mechanistic explanation of the boundary lubrication with DLC coatings was seldom provided [42] to [44], despite there being some excellent studies and frequently reported obvious empirical effects. This means that it is still questionable as to whether the lubricating mechanisms known from conventional steel (metal) surfaces are also valid for DLC coatings, or whether some other mechanisms are acting. In the ten years or so that there has been an interest in the boundary lubrication of DLC, a large quantity of empirical data has already been obtained, based on a variety of DLC coatings, base oils, additives, contact conditions, test devices, etc., which, in addition to providing new information, also makes understanding the behaviour and the performance of boundary-lubricated DLC coatings a complex task.

It is thus obvious that in order to improve and optimize the performance of DLC-lubricated systems, two specific requirements need to be fulfilled. Firstly, the real boundary-lubrication mechanisms of DLC coatings need to be revealed and understood from the mechanisms point of view, which means that studies have to be made in greater detail. Secondly, the results that were obtained so far, which are very scattered and poorly understood, need to be collected and compared, wherever this is possible. In this paper we attempt to summarize these previous results and analyse the behaviours that were reported during these studies. Due to the complexity and the variety of conditions and materials, only DLC/steel contacts are analysed in this paper. However, these are probably the most typical and often-used type of DLC contacts. This paper is thus complementary to our previous analyses of DLC/DLC contacts [45]. A presentation of the basic scheme of contacts using the different DLC coatings, additives and oils discussed in this paper is shown in Figure 2.

1 RESULTS

We have summarised the friction and wear results from already-published studies of lubricated DLC coatings in contact with steel [20], [32], [43],

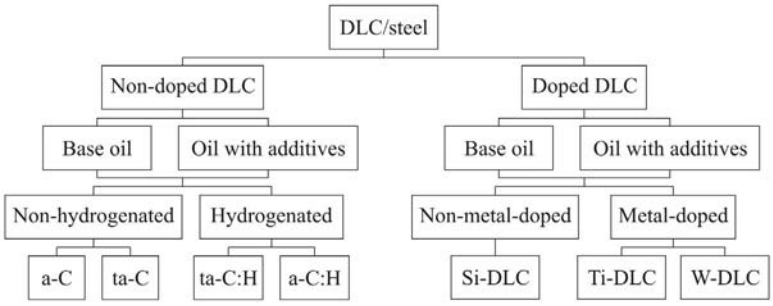

Fig. 2. *Schematic of the analysed contacts with respect to type of DLC and lubricants used*

[44], [46] to [57]. We then averaged all the values reported for specific coating/lubricant combinations with respect to the oils and the coatings shown in Figure 2. The presented results are shown as an average of the individual reported data, so that:

$$X = \frac{\sum_{i=1}^{n}\left[\sum_{j=1}^{p}\left(X_j + ... + X_p\right) + ... + \sum_{j=1}^{q}\left(X_j + ... + X_q\right)\right]}{n} \quad (1),$$

where n represents the number of researches, $p...q$ represent the number of results taken from each study, and X stands for the analysed value, i.e., the coefficient of friction or wear rate.

Such an analysis was chosen in order to avoid the influence of the different number of results given by each study – having in mind that many studies present a list of results for specific material-lubricant combination, e.g., at various sliding intervals, velocities, loads, etc., which are impossible to fully consider empirically. However, where a large scatter of results showed a notable effect, this is pointed out and specifically commented on.

With regard to the scheme shown in Figure 2, we have separated the lubricants into base oils and oils with additives, in order to observe the influences of both separately. In Table 1 and Table 2 a list of analysed base oils and additives is presented.

In literature, it is more typical to report contacts as ball/disc, however, for the clarity of the discussed coating materials, we report in this paper the coating material first, although it is usually the disc. Consequently, contacts are throughout the paper reported as COATING/STEEL, irrespective whether the coating was a ball or a disc.

Table 1. *Denotations and specifications of analysed base oils*

Denotation	**Specification**
PAO	polyalphaolefin
M	mineral oil
S	sunflower oil
SE	saturated ester
UE	unsaturated ester

Table 2. *Denotations and specifications of analysed additives*

Denotation	**Specification**
EP	dialkyl dithiophosphate containing 9.3% P and 19.8% S or sulfurized olefin polysulfide
AW/EP	mixture of amine phosphates containing 4.8% P and 2.7% N
AW-mild	mixture of diamine monohexyl phosphate and amine dihexyl phosphate
AW	zinc dialkyldithiophosphate (ZDDP) or ZDDP-based anti-wear additive
FM	molybdenum dithiocarbamate (MoDTC)
FM+AW	molybdenum dithiocarbamate (MoDTC) + zinc dialkyldithiophosphate (ZDDP)
GMO	glycerol mono-oleate

1.1 Friction Results

1.1.1 Non-Doped DLC/Steel Contacts

Figure 3 shows the average coefficients of friction for a non-doped-DLC/steel contact lubricated with different oils and additives. In experiments involving only the base oils (without additives) the results with mineral and sunflower base oils generally have a higher friction (Fig. 3a) than the results with a polyalphaolefin (PAO) base oil (Fig. 3b). However, there is no significant difference in the friction between industrial base oils, i.e., mineral and sunflower base oils, while for the ester-type base oils (saturated or unsaturated) no results have been published so far.

Two types of additive effect can be seen in Figure 3, i.e., a friction increase and a friction decrease in comparison with base oils. Namely, the addition of AW/EP additives to mineral and sunflower oils generally caused an increase in the coefficient of friction. However, when the EP additives are added to base oils a decrease in the friction was observed for the sunflower oil, and an increase in the friction was observed for the mineral oil [46]. In both, the mineral and the sunflower base oils, the effect of the AW/EP additive was more pronounced than that of the EP additive. In one particular study [51], a decrease in the friction was observed when an anti-wear (ZDDP) additive was added to the mineral base oil, Figure 3a. However, the decrease was not as pronounced as one would expect from Figure 3a, because even with a base oil (in this particular study) the coefficient of friction was as low as 0.09 – i.e., much lower than the average of all the studies, as presented in the same diagram in Figure 3a. The decrease in the coefficient of friction in this case was about 0.02 during the running-in phase and about 0.01 for the steady-state value. When used in PAO base oil the AW additives (mild or strong) always increase the friction, although when a friction-modifier (FM) additive was present, the coefficient of friction decreased, Figure 3b.

The lowest coefficient of friction was found when using the formulated PAO (with the addition of MoDTC and ZDDP additives or with the GMO additive), while on the other hand, the highest levels of friction were obtained with the AW/EP formulated mineral and sunflower base oils.

In experiments with non-hydrogenated DLC coatings a generally lower friction was measured than with hydrogenated DLC coatings. All the friction data with non-hydrogenated DLC coatings

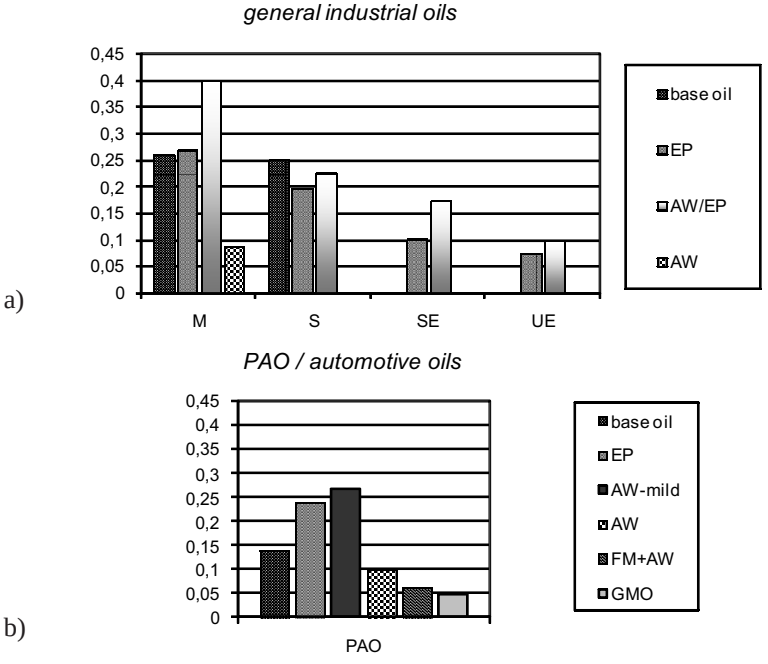

Fig. 3. *Average coefficient of friction for non-doped DLC/steel contact lubricated with (a) general industrial oils, and (b) PAO oils; with and without additives*

were lower than 0.1 – they were measured in (i) mineral oil with EP additives [50], (ii) PAO with MoDTC and ZDDP additives [43] and (iii) PAO with a GMO additive [20] and [44]. The lowest coefficient of friction (COF<0.05) among these was measured for the PAO with the GMO additive [44], which was also the lowest coefficient of friction found for a lubricated DLC/steel contact. With a-C:H coatings the coefficients of friction in the range 0.15 to 0.3 were measured using PAO with the EP or AW additives [52] and [53], and the amount of additive in the oil governed the friction behaviour. Sometimes an even higher friction was measured with the sunflower and mineral oils with the EP or AW/EP additives [46] and [49], which is also higher than in self-mated DLC/DLC contacts using the same oils and additives [58]. However, it should be made clear that these values are strongly test-dependent and are not just inherent contact properties.

1.1.2 Doped DLC/Steel Contacts

In Figure 4 the average friction is shown for doped DLC/steel contacts lubricated with different oils and additives. In tests with general industrial oils this friction was almost identical to the non-doped DLC coatings (Fig. 3). A similar situation could be inferred for the PAO/automotive oils. However, for the PAO oils a large scatter was calculated for the experiments with an EP additive. This is mostly the consequence of a substantial number of results reported for the EP additive with various concentrations mixed in base PAO oil in the contacts of W-DLC/steel, which, however, resulted in significantly different friction values. Namely, with some concentrations the friction increased, and with some it decreased [52] and [53]. This coating-lubricant combination (W-DLC/steel in contacts with EP additive) has also been studied for different test parameters, such as various temperatures, loads, sliding speeds, etc. [52], [53] and [55], and the EP additive was reported to have more influence on the friction than AW, particularly in the early stage of sliding. In some cases, when the EP additive was used, a significant reduction in the friction was reported after some period of sliding ("running-in"). Very similar results were reported for the mineral oils using the same additives [49], but the reduction of friction from the initial to the steady-state friction was found in

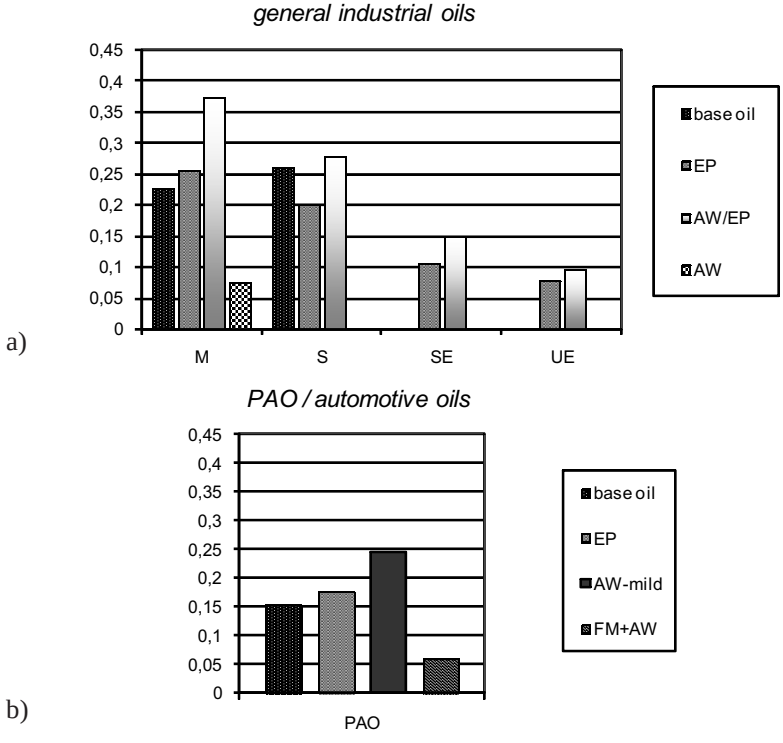

Fig. 4. *Average coefficient of friction for doped DLC/steel contact lubricated with (a) general industrial oils, and (b) PAO oils; with and without additives*

this case to be a consequence of coating removal and, therefore, the sliding of the steel ball over the Cr-interlayer (see Fig. 8), which resulted in a reduced friction [49]. In agreement with the latter conclusion, a complete removal of the coating (with some rare exceptions) was normally observed in these studies with additive concentrations lower than 2.5 % (typical conc. for formulations) – with mineral [49], but also with PAO oils [52], [53] and [55]. Therefore, this reduced friction was frequently found associated with excessive wear and coating removal, which is not a favourable tribological result for longer runs under such severe contact conditions.

From Figure 4a a decrease in the coefficient of friction with the use of the AW additive (ZDDP) in mineral oil [51] can be seen (last column at "M"). Si-DLC coatings were used in this particular study. It should be noted that the decrease was not so pronounced as it appears from this average value (single study), because even the base oil gave a rather low value compared to the average of many base-oil results that are encountered in the first column at "M". However, it is important to point out that the Si-DLC/steel contacts showed a larger decrease in friction than the non-doped DLC/steel combination. Furthermore, the friction decrease was shown to be dependent on the Si content in the coating – the highest Si/C ratio in the coating resulted in the greatest friction decrease when the AW additive was introduced into the base oil [51]. Another type of doped DLC coating that was investigated was the Ti-DLC coatings. The results showed that Ti-DLC coatings against steel result in the lowest friction and wear, even when tested with the PAO base oil only. This indicates that the interaction of the Ti-DLC with base oils is better and more protective than with other coatings. Namely, these results were even better than steel/steel, a-C:H/steel and a-C/steel [51], suggesting that this might be a promising coating/steel combination.

1.2 Wear Results

1.2.1 Non-Doped DLC/Steel Contacts

The interesting wear behaviour of non-doped DLC/steel contacts can be observed in Figure 5. A

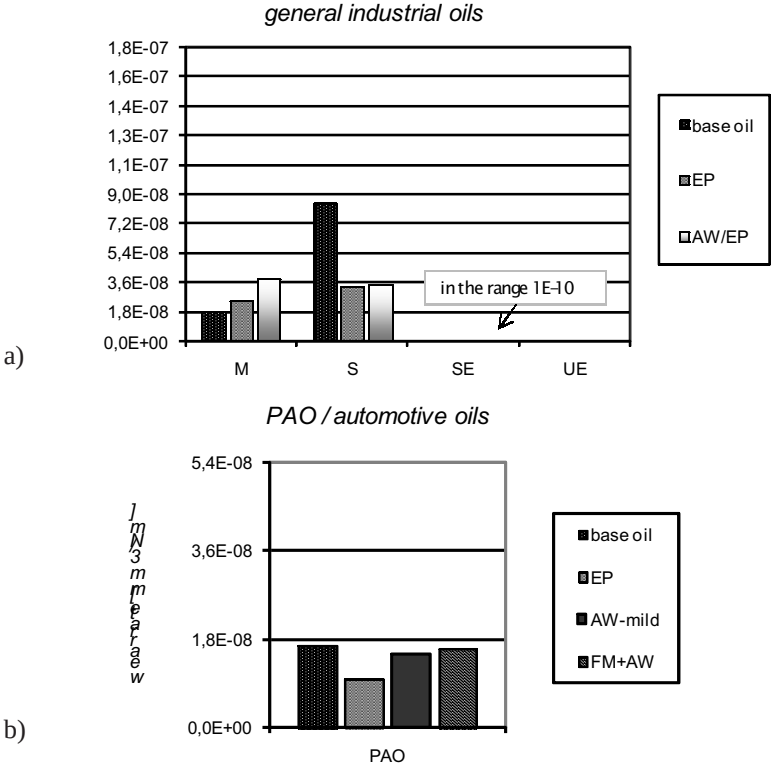

Fig. 5. *Average wear coefficient for non-doped DLC/steel contact lubricated with (a) general industrial oils, and (b) PAO oils; with and without additives*

huge difference in the wear rates can be seen for the general industrial oils, i.e., for the mineral and sunflower oils the wear was two orders of magnitude (100x) higher than that of the saturated and unsaturated esters, irrespective of whether additives were used or not. The wear rates in the PAO oils were generally slightly smaller, but in the same range as the mineral and sunflower base oils. Moreover, no significant effect of the additives was observed in the tests with PAO (Fig. 5b).

Two different responses were found for the a-C:H/steel contact with mineral and sunflower oils when additives were used. The inclusion of additives to mineral oil increased the wear of the steel ball and the highest wear was measured with the AW/EP additive. However, the inclusion of additives to the sunflower oil reduced the wear of the steel ball and the lowest wear was measured with the EP additive. Generally, the wear was slightly higher with the sunflower base oil than with the mineral base oil, which was also clearly visible from the SEM analysis of the worn surfaces that showed two different wear mechanisms for these oils [46]. Furthermore, when the AW/EP additive was used in mineral oil the sliding surface became soft and plastically deformed, while in sunflower oil the surface was brittle-like and contained small pits.

Another study was performed with a tungsten-carbide (WC) ball sliding against DLC. When the WC ball was tested against a non-hydrogenated (a-C) and hydrogenated (a-C:H) coating, and lubricated with a PAO-like oil (hydrogenated 1-decene homopolymer oil), the behaviour of the coatings was similar to that observed for the coatings tested in air, with only slightly lower wear of the coatings, indicating the positive influence of oil lubrication. The coating surfaces exhibited limited wear with a slight polishing-type wear, and with a specific wear rate of less than 6.4×10^{-9} mm^3/Nm [54].

1.2.2 Doped DLC/Steel Contacts

Most of results from Figure 6 require more discussion, as there are many specifics found in these studies, which affected the results. Namely, there are many more differences in the behaviour and more discrepancies in the results for doped

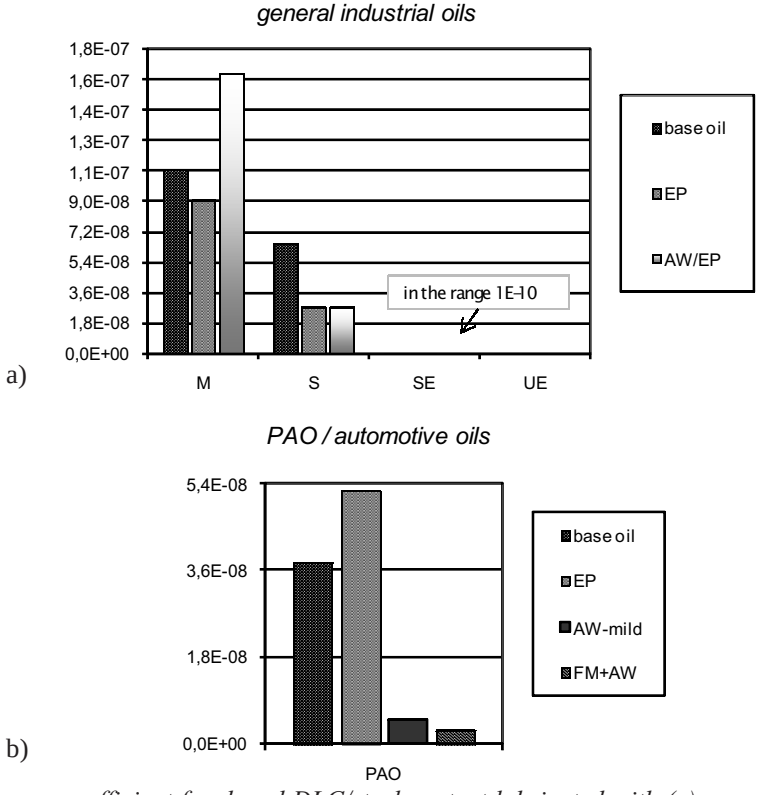

Fig. 6. *Average wear coefficient for doped DLC/steel contact lubricated with (a) general industrial oils, and (b) PAO oils; with and without additives*

DLC coatings against steel than can be seen from a diagram of the average values presented for several types of doped DLC coatings in Figure 6.

By using only mineral base oil, the W-DLC coating in contact with a steel counter-body suffered severe wear and was always worn through [46] and [49]. Other types of doped coatings (Ti-DLC, Si-DLC) showed better wear resistance, but the doped coatings always have higher wear, compared to non-doped coatings in contacts against steel, when tested with mineral base oil. When lubricated with sunflower base oil, the wear rate of these doped coatings was much lower, and this was true even for the W-DLC coating, where a three-times lower wear was measured for this combination. Moreover, with sunflower base oil, the wear of the W-DLC/steel was even smaller than that of the a-C:H/steel combination [46].

The additives generally reduced the wear of the doped DLC/steel contacts, Figure 6a. Most importantly, if the additives were successful in preventing the adhesion between the steel and the doped DLC, the wear was reduced compared to the wear with base oils, and was frequently lower than the non-doped DLC against steel (with additives). An exception was, however, found only for the W-DLC coating. Namely, the use of the AW/EP additive slightly reduced the wear of the W-DLC coating in the W-DLC/steel combination (still resulting in wearing out); however, the use of the EP additive resulted in higher wear. But, this case was unusual, because the coating was typically worn through and so severe adhesion could not be prevented. One of the reasons for this was explained in a study of mineral oils [49], where a clear formation of complex carbides, indicating the adhesion and dissolution of the WC (from the W-DLC) and the steel (from the ball counter-body) was found, as discussed and shown in Sections 1.3 and 1.4.

On the other hand, it was reported that when EP additives were used in PAO base oil, the additives improved the tribological behaviour of W-DLC/steel contacts, but this was strongly dependent on the concentration of the additive [52] and [53]. It was found that for concentrations from 0 to 1% of the EP additive, the W-DLC coating was removed from the surface. An increase in the EP additive concentration to the range from 2.5 % to 5 % gave excellent protection to the coated disc, almost eliminating its wear. However, at 10 % of EP in PAO oil, the effect of the additive was changed again; the friction increased and the surface layers became the same as with the steel/steel contacts, i.e., without any tungsten, but the wear was reported to remain very low. Presumably, the formation of a WS_2-containing layer is responsible for this beneficial effect, however, these results need to be further verified. Namely, the formation of WS_2 was found only for 0.5 % of the EP additive, for which the sliding actually led to a worn through coating [52]. Therefore, this explanation of a protective WS-type layer seems questionable and may even be used to support the opposing view, i.e., explaining how the coating was worn out due to the consumption of W from the coating at this low EP concentration. Moreover, the latter suggestion is in agreement with the high wear at 0.5 and 1 % of EP additive and another high-wear mechanism, i.e. the formation of complex carbides $W_{6"x}Fe_xC$ that were found in another similar study with 1 % of EP [49], and together they provide a reasonable explanation for such high wear and the wearing out of this coating in those severe boundary-lubricated conditions [49], [52] and [53].

When using PAO oil with MoDTC and ZDDP additives (i.e., FM+AW), the Ti-DLC/steel contacts showed very little wear, which can be seen in the results in the last column of Figure 6b [43]. Moreover, with the PAO base oil the wear of the steel counter body in the Ti-DLC/steel contacts was smaller than for the a-C:H/steel or a-C/steel combinations [43].

The wear was generally lower when both contact surfaces were coated with doped DLC [59] than when only one counter-body was coated, which was observed for different doped coatings in mineral oils [46] and [49], as well as for the Ti-DLC coating lubricated with additivated PAO [43]. Of course, this depends on the loads, the roughness, etc., and the amount of wear on the steel and the coated samples has to be evaluated separately. But, it should be noted that even if the coated surface tends to wear much less than the steel, the amount of wear on the steel side must also be evaluated, because steel is much softer than DLC coatings and thus it may became a critical part of the contact through various wear mechanisms (adhesion, abrasion, etc.) and sometimes even become unacceptable for the application.

1.3 DLC–Base-Oil Interactions

1.3.1 Non-Doped DLC/Steel Contacts

When experiments with PAO oils were considered, it was clear that the friction in non-doped DLC/steel contacts was higher, while the wear was lower than in self-mated non-doped DLC/DLC contacts. Among the non-doped DLC coatings in these DLC/steel contacts (with the base oil only), a higher coefficient of friction was measured with the hydrogenated a-C:H coating than with the non-hydrogenated a-C coating. But this was just the opposite to experiments with PAO that contained FM and AW additives (MoDTC and ZDDP) [43], where lower friction was found for the a-C:H coating than for the a-C coating. The wear in the contacts of the non-hydrogenated a-C coatings was, however, higher than the wear with the hydrogenated a-C:H coatings.

In agreement with this, in studies where mineral oils were used, almost no signs of wear could be found on the surfaces of the non-doped DLC. The major reason for this was the absence of any adhesion or transfer layers in these contacts [49], which is, however, the major difference in comparison to doped DLC coatings.

In some studies [20], [43] and [44] the coefficient of friction was much lower when using PAO base oil than when a mineral base oil was used [46], [49] and [50]. This discrepancy was so large that it hardly seems possible that it is a natural characteristic of the PAO base oil compared to the mineral oil. In order to evaluate this difference in the coefficient of friction, several additional tribological tests were conducted in our laboratory, including performing the tests with the PAO and a paraffin mineral base oil under exactly the same conditions: using the same tester and the same operating parameters. As can be seen from Figure 7, the results with the PAO and the mineral base oil were shown to be very close to each other, and this was true for non-doped and doped coatings, indicating that differences in literature, summarized

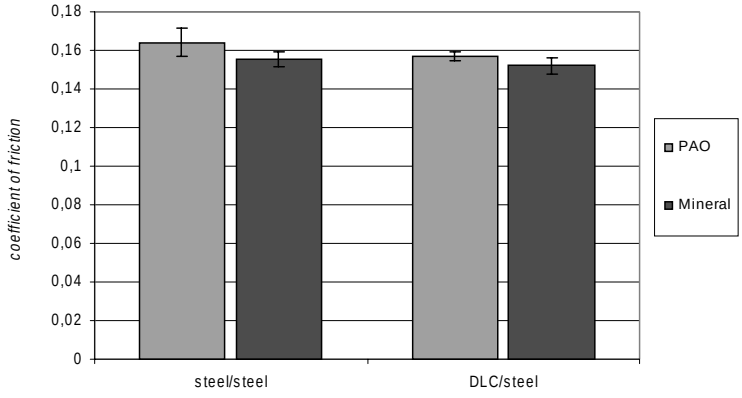

Fig. 7. *Coefficient of friction for steel/steel and DLC/steel contacts lubricated with PAO and mineral base oil*

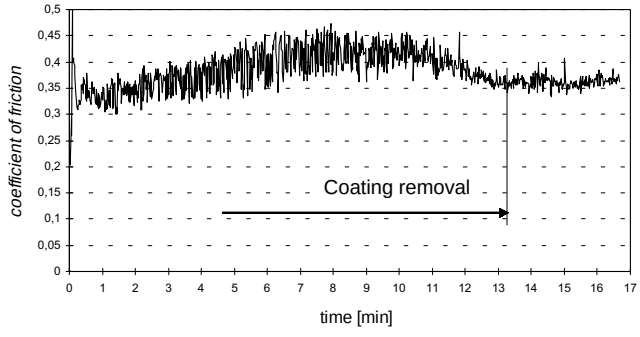

Fig. 8. *Coefficient of friction for W-DLC/steel contacts lubricated with a mineral base oil*

in Figure 3 and Figure 4, are most probably the consequence of different testing parameters and testing equipment used in different studies.

1.3.2 Doped DLC/Steel Contacts

The most distinctive and studied contact of doped DLC coatings against steel in the presence of PAO base oils was the W-DLC coating. Generally, positive results with regard to friction are reported; however, these are somewhat contradictory compared to the wear behaviour. Namely, when sliding a steel ball against a W-DLC coated surface in PAO base oil, the transfer of the coating material from the W-DLC coated disc to the steel ball was observed. A transfer layer with WC particles was formed on the contact surface of the steel ball, which was reported to be responsible for the reduction of friction as compared to the steel/steel combination [52]. However, at the same time, the wear is high, obviously because of the transfer of the coating material. Thus, wearing through of the coating was reported. It is said that localized de-cohesion within the coating was followed by gradual wear, and eventually led to local exposure of the substrate [52]. This actually means that the coating was removed, although the friction was reduced.

Similarly, in another study of W-DLC/steel using mineral oil instead of PAO the coating was also always worn out [49]. Moreover, regarding the reduced friction, which also occurred after a certain sliding distance, it was shown that this friction reduction was measured at a time when the coating was worn through and the Cr interlayer was reached, thus leading to sliding between the steel and the Cr layer, which resulted in this friction reduction. This behaviour for the EP-added oil is presented in detail in [49], while Figure 8 shows very similar behaviour for the mineral base oil only. This finding seems to agree with the above observations of the PAO base oil reported in [52] and others. Moreover, in this comprehensive analysis using mineral oil [49], it was found that transfer and adhesion typically occur between the metal-doped DLC and the steel surfaces in the presence of a base oil only. This was obviously the case for both the Ti-DLC and the W-DLC. Furthermore, in the case of W-DLC/steel contacts, adhesion and substantial transfer layers were observed (Fig. 9a), including the formation of complex carbides (η-phase) $W_{6-x}Fe_xC$ in the form of dendrites (Fig. 9b). Thus, if adhesion is not prevented, the wear between the steel and the metal-doped DLC coatings could be very high. Accordingly, appropriate additives are obviously required for a reduced adhesion and the improved wear performance of these contacts.

Moreover, from a study comparing the tribological behaviour of W-DLC, Ti-DLC and Si-DLC coatings in contact with a steel counter-body [49] different wear mechanisms were found for the non-metal (Si) doped and metal (W, Ti) doped DLC coatings in contact with steel. Figure 10a shows an overview of a metal-doped Ti-DLC disk surface tested against a steel ball with mineral base oil without any additive. A relatively thick layer of adhered debris covered almost the whole wear surface, as seen from the corresponding EDS spectra

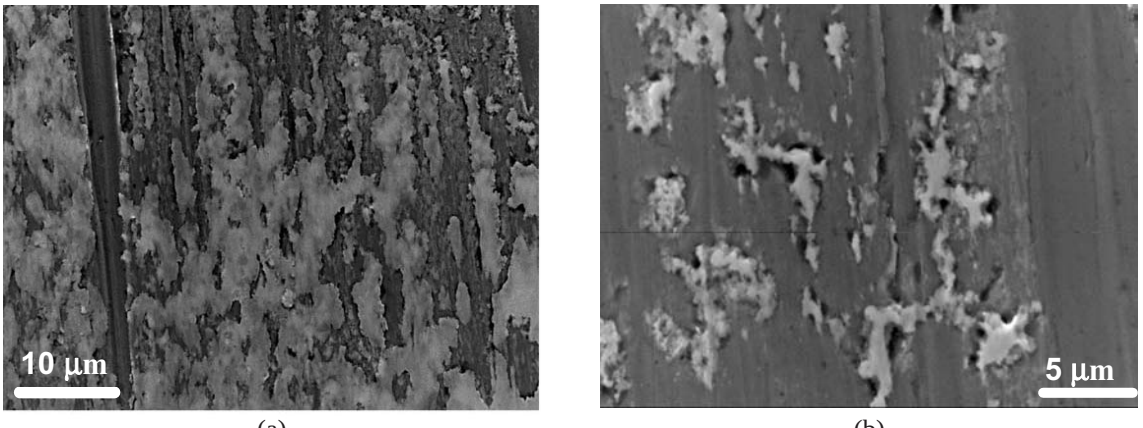

(a) (b)

Fig. 9. *(a) Transfer of the doped W-DLC coating to the steel ball and (b) formation of complex carbides; i.e. dendrites*

in Figure 10b, while the transferred wear debris from the Ti-DLC were found on the steel balls. However, with additives in the oil, the adhesion of the Ti-DLC was successfully prevented, as seen from very limited material transfer in Figure 10c.

In contrast to the typical adhesion-based wear mechanisms found for metal-doped coatings (W-DLC and Ti-DLC), a non-metal-doped coating (Si-DLC) tested in mineral base oil against a steel counter body showed different wear behaviour, Figure 11. The amount of adhesion, even when using only base oil without additives, was negligible (Fig. 11a) compared to the Ti-DLC and W-DLC coatings. This suggests a limited chemical compatibility of the Si-DLC coatings with the steel surfaces, indicating that they are more like the non-doped DLC coatings than the metal-doped coatings. The observations of the ball surfaces were in agreement with the disc surfaces, as no sign of any transfer of the Si-DLC wear debris was found. The surfaces were mechanically damaged, showing poor lubricant protection, but no adhesion was present. Furthermore, when additives were added to the base oil, the surfaces changed their appearance, indicating that a thin and apparently soft layer formed on the Si-DLC surface, which might suggest that an interaction occurred between the additive, the steel and the coating, Figure 11b.

From this study [49] it is clear that in contrast to the non-metal-doped DLC coatings (Si-DLC), the metal-doped coatings (Ti-DLC and W-DLC) in contact with steel always experienced severe adhesive wear and mutual wear debris transfer if a mineral base oil without additives was used. Therefore, metal elements most probably induce metal-like behaviour of the metal-doped coatings, while the non-metal-doped coatings behave more like non-doped DLC coatings, which was also noted for self-mated DLC/DLC contacts [59]. On the other hand, the addition of EP additives was very successful on Ti-DLC, but this was not the case for W-DLC.

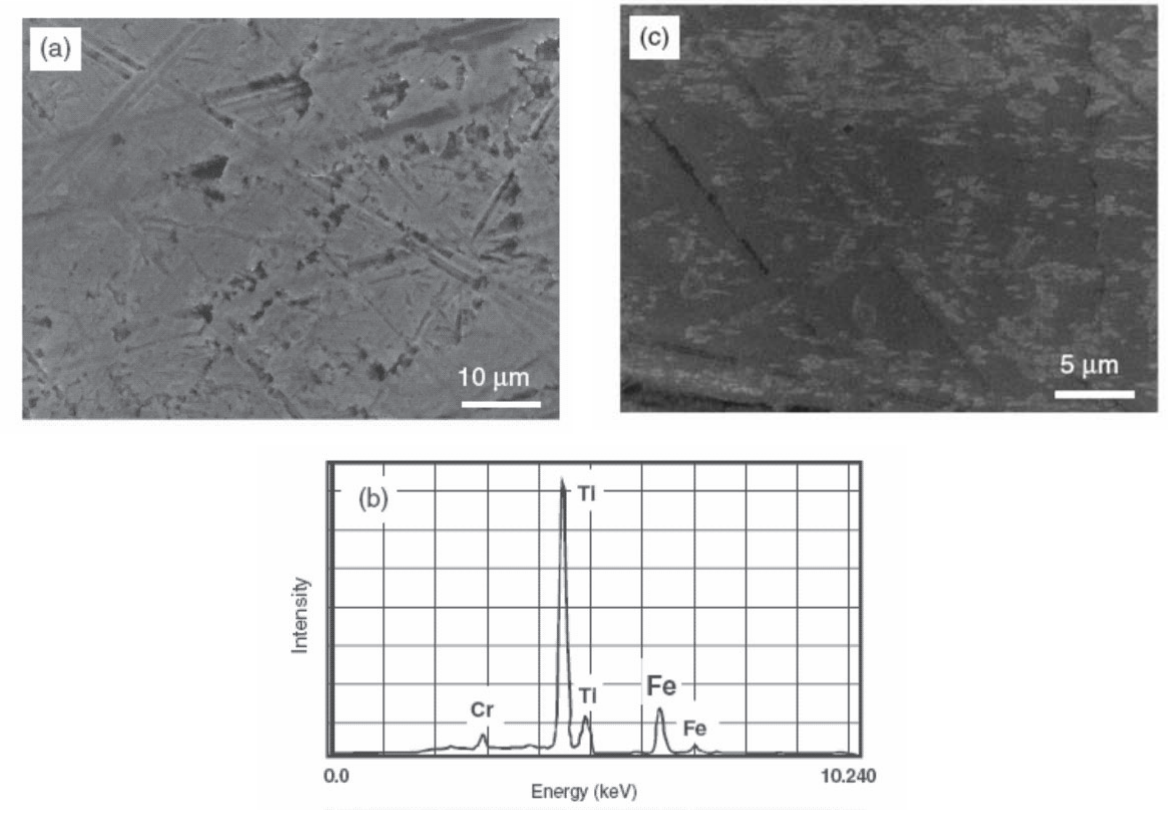

Fig. 10. *(a) SEM image of the Ti-DLC worn disc surface tested with mineral base oil and (c) mineral base oil with AW/EP additive. The figure in (b) corresponds to the EDS spectra of the layer from the figure in (a).*

1.4 DLC-Additive Interactions

1.4.1 Non-doped DLC/Steel Contacts

In a study of non-doped DLC coatings lubricated with mineral or sunflower oil containing the AW/EP additive no signs of tribofilm formation could be found on the worn DLC-coated surfaces using EDS analysis [46]. However, P-peaks were observed in the EDS spectra from the steel counter-body, indicating the formation of a tribofilm on the steel side of the contact, but not on the coating itself. Generally, the sunflower base oil showed less friction than the mineral base oil, and thus the effect due to the use of additives was also relatively smaller, while remaining distinct. The use of EP additives, however, always resulted in increased friction for both the sunflower base oil and the mineral base oil [46].

When the PAO base oil was used, with or without MoDTC (FM) and ZDDP (AW) additives, the hydrogenated a-C:H coating produced less friction than the non-hydrogenated a-C coating [43] in a contact with the steel counter-body. This positive effect of the hydrogen content on the lubrication properties of the DLC coating is similar to that observed in self-mated contacts with the same lubricants. Table 3 shows the elemental composition of the tribofilms formed in the contacts lubricated with the PAO oil containing the MoDTC and ZDDP additives, which formed on the hydrogenated a-C:H and non-hydrogenated a-C coatings after sliding in contact with a steel counter-body [43]. From the analyses it was found that the Mo3d (Mo(IV)) peak corresponds to MoS_2 and the Mo3d (Mo(VI)) peak corresponds to MoO_3. This shows that the MoS_2/MoO_3 ratio for the hydrogenated a-C:H coating is much higher than that of the non-hydrogenated a-C coating, which indicates the higher reactivity of these oils with hydrogenated DLC than with non-hydrogenated DLC. However, no significant effect of the steel counter-body on the chemical composition of the tribochemical layer was detected in this study.

In contrast to the above discussion on the effect of the hydrogen content in the presence of PAO with MoDTC and ZDDP additives, just the opposite behaviour can be concluded for the GMO additive. Namely, ultra-low friction was found with the non-hydrogenated ta-C coatings sliding against steel, when lubricated with PAO containing GMO [20,44], while with the hydrogenated DLC, the friction increased significantly. This difference in the friction behaviour due to hydrogen content in the DLC coating with different additives is schematically presented in Figure 12.

1.4.2 Doped DLC/Steel Contacts

In a study of sliding the steel ball against W-DLC-coated disks using PAO oil containing the EP additive, a tribofilm composed of the coating material (W and C) and sulphur (S) was formed on the steel surfaces (only) with EP concentrations from 0.5 to 5 %. Moreover, under a specific concentration of 0.5 % of EP additive, the WS_2 species were found using XPS analyses [52] and [55]. From "conventional" boundary-lubrication

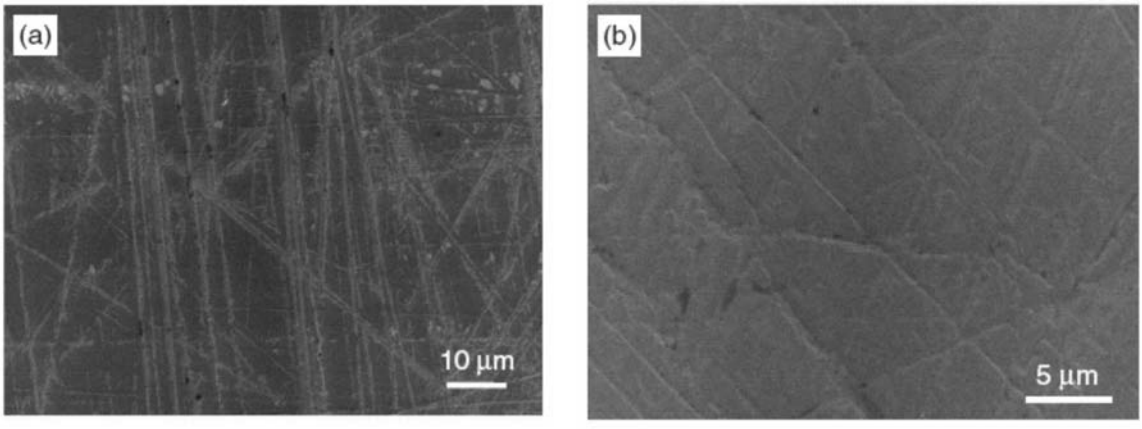

Fig. 11. *(a) SEM image of Si-DLC worn disc surface tested in mineral base oil and (b) mineral base oil with AW/EP additive*

Table 3. *Elemental composition (at. %) of tribofilms formed on a-C:H and a-C coating surfaces from DLC/steel contact using PAO with a mixture of MoDTC and ZDDP additives [43]*

Elements	Energy (eV)	Elemental composition (%)	
		a-C:H	a-C
C1s	284.8-285.5-287.6	94.6	92.4
O1s	531.0-532.8	3.1	5.2
S2p (sulphide)	162	0.8	0.9
Mo3d (Mo(IV))	229	0.4	0.4
Mo3d (Mo(VI))	232	0.1	0.9
P2p	133.2	≈ 0	≈ 0
Zn2p	10232.4	1.0	0.2

The data were obtained after the treatment of the XPS spectra.

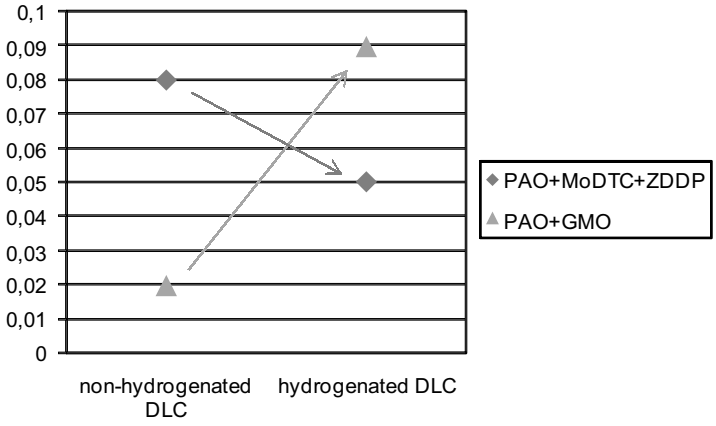

Fig. 12. *Effect of hydrogen content in the DLC coating on the friction coefficient using PAO oil containing (i) MoDTC and ZDDP and (ii) GMO additive. Schematic is designed from the data in [20], [43] and [44].*

practice it is known that the friction-reduction mechanism of the widely used MoDTC is based on the formation of nano-metric MoS_2 layers on the contact surfaces. Due to the fact that molybdenum (Mo) and tungsten (W) are chemically similar elements, it was proposed, based on the HSAB principle, that W transferred from the W-DLC coating to the steel counter-body, and in combination with the S-based EP additive, formed a lamellar WS_2-type tribofilm on the steel surface, which was further assumed to have similar tribological characteristics to that of MoS_2. Therefore, it was suggested that the tribofilm that contained the WS structures is similar to the MoS_2 films, and therefore it caused friction and wear reduction in the contacts lubricated with PAO oil containing from 2.5 % to 10 % of EP additive [52] and [55].

However, as discussed earlier, the explanation of the beneficial effect of a WS_2 layer appears questionable, because the WS_2 species were found by XPS only at 0.5 % of the EP additive (not at 2.5–10%), for which the sliding actually led to wearing out and removal of the coating [52] and [55]. Actually, this XPS evidence may suggest the opposite mechanism, i.e., how the coating was worn out so quickly at 0.5 % of EP, which occurred also at 1 % of EP, through the consumption of W from the coating. Thus, the only effect of WS_2 that was actually confirmed (at 0.5 % EP) is negative - not beneficial, because the coating was worn through and the friction was high at those conditions. Therefore, this result contradicts the explanation of the positive effect of using 2.5 to 10 % of EP, where low wear and friction were found, but the detailed chemical composition of the layer remained unknown. Therefore, it is not clear whether the same WS species, i.e. WS_2, are formed at concentrations of 2.5, 5 and 10 % of EP. What is more, at 10 % of EP, no W at all was found in the tribofilm that was, however, still rich in sulphur (the same as with the steel/steel contacts), but the

wear was equally low as with 2.5 % or 5 % of EP [52]. Obviously, at 10 % of EP the mechanism for low wear and friction was not the same as with lower EP concentrations.

Furthermore, the lowest friction in that study was found for 2.5 % of EP, providing value of about 0.145, which is around 36 % lower than for PAO base oil (0.23). However, at 1 % of EP, where the coating was worn-through and removed, the friction of about 0.16 was measured, which is about 30 % lower compared to PAO base oil. Moreover, at 5 % and 10 % of EP, where the best tribological performance was reported, the friction was about 0.165 and 1.175 respectively, which is even higher than at 1 % of EP where coating was removed during steady state [52]. This shows that almost equally low or even lower steady-state friction as with optimal conditions at 2.5 % of EP can be maintained at very high wear rates even without the presence of the W-DLC coating (at 1 % of EP), or without W-containing tribofilm (at 10 % of EP). This conclusion agrees with another study of the same contact lubricated with paraffin mineral oil, where reduced steady-state friction was found as a consequence of W-DLC coating removal and sliding of steel ball over the Cr interlayer, as shown for 1 % of the same EP additive [49], as well as for the base oil only, see Figure 8.

Accordingly, three regions were identified with different wear behaviours depending on the EP concentration (0.5 to 1, 2.5 to 5 and 10 % of EP), while friction behaviour seems to be even more complex, suggesting that they cannot be governed by a single surface mechanism. Therefore, from the above discussion it follows to be very unlikely that the formation of the WS_2 layer could be the reason for the low wear (and friction) observed under the conditions of 2.5 to 10 % of EP in the oil, as suggested in [52] and [55]. On the other hand, the formation of complex carbides $W_{6"x}Fe_xC$ was found with the same contacts using 1 % of EP additive [49], which confirms the well-known high chemical compatibility and instability (dissolution) of the W–Fe–C system, which supports those results and provides a reasonable explanation for such high wear and wearing out of the coating that was typically found in all these studies [49], [52] and [55] – at concentrations lower than 2.5 % of EP, which is, however, already a very high concentration for any oil EP formulation. The W-DLC coating lubrication and interactions with additives, including the conditions to prevent its adhesion/dissolution with steel therefore need to be further clarified, but it seems obvious that the long-term performance of the W-DLC/steel contacts cannot be improved using the presently proposed mechanism with typical EP concentrations (around 1 %) if the coating has to be worn at such a high rate to provide "protective" and/or low-friction films. Moreover, in a thesis, where these tribofilms were in-depth investigated and analysed [60], it was concluded that to facilitate a long life of W-DLC coating in contacts with steel, more suitable S-based additives, and a process as well as the coating composition that allows deposition of thick coatings, are required because of the continuous high consumption of the coating and additive.

A very recent study [61] shows that similar metal-like adhesion behaviour of doped-DLC

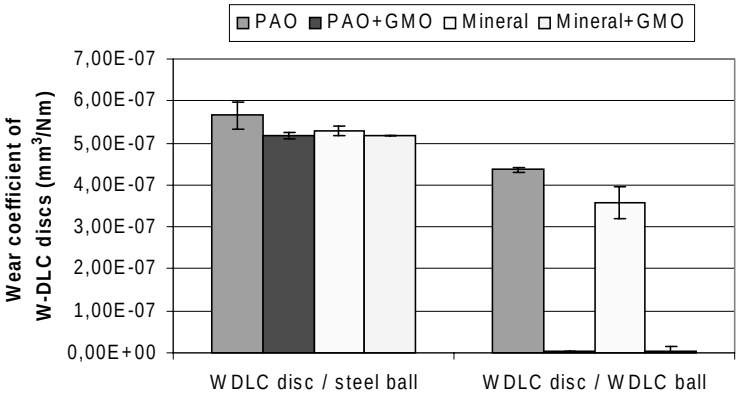

Fig. 13. *Wear of the W-DLC discs in W-DLC/steel and W-DLC/W-DLC contacts when tested with PAO and mineral oil, with and without GMO friction modifier*

against steel is obtained also with friction modifiers, such as GMO. Although GMO greatly improved the wear behaviour of W-DLC/W-DLC contacts, i.e. practically eliminated the wear of balls and discs, both in PAO and mineral oil, the wear of W-DLC/steel contacts was almost the same irrespective whether GMO was used or not, Figure 13. In a self-mated contact of Ti-DLC/Ti-DLC with another friction modifier, i.e. MoDTC, improved tribological behaviour was also found [43]. This shows that despite the obvious interactions of additives with metal-doped coatings [43], [45] and [59] and usually observed improvements, high chemical compatibility between these coatings (especially W-DLC) and steel is a critical parameter that determines their adhesion and wear, if the additives are not successful enough, as already suggested earlier [49].

2 DISCUSSION

Different friction and wear behaviours were observed depending on the different DLC-lubricant combinations presented in this paper (Fig. 2). In most reported studies the additives significantly affected the wear and friction of the boundary-lubricated DLC contacts; however, the extent of the change depends on the type of oils, the additives, coatings, etc. Different behaviours were observed for non-doped and doped coatings. Generally, it is suggested that metals, and possibly also other doping elements, provide sites for the coating-lubricant interactions in accordance with conventional metal-lubrication theories [39] to [41]. Such behaviour could be observed for Ti-DLC coatings, as well as for W-DLC coatings [49], [52] and [55]. However, this is not always plausible and can lead to severe wear if the adhesion between the doping elements and the steel counter-body is not prevented. Thus, appropriate additives need to be used or developed, but this challenge still remains for the future. Nevertheless, all these results confirm that in some cases even today's additives are relatively successful, which supports earlier findings on the reactivity between the DLC coatings and the additives [42] to [44]. The chemical structure of the coating seems to play the key role in the boundary-lubrication mechanisms of DLC/steel contacts as the differences between various, primarily doped, coatings are very large. However, also for the non-doped coatings, it is clear that the hydrogen content in the coating material, as well as the molecular structure of the base oil and the additives, play the key role in achieving the positive lubricating effect of the non-doped-DLC-–oil combinations. Finally, the contact conditions, especially the contact temperature need to be considered in much more in detail [62], as this can vary a lot in the temperature values [62] and [63] and the DLC response [42].

Several consistent trends and tribological behaviours were identified in this paper; however, some clear inconsistencies and discrepancies were also found. The main problem is that verified lubrication mechanisms that would indisputably explain certain behaviour are to a large extent missing. Accordingly, it is obvious that more results and more in-detail studies are required to better understanding DLC-coating/steel contacts, but the most obvious findings from the present analyses are summarized in the following section.

3 CONCLUSIONS

- Steel counter-bodies and their reactivity with oils and additives have an important effect on the friction in all the DLC/steel contacts. This is the reason for approximately the same friction values being measured for the doped and non-doped coatings under the same conditions.
- The addition of the AW/EP additive to the mineral base oil usually increases the friction. In contrast, the addition of the EP additive and friction modifier (GMO) to the mineral base oil decreased the friction.
- Non-hydrogenated DLC coatings typically have a lower friction than hydrogenated DLC coatings.
- With respect to the different oils, significantly lower friction was measured with PAO oils than mineral or other industrial oils, but this seems to be test-dependent rather than a property of the base oil (in combination with particular DLC coating).
- The lowest friction in the DLC/steel contacts was measured when friction modifiers were used.
- The wear of metal-doped DLC coatings is typically higher than that of non-doped DLC coatings, which is even more pronounced if the additive's efficiency is lower, and particularly with base oils.

- The wear of metal-doped-DLC/steel contacts strongly depends on the efficiency of the additives. If the additive protection is successful, wear can be reduced, otherwise the wear is very high due to the strong adhesion between the steel and the metal-doped DLC. Non-metal-doped DLC coatings appear to have a different wear behaviour compared to the metal-doped DLC coatings.
- The metal elements in DLC coatings most probably induce their metal-like behaviour, while the non-metal-doped coatings behave more like non-doped DLC coatings.
- For the performance of doped-DLC/steel contacts, it is clear that there is an important positive effect from additives possible, but it varies depending on the type of additives and coatings. Potential lubrication mechanisms remain uncertain due to inconsistencies and discrepancies in reported results. Presently suggested mechanisms for W-DLC coatings with EP additives are not appropriate for improved tribological performance due to high additive and coating consumption, i.e. wear.
- The hydrogen content in non-doped DLC coatings significantly affects their tribological performance. However, different friction behaviours were observed for different friction modifiers, depending on the hydrogen content. Some plausible mechanisms have already been proposed in the literature.

4 REFERENCES

[1] Erdemir A. Diamond-like Carbon Films, In: J.Vižintin, M. Kalin, K. Dohda, S. Jahanmir (Eds.), *Tribology of mechanical systems: a guide to present and future technologies*, ASME Press, New York, 2004. p. 139-156.

[2] Grill A. Diamond-like carbon: state of the art, *Diamond and Related Materials*, 8 (1999) 428-434.

[3] Donnet C., Grill A. Friction control of diamond-like carbon coatings, *Surface and Coatings Technology* 94-95 (1997) 456-462.

[4] Matthews A., Leyland A., Holmberg K., Ronkainen H. Design aspects for advanced tribological surface coatings, *Surface and Coatings Technology* 100-101 (1998) 1-6.

[5] Erdemir A., Fenske G.R., Terry J., Wilbur P. Effect of source gas and deposition method on friction and wear performance of diamondlike carbon films, *Surface and Coatings Technology* 94-95 (1997) 525-530.

[6] Fontaine J., Donnet C., Grill A., Mogne T.L. Tribochemistry between hydrogen and diamond-like carbon films, *Surface and Coatings Technology* 146-147 (2001) 286-291.

[7] Andersson J., Erck R.A., Erdemir A. Friction of diamond-like carbon films in different atmospheres, *Wear* 254 (2003) 1070-1075.

[8] Robertson J. Deposition and properties of diamond-like carbon, *Material Research Society Symposium Proceedings*, 555 (1999) p. 12.

[9] Erdemir A. The role of hydrogen in tribological properties of diamond-like carbon films, *Surface and Coatings Technology*, 146-147 (2001) 292-297.

[10] Neville S., Matthews A. A perspective on the optimisation of hard carbon and related coatings for engineering applications, *Thin Solid Films*, 515 (2007) 6619-6653.

[11] Ronkainen H., Varjus S., Koskinen J., Holmberg K. Differentiating the tribological performance of hydrogenated and hydrogen-free DLC coatings, *Wear*, 249 (2001) 260-266.

[12] Kano M., Tanimoto I. Wear mechanism of high wear-resistant materials for automotive valve trains, *Wear*, 151 (1991) 229-243.

[13] Cruz R., Rao J., Rose T., Lawson K., Nicholls J.R. DLC–ceramic multilayers for automotive applications, *Diamond and Related Materials*, 15 (2006) 2055-2060.

[14] Franklin S.E., Baranowska J. Conditions affecting the sliding tribological performance of selected coatings for high vacuum bearing applications, *Wear* 263 (2007) 1300-1305.

[15] Vanhulsel A., Velasco F., Jacobs R., Eersels L., Havermans D., Roberts E.W., Sherrington I., Anderson M.J., Gaillard L. DLC solid lubricant coatings on ball bearings for space applications, *Tribology International* 40 (2007) 1186-1194.

[16] Jiang J.C., Meng W.J., Evans A.G., Cooper C.V. Structure and mechanics of W-DLC coated spur gears, *Surface and Coatings Technology* 176 (2003) 50-56.

[17] Kalin M., Vižintin J. The tribological performance of DLC-coated gears lubricated with biodegradable oil in various pinion/gear material combinations, *Wear* 259 (2005) 1270-1280.

[18] Tung S.C., McMillian M.L. Automotive tribology overview of current advances and challenges for the future, *Tribology International* 37 (2004) 517-536.
[19] Etsion I., Halperin G., Becker E. The effect of various surface treatments on piston pin scuffing resistance, *Wear* 261 (2006) 785-791.
[20] Kano M. Super low friction of DLC applied to engine cam follower lubricated with ester-containing oil, *Tribology International* 39 (2006) 1682-1685.
[21] Hershberger J., Ozturk O., Ajayi J.B., Woodford J.B., Erdemir A., Erck R.A., Fenske G.R. Evaluation of DLC coatings for spark-ignited direct-injected fuel systems, *Surface and Coatings Technology* 179 (2004) 237-244.
[22] Dai M., Zhou K., Yuan Z, Ding Q. and Fu Z. The cutting performance of diamond and DLC-coated cutting tools, *Diamond and Related Materials*, 9 (2000) 1753-1757.
[23] Sato T., Besshi T., Tsutsui I., Morimoto T. Anti-galling property of a diamond-like carbon coated tool in aluminium sheet forming, *Journal of Materials Processing Technology* 104 (2000) 21-24.
[24] Kalin M., Majdič F., Vižintin J., Pezdirnik J., Velkavrh I. Analyses of the long-term performance and tribological behaviour of an axial piston pump using diamondlike-carbon-coated piston shoes and biodegradable oil, *Journal of Tribology* 130 (2008) 011013 p. 1-8.
[25] Sheeja D., Tay B.K., Nung L.N. Feasibility of diamond-like carbon coatings for orthopaedic applications, *Diamond and Related Materials* 13 (2004) 184-190.
[26] Shi B., Ajayi O.O., Fenske G., Erdemir A., Liang H. Tribological performance of some alternative bearing materials for artificial joints, *Wear* 255 (2003) 1015-1021.
[27] Tan A.H. Corrosion and tribological properties of ultra-thin DLC films with different nitrogen contents in magnetic recording media, *Diamond and Related Materials* 16 (2007) 467-472.
[28] Zhao X., Bhushan B. Comparison studies on degradation mechanisms of perfluoro-polyether lubricants and model lubricants, *Tribology International* 9 (2000) 187-197.
[29] Gatzen H.H., Beck M. Tribological investigations on micromachined silicon sliders, *Tribology International*, 36 (2003) 279-283.
[30] Numata T., Nanao H., Mori S., Miyake S. Chemical analysis of wear tracks on magnetic disks by TOF-SIMS, *Tribology International* 36 (2003) 305-309.
[31] Gahlin R., Larsson M., Hedenqvist P. ME-C:H coatings in motor vehicles, *Wear* 249 (2001) 302-309.
[32] Haque T., Morina A., Neville A., Kapadia R., Arrowsmith S. Non-ferrous coating/lubricant interactions in tribological contacts: Assessment of tribofilms, Tribology International 40 (2007) 1603-1612.
[33] Dahotre N.B., Nayak S., Nanocoatings for engine application, *Surface and Coatings Technology*, 194 (2005) 58-67.
[34] Erdemir A. Review of engineered tribological interfaces for improved boundary lubrication, *Tribology International* 38 (2005) 249-256.
[35] Hsu S.M., Gates R.S. Boundary lubricating films: formation and lubrication mechanism, *Tribology International* 38 (2005) 305-312.
[36] Neville A., Morina A., Haque T., Voong M., Compatibility between tribological surfaces and lubricant additives—How friction and wear reduction can be controlled by surface/lube synergies, *Tribology International* 40 (2007) 1680–1695.
[37] Sanchez-Lopez J.C., Erdemir A., Donnet C., Rojas T.C. Friction-induced structural transformations of diamondlike carbon coatings under various atmospheres, *Surface and Coatings Technology*, 163-164 (2003) 444-450.
[38] Grischke M., Hieke A., Morgenweck F., Dimigen H. Variation of the wettability of DLC-coatings by network modification using silicon and oxygen, *Diamond and Related Materials*, 7 (1998) 454-458.
[39] Mortier R.M., Orszulik S.T. *Chemistry and technology of lubricants,* Blackie Academic & Professional, Glasgow, 2nd ed., 1993.
[40] Dorinson A., Ludema K.C. *Mechanics and chemistry in lubrication, Tribology Series, vol. 9*, Elsevier, Amsterdam, 1985.
[41] Pawlak Z. *Tribochemistry of lubricating oils, Tribology and interface engineering series, vol. 45*, Elsevier, Amsterdam, 2003.
[42] Kalin M., Roman E., Vižintin J. The effect of temperature on the tribological mechanisms and reactivity of hydrogenated, amorphous diamond-like carbon coatings under oil-

lubricated conditions, *Thin Solid Films* 515 (2007) 3644-3652.

[43] De Barros'Bouchet M.I., Martin J.M., Le-Mogne T., Vacher B. Boundary lubrication mechanisms of carbon coatings by MoDTC and ZDDP additives, *Tribology International*, 38 (2005) 257-264.

[44] Kano M., Yasuda Y., Okamoto Y., Mabuchi Y., Hamada T., Ueno T., Ye J., Konishi S., Takeshima S., Martin J.M., De Barros Bouchet M.I., Le Mogne T. Ultralow friction of DLC in presence of glycerol mono-oleate (GMO), *Tribology Letters*, 18 (2005) 245-251.

[45] Kalin M., Velkavrh I., Vižintin J. Review of boundary lubrication mechanisms of DLC coatings used in mechanical applications, *Meccanica* (In Press).

[46] Kalin M., Vižintin J. A comparison of the tribological behaviour of steel/steel, steel/DLC and DLC/DLC contacts when lubricated with mineral and biodegradable oils, *Wear*, 261 (2006) 22-31.

[47] Kalin M., Vižintin J. The tribological performance of DLC coatings under oil-lubricated fretting conditions, *Tribology International*, 39 (2006) 1060 – 1067.

[48] Vercammen K., Van Acker K., Vanhulsel A., Barriga J., Arnšek A., Kalin M., Meneve J. Tribological behaviour of DLC coatings in combination with biodegradable lubricants, *Tribology International*, 37 (2004) 983-989.

[49] Kalin M., Vižintin J. Differences in the tribological mechanisms when using non-doped, metal-doped (Ti, WC), and non-metal-doped (Si) diamond-like carbon against steel under boundary lubrication with and without oil additives, *Thin Solid Films*, 515 (2006) 2734-2747.

[50] Ronkainen H., Varjus S., Holmberg K. Friction and wear properties in dry, water- and oil-lubricated DLC against alumina and DLC against steel contacts, *Wear*, 222 (1998) 120-128.

[51] Ban M., Ryoji M., Fujii S., Fujioka J. Tribological characteristics of Si-containing diamond-like carbon films under oil-lubrication, *Wear* 253 (2002) 331-338.

[52] Podgornik B., Hren D., Vižintin J. Low-friction behaviour of boundary-lubricated diamond carbon coatings containing tungsten, *Thin Solid Films*, 476 (2005) 92-100.

[53] Podgornik B., Vižintin J. Tribological reactions between oil additives and DLC coatings for automotive applications, *Surface and Coatings Technology*, 200 (2005) 1982-1989.

[54] Stallard J., Mercs D., Jarratt M., Teer D.G., Shipway P.H. A study of the tribological behaviour of three carbon-based coatings, tested in air, water and oil environments at high loads, *Surface and Coatings Technology*, 177-178 (2004) 545-551.

[55] Podgornik B., Hren D., Vižintin J., Jacobson S., Stavlid N., Hogmark S. Combination of DLC coatings and EP additives for improved tribological behaviour of boundary lubricated surfaces, *Wear*, 261 (2006) 32-40.

[56] Pettersson U., Jacobson S. Friction and wear properties of micro textured DLC coated surfaces in boundary lubricated sliding, *Tribology Letters*, 17 (2004) 553-559.

[57] Pettersson U., Jacobson S. Influence of surface texture on boundary lubricated sliding contacts, *Tribology International*, 36 (2003) 857-864.

[58] Kalin M, Vižintin J., Vercammen K., Barriga J., Arnšek A. The lubrication of DLC coatings with mineral and biodegradable oils having different polar and saturation characteristics, *Surface and Coatings Technology* 200 (2006) 4515-4522.

[59] Kalin M., Vižintin J., Barriga J., Vercammen K., Van Acker K., Arnšek A. The effect of doping elements and oil additives on the tribological performance of boundary-lubricated DLC/DLC contacts, *Tribology Letters*, 17 (2004) 679-688.

[60] Stavlid, N. *On the formation of low-friction tribofilm in Me-DLC – steel sliding contacts*. Acta Universitatis Upsaliensis, PhD thesis, Uppsala, 2006.

[61] Ožbolt L., Kalin M., Vižintin J. Influence of GMO on tribological behaviour of W-doped diamond.like carbon, in preparation.

[62] Kalin M., Vižintin J. Contact- vs. test-temperature: criteria for reactivity of diamond-like carbon coatings with oil additives, in preparation.

[63] Kalin M. Influence of flash temperatures on tribological behaviour in low-speed sliding: a review, *Materials Science and Engineering* A 374 (2004) 390-397.

Strojniški vestnik - Journal of Mechanical Engineering 54(2008)3, 207-218
UDC 658.5
Paper received: 22.8.2007
Paper accepted: 19.12.2007

Quality and Cost in Production Management Process

Magdalena Rosu*[,1] - Cristian Doicin[1] - Mirko Soković[2] - Janez Kopač[2]
[1]University Politehnica of Bucharest, Romania
[2]University of Ljubljana, Faculty of Mechanical Engineering, Slovenia

The paper presents an overview of the approaches usually used in production process, specific in planning and control. The goal is to supply "the big picture" of the methods and techniques often met in the entire production process, including the planning and control phases.

Thus, some important concepts and techniques like Six Sigma, Concurrent Engineering (CE), Quality Function Deployment (QFD), Enterprise Resource Planning (ERP) and Reverse Engineering (RE) are briefly described, together with techniques and methods for reducing the value of the lead time.

The description is sustained by diagrams showing the flow of the activities involved in each method.

Keywords: production management, process management, quality management, costs, lead time reduction

0 INTRODUCTION

The goal of each production company is to maximize its profit and value. Following this, the companies try to implement new methods for production scheduling and control, but also for assuring the best possible quality, at the same price, if possible. The approach is an effect of the changing in the customers' needs.

The customer's requirements regarding features and quality of products are continuously increasing but they don't want to pay more for better products. Only the companies which offer their customers the right products to the best price will obtain a great success on actual market.

In such an economical environment, a combination between systems and methods for production planning and control, on one hand, and quality assurance, on the other hand, is a key factor making the difference between a successful and a bankrupt business.

1 PRODUCTION PLANNING AND CONTROL SYSTEMS

1.1 Overview

Production can be defined as the transforming process of material in finite goods or services using time, resource and money. That transforming will have good results if these resources are used in efficient mode.

The major role of production management is to answer at the following question: how to do this transformation in the best conditions and to obtain the optimum level between three characteristics: time, resource and money.

The cost of production is a very important factor because this factor its assessed by the customers. The price and the quality of production must be correlated in order to satisfy the client. To obtain quality products is a very important goal of production manager and of production team.

Six Sigma methodology applications can be a good solution for this scope, to obtain the quality product with a lower cost because the rate of failure is very lower [12].

We can approach the production process like a production project and we can use the methodology from project management for each subproject which consist Six Sigma methodology.

But, the problem which will arise in this approach is related to the cost. Production approach like a project will be a very expensive process and can be applicable only in some cases like aeronautics, military production, for small series of product, etc.

In production management process, we can see the Six Sigma methodology like a main project. This main project was divided in five project

*Corr. Author's Address: University Politehnica of Bucharest, Splaiul Independentei 313, 060032 Bucharest, Romania, magdalenarosu@yahoo.com

management phases abbreviated DMAIC; D – Define, M – Measure, A – Analysis, I – Improve and C – Control.

Regarding DMAIC, the questions and the problems for which the leadership must find a solution are presented in the Figure 1 [9].

If we will approach this methodology like a project, in planning phase it is necessary to recognize and establish relevant quality requirements:

- a process development plan for new products or modified products;
- the production equipment and working environment; maintenance for equipment and the working environment for ensure the availability of the production systems;
- the procedures and methods for process quality assurance;
- the operation in concordance with rules and standards, laws, defined responsibilities, quality management, as well as customers requirement;
- the monitoring and documenting of all process parameters and product characteristics, available to all competent services and departments.

In process planning stage the failure mode and effect analysis (FMEA) method is widely used.

CFD is a CE methodology that enforces the notion of concurrency and deploys simultaneously a number of completing product values in addition with quality [12]. Using the QFD concept it is possible to simultaneously address different houses of values, like house of quality, house of X-ability, house of tools and technology, house of costs, house of responsiveness, house of infrastructure, and enabling better transparency between customer's requirements and technical abilities of the company, at the same time reducing the time of product design.

1.2 How to Achieve Short Delivery Times of Orders Through Reduction of Lead Time of Operation?

The goal of each production company is to maximize its profit and value. It is possible to achieve this goal by minimizing lead times, minimizing deviations from the agreed dates, minimizing inventory, and maximizing use of resources. The connections between these elements are presented in Figure 2.

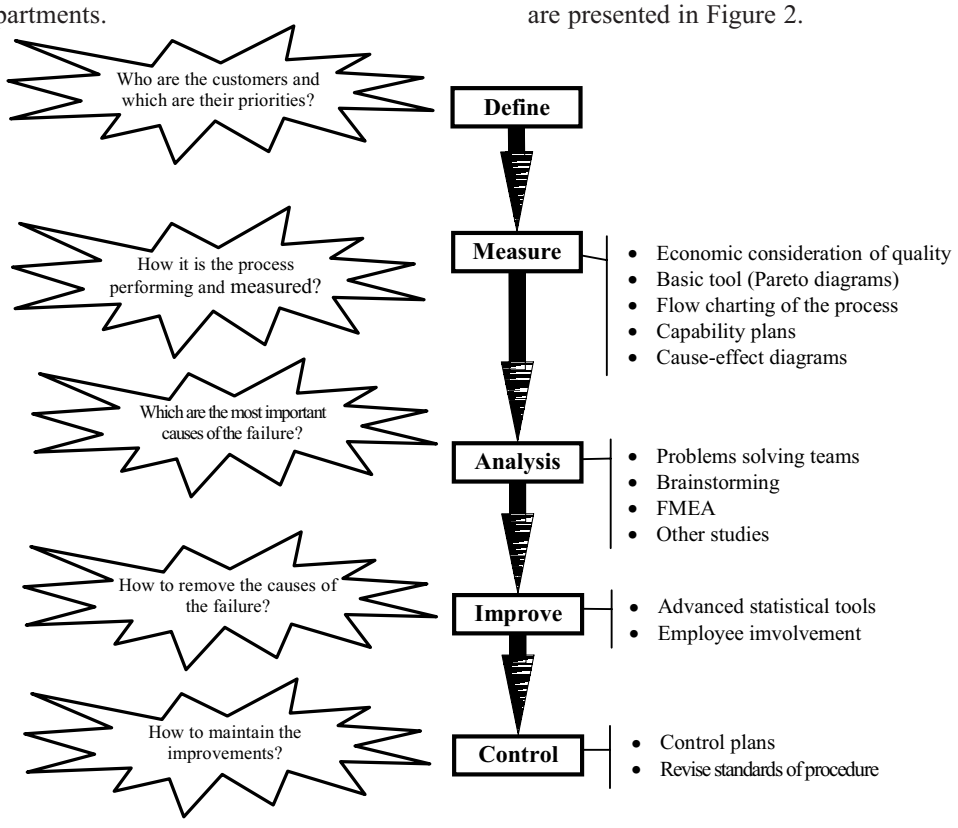

Fig. 1. The five project management phases DMAIC [9]

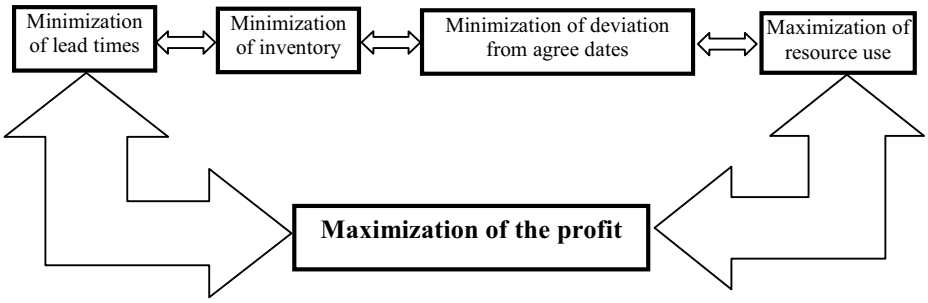

Fig. 2. Goals of economical production

1.2.1 Reduction of lead time of operation

Lead time of operations is defined as an interval calculated from the time of completing the job in previous workplace till the time of completing the job in analyzed workplace [14]. For reducing the lead time, researchers from Production Systems Laboratory may organize a creativity workshop and the problems could be solved in brainstorming groups. For this it is necessary that two stages to be completed:

1. *Analysis of workplaces in a workshop*; and for this it is necessary to carry out the following phases: designing the workshop models, designed the workplace model, designing the flow diagram and drawing the logistic curves.
2. *Searching the critical workplaces* (bottlenecks) and propose the measures for reduce the lead time of operations.

Starbek et al. [14] consider each workplace from workshop like a funnel. The objects of work are flowing into it (workload) and out of it during the treated interval.

By registering the data on the flow of jobs through the workplace it is possible to gradually draw the diagram of logistic curves that present the important logistic goals: average lead time of operation, average inventory of the operation, and performance of the operation. The logistic curve diagram presents the relations between performance, lead time, and range of workplace.

The critical workplaces are identified after analysis of the workplaces in workshop, and it is necessary to implement correction measures for reduce the lead time of operation. For a global reduction of lead time it is necessary to introduce continuous control of average lead time operation.

One of procedure described by Starbek contains three steps:

Step 1: Definition of working system features in workshop and describing the reasons for excessive lead times of orders.
Step 2: Finding most important working system in a workshop. This is the workplace that has the bigger influence on excessive lead time in analyzed period.
Step 3: Selection and implementation of specific measures in this working system.

In first step are defined the following features: mean orders time TOm, standard deviation of orders work TOs, coefficient of variation of orders work TOv, weighted mean lead time of orders TLw, standard deviation of weighted lead time LTs, coefficient of variation of weighted lead time TLv, mean performance of working systems PEm, number of finished orders n, mean inventory of orders Im, relative inventory of orders Irel.

In second step it is necessary to implement measures in order to reduce the weighted mean lead time of orders. That can be made using ABC analysis and these measures should be implemented in all working systems of workshop. As a result of these activities, the total weighted lead time during the processing of all orders in all workplaces of workshop will be reduced [2].

The third step is to identify the relation between relative inventory of orders indicator Irel and references relative inventory of orders indicator $Irel^*$. The practice show that when $Irel > Irel^*$, it is possible to reduce lead times in this workplace which have the bigger influence by using the optimization methods.

This procedure has been implemented to ETI d.d. company from Izlake and the results of this experiment was a good selection of measures which should ensure the shorter lead times of order. Another problem in actual production system is to

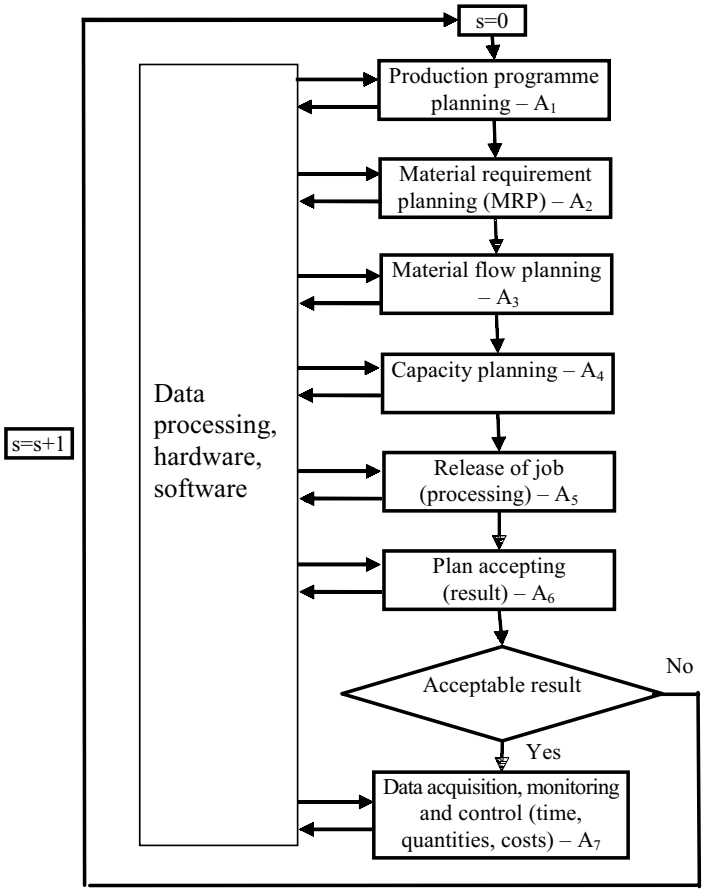

Fig. 3. Production planning and control systems [13]

find a way to achieve the optimum scheduling of job.

In paper [13], Starbek et al. present some elements which have influence in production planning and control systems.

Production planning and control systems consist of 7 modules (task), $A_{1\text{-}7}$ as it is shown in Figure 3. The first four modules are a *planning task* and last three modules are a control task. The importance of tasks increases from the first to the seventh task.

In the framework of the actual production system, the efficiency depends on the selecting scheduling method. The scheduling methods are divided in two groups: optimization methods and non-optimization methods. After choosing the method we estimate that analytical methods which use priority rules are simple and they need minimum amount of data to generate the schedule.

In generally the following priority rules are used:

1. LRPT – activity with the longest remaining processing time are scheduled first;
2. MS – minimum slack, is scheduled first the activity with minimum slack;
3. SRPT – it is the scheduled the activity with shortest remaining processing time;
4. EDD – are scheduled the activity with the earliest start data;
5. SPT – it is the scheduled the activity with minimum processing time (activity duration);
6. FCFS – are scheduled the activity in accordance with the release data sequence;
7. LPT – are scheduled activity with the longest processing time.

The result of scheduling simulation is a set of possible schedules and the planner must select the optimum schedule. The selection of optimum schedule is a process which uses predefined criteria and different decisions models. In practice it is necessary to define the level of importance or relative weights of these criteria.

In conclusion, planning and control have a big effect in actual production systems through scheduling simulation module which allows scheduling simulation taking in account different methods and criteria for scheduling.

2 CONCURRENT ENGINEERING

The customer's requirements regarding features and quality of products are continuously increasing but they don't pay more for better products. Only the companies which offer their customers the right products to the best price will obtain a great success on actual market. A new approach of development process of products is concurrent engineering (CE).

2.1 Sequential and Concurrent Engineering

The main feature of *sequential engineering* is sequential implementation of stages in product development process [8]. The referent process stage may begin only after preceding stage has been completed. Data on the reference process stage are collected gradually and they are completed when the stage has finished, then the data are forwarded to the next stage.

The main feature of *concurrent engineering* is concurrent implementation of stages in product development process. In this case the reference stage can begin before the preceding stage has been completed. Data on the reference stage can begin before its preceding stage are collected gradually and are forwarded continuously to the next stage. Winner proposes the use of 3-T loops, where interactions exist between three levels of product development process. The differences between sequential and concurrent engineering is presented in Figure 4 [8].

This methodology improves parallelism achieved by overlapping. The main advantage of this methodology is the interaction between tracks. In each loop, transformations of inputs and outputs are performed on the basis of requirements and limitations.

The concurrent engineering is not possible to be applied without a good organization team work. *Concurrent engineering* is based on multidisciplinary product development team. The members of team have to be experts from various departments of company and representatives of strategic suppliers and customers.

The team consists of different workgroups in different phases of product development process, and each workgroup consists of four basic teams: logical team (the whole product development process is split into logical units – operation, tasks and defines interfaces and connections between individual process units); personnel team (it trains and motivates the personnel, and provides appropriate payment); technology team (responding for creating a strategy and concept, assign the quality and minimum cost); virtual team (provides other product development team members the required dates).

The goal of engineering is to achieve the best possible co-operation between the four above teams (Fig. 5a).

In the small companies the product development team consists of only two level teams.

The product development team is approached like a core team (see Fig. 5b).

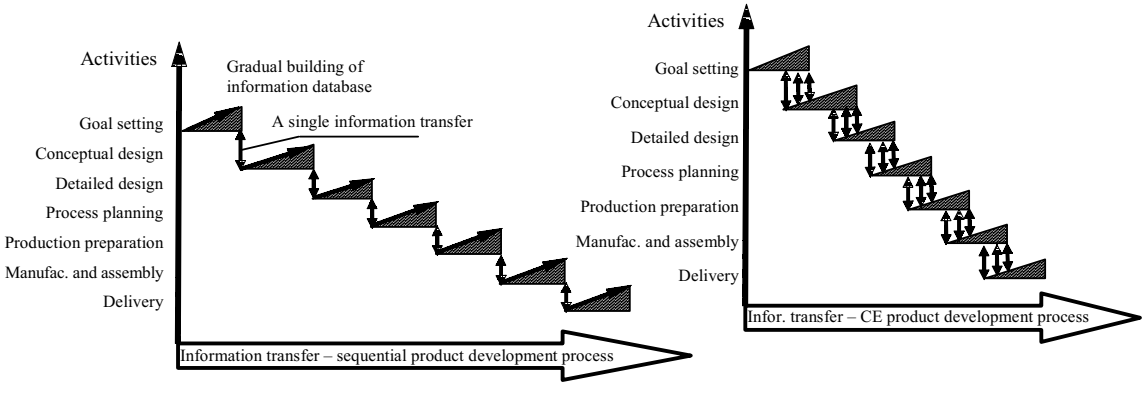

Fig. 4. Difference between sequential and concurrent engineering [8]

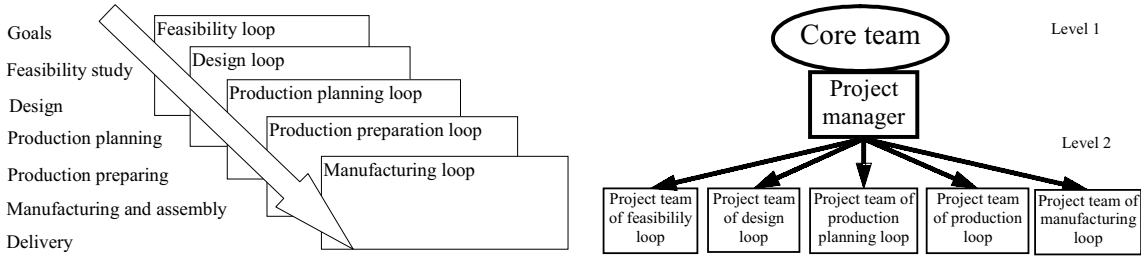

Fig. 5. Product development team

The basic element of concurrent product development is a *team-work*.

2.2 Implementation of Concurrent Engineering

The transition from sequential to concurrent product development should perform in the following two phases:

First phase: preparation for concurrent product development;

Second phase: implementation of concurrent product development.

Quality Function Deployment (QFD) and Concurrent Function Deployment play an important role in CE product development process. QFD is a central tool supporting the CE, the aims of QFD is to provide the team a classification method of deployment actions. The most widely described model of QFD is a four-level of model know as Clausing model or ASI model. The first step in part characteristic deployment is to develop a function tree – the total product is divided into subsystems and the subsystems are divided into parts and their characteristics will be evaluated.

Concurrent Functions Deployment (CFD) can be view like an upgrade of QFD. The basic organizational of CFD are:

- to increase innovation;
- organize infrastructure and improve the company's responsiveness;
- improve the cooperation inside the company and with external entities;

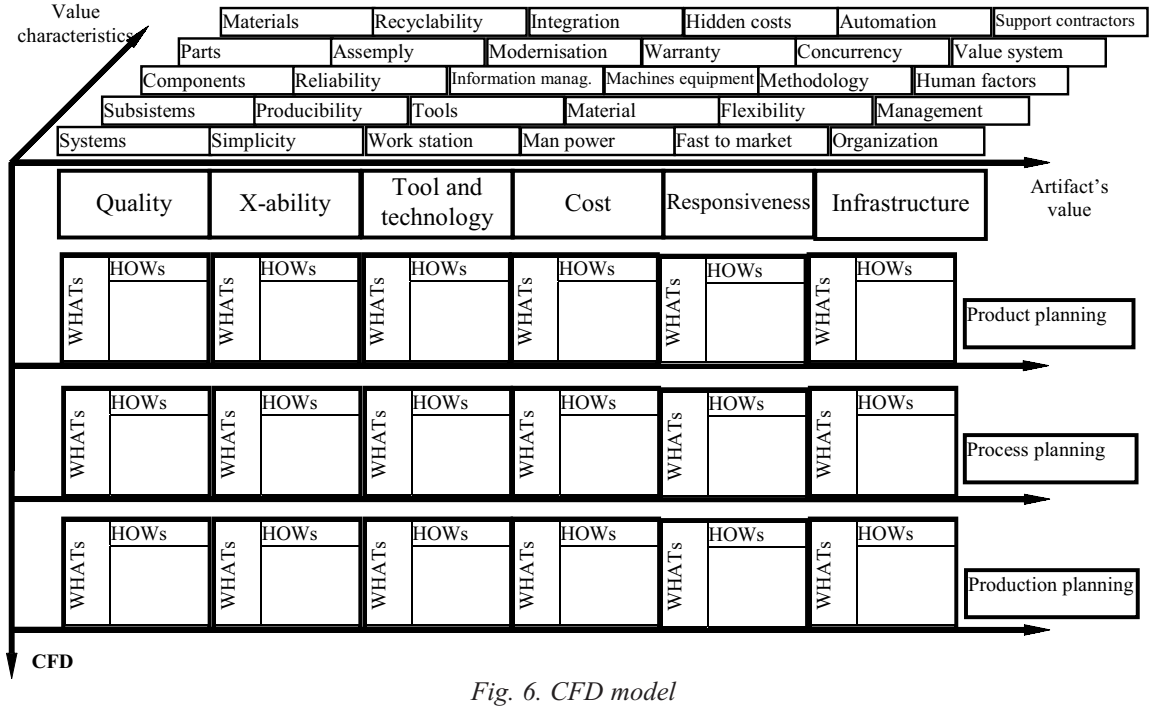

Fig. 6. CFD model

- quickly introduce new products to market in a cost-efficient manner.

CFD is a CE methodology that enforces the notion of concurrency and deploys simultaneously a number of completing product values in addition with quality [15]. With the QFD concept it is possible to address simultaneously different houses of values, like house of quality, house of X-ability, house of tools and technology, house of costs, house of responsiveness, house of infrastructure, and enabling better transparency between customer's requirements and technical abilities of the company, at the same time reducing the time of product design.

The QFD deployment process using the CFD methodology is presented in Figure 6 (Prasad 1997 quoted by Tomazevic [15]).

The CFD methodology has been implemented in small and medium enterprises and the result was an optimum result for all product values because the QFD methodology takes into account only product quality and the CFD methodology takes into account other product values like X-ability, responsiveness, tool and technology, infrastructure and cost.

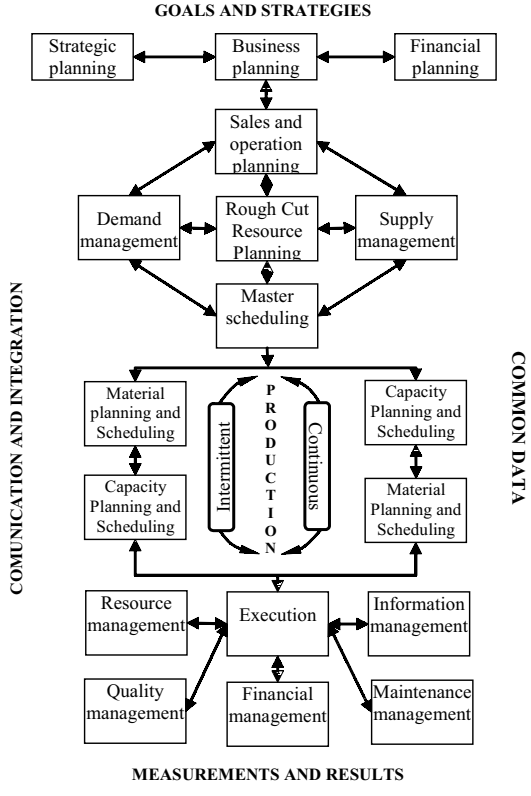

Fig. 7. Enterprise resource planning, ERP

The successful of the tools and methods that support concurrent engineering is a condition for a later transition to concurrent engineering development of a new type of product.

3 ENTERPRISE RESOURCE PLANNING

3.1 Virtual Enterprise Approach

The modern production systems have to be adaptable to changes of market. A solution of production systems to be adaptable to the changes of market is virtual enterprise approach.

Virtual enterprise is a temporary partner union of companies that join in order to share their professional knowledge, competence, resource and can thus better respond to business opportunities in their environment. Collaboration of enterprise in a virtual enterprise is based on the information and communication infrastructure [1]. In a virtual enterprise each individual partner enterprise does not manufacture a complete product, just only some operation of a product or some parts of a product.

Virtual enterprises may have different structures, for example: short time, consortium forms and extended virtual enterprise. The extended virtual enterprise form is recommended for long-term operation of virtual enterprise and this form consist in a good connection between partners, suppliers and customers for to obtain the common goals.

Responsibility for new product development within the virtual resource is taken by all partners.

Enterprises which are parts of extended virtual enterprise have to coordinate their internal enterprise resource planning systems with other ERP systems in the supply chain.

ERP is a technological evolution of MRP II. Advancement in the areas of logistics, human resources, quality, finance, maintenance, and documentation management provide today's enterprise with a tool for process better planning and control the business. Many authors define the term ERP like "Advanced Manufacturing Resources Planning", as represented in Figure 7 [1].

In ERP environment is introduced the scheduling by simulation module. The module includes all elements that are necessary for realistic scheduling.

Different methods for simulation of scheduling are used. The result of simulated scheduling is a set of different schedules and this different schedules are analysed on bases as different characteristics and criteria is selected the optimum schedule.

The optimum schedule of orders is sent to the ERP systems database.

3.2 Implementation of ERP Into Actual Production Systems

Implementing such a complex and huge software system in a company usually involves many analysts, programmers and users, and often comprises an expensive project in itself for large companies, especially trans-nationals.

In order to implement ERP systems, companies often seek the help of an ERP vendor or of third-party consulting companies. Consulting in ERP involves two levels, namely business consulting and technical consulting. A business consultant studies the organisation's current business processes and matches them to the corresponding processes in the ERP system, thus configuring the ERP system according to the organisation's needs. Technical consulting often involves programming.

The implementation must:

- be done concomitant from management;
- be done from a task force personnel from all functional areas,;
- take care of hardware requirements;
- be done step by step rather than sudden introduction;
- be done with patience, because ERP implementation takes time.

ERP implementation involves the next phases: project planning, business and operational analysis (including GAP analysis), Business Process Reengineering, installation and configuration, project team training, business requirements mapping to software, module configuration, system modification and interfaces, data conversion, custom documentation, end user training, conference room pilot, acceptance testing, production and post-implementation audit/support [1].

For small companies the implementation of computer aided monitoring and control is carried out in the following steps [1]:

Step 1: *Selection and implementation* of the ERP system in combination with PPC module. This selection can be made on the basis of system tests.
Step 2: *Automatic data acquisitions on manufacturing events*. After implementations of ERP systems it is necessary to add permanently new data.
Step 3: *Software for monitoring the actual state of production*. In this step it is necessary a permanently monitoring of process control and feedback reaction in order to improve the status of work systems and of the whole production systems.
Step 4: *Definition of reference values of lead time, inventory, range and use*.
Step 5: *Continuous improvement of process (*Deming's cycle*)*.

ERP is an integrated management process for company-wide management of a business enterprise. The concepts and techniques of ERP must be applied across all company functions. ERP integrates management processes to assure that decisions and planning are born out of the same databases, assumptions and methodology and language. ERP solutions focus on optimizing productivity by focusing on planning and executive reporting of the enterprise as an integrated unit [5]. By integration of monitoring and control modules in ERP systems are provides realistic data for planning and are taking corrective measures in order to improve the situation.

ERP is much more than a manufacturing software tool. It is a management philosophy for making and keeping promises to a better management the supply and demand sides of the business using directly integrated management systems [5]. The focus is on results, improvement of the competitiveness in the marketplace and improvement of the overall company business performance.

4 REVERSE ENGINEERING

The customer requirements it's the most important factor which the leadership of production factory have to take in account.

Because every day the market demand asks to change the production, the factory has to find the way to be aligned with the demand of the market. If the production factory doesn't find the way to align of the demand market, this factory will not survive and will fail.

The one of new success approach in design and development of products it's Reverse Engineering. This method it's an unconventional approach for design and development of products.

In conventional design of products, the process starts with the geometrical modelling using a CAD systems, then the information are exported in standard format (like IGES points/STL binary, ASCII data, DXF polyline, VDA point or IGES/ STL surfaces) and imported in the same format to CAE systems (allowing numerical model simulation) and/or to a CAM systems (allowing to generate the trajectories of tool).

This unconventional approach can be applied when the scope is improvement or optimising some parts of existing products or when do you want to simulate or redesign some parts of product for which don't have a CAD data format. The three steps in RE process are: *digitising, data segmentation* and *data* fitting [6], [10] and [11].

The *digitising phase* is generating conceptual model from physical model through 3D-scanninig techniques aided by specialised software's for model reconstructions. This phase is the process of gathering data from a 3D surface.

This process of acquiring data can be made in different forms using new technologies for data capture as laser, camera, and vision and analogue probe systems. This phase, called *digitising*, is described in Figure 8.

Technologies for gathering data are adopted in accordance with the physical model. Therefore, CCD cameras and laser have the advantages for a fast and precise gathering data and can be used for soft materials because are two non contact methods, but the price is very high and can't be used for reflective materials or for oil and wet parts.

Classical contacts have good precisions in all axes, have a low prise, it's possible to scan all types of material (beside the soft materials) and can be used for the very big products (like airplanes, ships, big machines and devices), but the scanning speed is lower and can't be used for soft materials, it's not possible to determinate the roughness of the surfaces [10].

5 INTEGRATION CONCEPT IN MODERN MANAGEMENT

5.1 Concepts and Theories

Growing globalization and more complex business environment are conditions which have requests to rapidly increasing management effectiveness and require application of new management theories which can respond to modern business conditions. Modern management theories offer some concepts for increase effectiveness of organizations.

Those theories, described by Bobrek et al., are General system theory, Balanced Scorecard, CASE tool for information systems design [3].

Another theory is "Six competitive games" of Gharajedaghi quotation by Bobrek et al. [3]. Together, these six games have dominated the

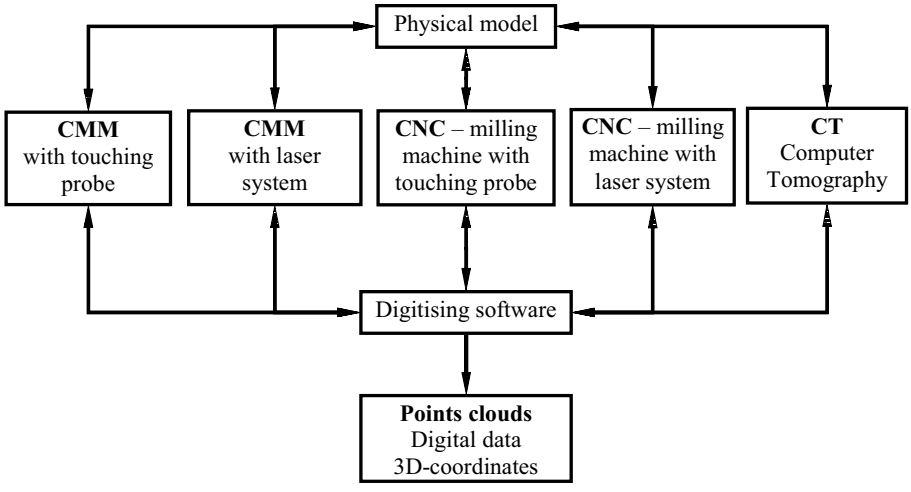

Fig. 8. Digitising phase using different technologies for gathering data from 3D-geometries and generated data [11]

management scene and each paradigm has its own unique mode of organization.

A new theory is developed on the Dale examination and the result of that is summarised into four areas of interest: *integration in organisational behaviour* (integration is considered as the degree of coordination and cooperation necessary to overcome the differentiation and establishment of common outlook), *integration in the systems concept* (integration and alignment increase the efficiency and the effectiveness), *integration in the quality management* (that is the degree of the alignment and the harmonisations with the European model of TQM, levels of TQM activity stages of quality culture) and *integration in the management systems standards* (is associated with alignment, harmonisation and compatibility and implies a single top-levels system) [4].

The benefits of systems' integration can be: improved operational performance, internal management methods, higher motivations of staff, fewer multiple audits, enhanced customer confidence, reduced costs.

The design approach is useful in creating management systems of organizations in economic field and is fully accepted in international standards of management.

Integrating all requirements, techniques and tools in those standards leads to a unique concept of management which appears in the term Integrated Management Systems (IMS) [3].

The system definition is *an element structure and its relation and processes accomplishing the purpose of the system.*

The graphic model of the system **S** is presented in Figure 9, and for a complete

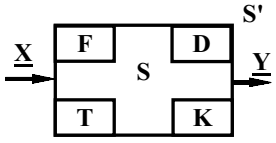

Fig. 9. Graphic model of the system

identification of a system is necessary to define the following systems quantities:

F is system goal functions, that determines the goal of which the systems exists and systems should achieve at a specific point in time.

K represents system characteristics; these are the characteristics of system and its elements by which are identified and compared with other systems of the some class. The systems characteristics are in connection with the process of measurement, analysis and development.

X represents inputs, that are independent variables and these can be materials, energy or information's.

Y is output and this represent the result of the work transformation in the system and this can be materials, energy or information.

T represents the system transformation operator and this is the rule based on which the input into system are turns into an output.

D represents the system status and this is understood as the capability of system to perform process or not.

S' represents environment of the system.

Scientific management approach application, for every concrete system, means application of different methods and tools group, which in concrete conditions results the best effects [3]. In traditional management the commonly used tools are: strategic planning, costs management functional organizational structure, detailed description of work tasks, standard work between performers and promoters, management by objectives, financial measurements, etc.

The modern management theory is a comprehensive number of techniques and tools, which could be effectively used to design management systems. It is very important to choose adequate techniques, which can contribute to integration of different goals of management and affirmation synergetic effect on all levels of organisation. One of scientific approach to management is Conductor Orchestra method of Drucker quoted by Bobrek et al. [3].

5.2 Management System Design Methodology in Management Standards

The management systems design processes are given by ISO 9001:2000. Advanced Product Quality Planning (APQP) is a logical methodology for general product design, which has been developed in the automotive industry.

Product quality planning is a structured method of defining and establishing the steps necessary to assure that product satisfies the customer [4]. The goal of product quality planning is to facilitate communication with everyone

involved to assure that all required steps are completed in time. The basic principles of implementing APQP plan [4] are:

- *organise the team* – assign responsibility to a cross of functional team;
- *define the scope* – it is identify the customers needs, expectations and requirements;
- *team to team* – that include regular meetings with other teams;
- *training* – assign a training program for communicates all requirements and development skills to fulfil customer needs and expectations;
- *customers and supplier involvement* – customer may initiate the quality planning process with supplier;
- *control plans* – are written descriptions of the systems for controlling parts and processes;
- *concern resolutions* – during the planning process the team will encounter product design;
- *product quality timing plan* – that is the first task which should be developed by planning's team;
- *plans relative to the timing chart* – the success of any program depends on meeting customers needs and expectation in a timely manner at a cost that represent value.

It is possible to find an analogy between APQP principles and methodology of QMS implementation. The object of designing in the management systems fields is an unequivocal process structure of the business system and process model. This approach is founded by Deming and is very well know the 14 management principles, which are new ISO 9000:2000 standards condensed into eight principles.

The whole implementation of the teamwork principles and concurrent engineering is possible by using a computer aided tool (CASE - Computer-Aided Software Engineering), which involves technology of communication for interchange the information of the project teams in different design phases. *CASE is the use of computer-based support in the software development process.* This definition includes all kinds of computer-based support for any of the managerial, administrative, or technical aspects of any part of a software project.

In paper [4] the authors find that adequate theory, practical methods and tools for design of the organizational and management systems exists. In the same time, some correspondences with computer-aided tools are revealed. These connections may improve the design procedure effectiveness and efficiency and it is possible to use APQP model as a basis for the standardisation of management systems design procedure.

6 CONCLUSIONS

Nowadays, the modern production systems must be adaptable to the changes on the market.

Most of the products are manufactured by order and for this reason, the production lots has been reducing. On the other hand, following the customers' needs and trying to always have only satisfied customers, the manufacturers discovered the importance of implementation of some new methodologies: Concurrent Engineering in combination with Six Sigma, often in the framework of an ERP environment.

The implementation of concurrent engineering starts by creating a specific environment that facilitates communication and collaboration between members of team work, but also between separate organisations and departments within the same company.

In the same time, the companies who apply concurrent engineering must see the implementation process as a project. This approach makes concurrent engineering a powerful development tool that can be implemented early in the conceptual design phase, when the majority of the products' costs are committed.

Close to the techniques developed in Concurrent Engineering, and often combined with them, the Six Sigma methodology assures the increase of the quality of manufactured products, and also the visible decrease of the number of rebuts and of the production costs.

In the framework of the Six Sigma environment, the collecting and analysis of data is an individual process which doesn't take care about the synchronisation between departments. Another weakness of the Six Sigma methodology is the lack of control used to sustain improvements achieved. Taking into account all these elements, in order to assure a superior quality for all the products, and also just in time products, the manufacturing companies have to join in efficient mode, both methodologies, combining them in a creative way. Growing globalisation on a market is the element

which gave requests for organisations to rapidly increase the management effectiveness and to require the application of the new management theories.

Six Sigma and Concurrent Engineering may give a solution which helps them to obtain a fast response to customer needs and to line up to modern business requirements.

7 NOMENCLATURE

CE	Concurrent Engineering
QFD	Quality Function Deployment
CFD	Concurent Function Deployment
DMAIC	Define, Measure, Analysis, Improve, Control
FMEA	Failure Mode and Effect Analysis
LRPT	activity with the Longest Remaining Processing Time
MS	Minimum Slack
SRPT	scheduled activity with Shortest Remaining Processing Time;
EDD	scheduled the activity with the earliest start data;
SPT	scheduled activity with minimum processing time (activity duration)
FCFS	scheduled activity in accordance with the release date sequence;
LPT	scheduled activity with the Longest Processing Time
ERP	Enterprise Resource Planning
MRP II	Material Resource Planning II
CAD	Computer Aided Design
CAM	Computer Aided Manufacturing
RE	Reverse Engineering
IMS	Integrated Management Systems
APQP	Advanced Product Quality Planning
CASE	Computer-Aided Software Engineering

8 REFERENCES

[1] Berlec, T., Kusar, J., Starbek, M. Monitoring and control of material flow in a company. *5th International Conference on Industrial Tools*, 2005.

[2] Berlec, T., Kusar, J., Starbek, M. Procedure for achieve short delivery times of orders. *4th International Conference on Industrial Tools*, 2003.

[3] Bobrek, M., Sokovic. M. Integration concept and synergetic effect in modern management. *Journal of Material Processing Technology*, vol. 175, 2006, no. 1/3, p. 33-39.

[4] Bobrek, M., Sokovic, M. Implementation of APQP concept in design of QMS. *Journal of Material Processing Technology*, vol. 162/163, 2005, p. 718-724.

[5] Brezovar, A., Kusar, J., Tomazevic, R., Starbek, M. Scheduling of operation in distributed production units. *5th International Conference on Industrial Tools*, 2005.

[6] Budak, I., Hodolic, J., Sokovic, M. Development of a programme system for data point pre-processing in Reverse Engineering. *Journal of Material Processing Technology*, vol. 162/163, 2005, p. 730-735.

[7] Duhovnik, J., Starbek, M., Dwivedi, S.N., Prasad, B. Development of new products in small companies. *Concurent engineering: Research and applications*, vol. 9, no. 3.

[8] Kusar, J., Starbek, M., Brezovar, A. Introduction of concurrent product development in small companies. *4th International Conference on Industrial Tools*, 2003.

[9] Pavletic, D., Sokovic, M. Six Sigma: A complex Quality Initiative. *Journal of Mechanical Engineering*, 48(2002)3, p. 158-168.

[10] Sokovic, M., Kopac, J. Information flow in the process of rapid product design and manufacturing, *IPOM*, 2004.

[11] Sokovic, M., Kopac, J. RE (reverse engineering) as necessary phase by rapid product development. *Journal of Material Processing Technology*, vol. 175, 2006, no. 1/3, p. 398-403.

[12] Sokovic, M., Pavletic, D., Fakin, S. Application of Six Sigma methodology for process design. *Journal of Material Processing Technology*, vol. 162/163, 2005, p.777-783.

[13] Starbek, M., Kusar, J., Brezovar, A. Optimal scheduling of jobs in FMS, *CIRP Journal of manufacturing systems*, vol. 32, 2003.

[14] Starbek, M., Berlec, T. Reduction of lead time of operation. *CIRP Journal of manufacturing systems*, vol. 32, 2003.

[15] Tomazevic, R., Kusar, J., Starbek, M., Savnik, L. Introduction of concurrent engineering deployment method into CE organization in SMEs. Concurrent engineering. The worldwide engineering grid, Tsinghua University press, Springer.

Strojniški vestnik - Journal of Mechanical Engineering 54(2008)3, 219-224
UDC 620.17:62-462.2
Paper received: 18.4.2007
Paper accepted: 27.6.2007

Equivalent Stress Analysis of Processing Tube Tension-Reducing of the New Steel 33Mn2V for Oil Well Tubes

Fuzhong Wang*[,1] - Lu Lu[1,2] - Huichun Zhang[1] - Ying Fei[2] - Guoquan Liu[3] - Jiahe Ai[3]
[1]Tianjin Polytechnic University, Department of Physics, China
[2]Bo Hai University, Center for Science & technology Experiment, China
[3]University of Science and Technology Beijing, School of Materials Science and Engineering, China

Finite element method (FEM) is used for simulation of two-pass processing tube tension-reducing of the new steel 33Mn2V for oil well tubes. The simulated results visualise dynamic evolution of equivalent stress, especially inside the work-piece. It is shown that the non-uniform distribution of equivalent stress on the longitudinal and transverse sections is a distinct characteristic of the processing tube tension-reducing, which can be used as basic data for improving tool and technics design, predicting and controlling the micro-structural evolution for manufacturing oil well tubes.

Keywords: oil well tubes, steel 33Mn2V, finite element methods, tube tension-reduction, equivalent stress

0 INTRODUCTION

In recent year, with the improvement of FEM (finite element method) and the development of computer technology, numerical simulation technology based on FEM is increasingly becoming a powerful tool to analyze the hot rolling and the hot forging process of steel and so on [1] to [5]. The processing tube tension-reducing is an important and complex deformation process in the producing seamless tubes, which is influenced by the materials properties, deformation temperature and rolling rate, stress, contact and friction condition, reducing size and others, which are a non-isothermal steady-state coupled with non-steady-state three-dimensional thermo-mechanical process. While numerically simulating the above process, it is necessary to conduct a coupled analysis, and give a consideration to the contact heat transfer by contact between the work-piece and the roll, convection and radiation between the work-piece and the environment, and the heat generation due to plastic work and friction force. This paper's aim is to get metal flow and distributions of equivalent stress on some special sections such as longitudinal and transverse sections under processing tube tension-reducing.

1 EXPERIMENTAL MATERIAL

The chemical composition of the experimental material 33Mn2V steel is shown in Table 1.

3-D thermo-mechanical coupled elasto-plastic FEM was used for simulation of two-pass processing tube tension-reducing of the new steel 33Mn2V for oil well tubes using MARC/AutoForge3.1 software. The material database of MARC/AutoForge3.1 software do not have the data of the flow stress of steel 33Mn2V, so its database should be set up. The experimental material was taken from the same part of a barren tube billet, and then manufactured into dozens of specimens with a diameter of 8mm and a length of 15mm. According to various process parameters based on practice production, the hot upsetting experiments was conducted on a thermal/dynamic simulation tester and then their flow stress curves were written down, and stored into the computer by MARC/AutoForge3.1 software's format. The whole flow

Table1. *Composition of experimental material in wt %*

C	Mn	Si	S	P	V	N	Ti	other one
0.32	1.70	0.29	0.006	0.013	proper	proper	proper	proper

*Corr. Author's Address: Tianjin Polytechnic University, Department of Physics, Tianjin 300160, China, wangfuzhong@163.com

Table 2. *Thermo-physical property parameters of 33Mn2V steel*

Temperature [°C]	Young's modulus [G Pa]	Poisson's ratio	Conductivity [W/m K]	Specific heat capacity [J/kg K]	Thermal expanding coefficient [10^{-6}/K]
20	206	0.300	-	-	-
100	203	0.300	35.0	469	12.2
200	179	0.305	35.8	502	13.9
300	190	0.310	33.2	527	13.5
400	183	0.310	31.3	543	13.8
500	174	0.310	29.3	548	14.0

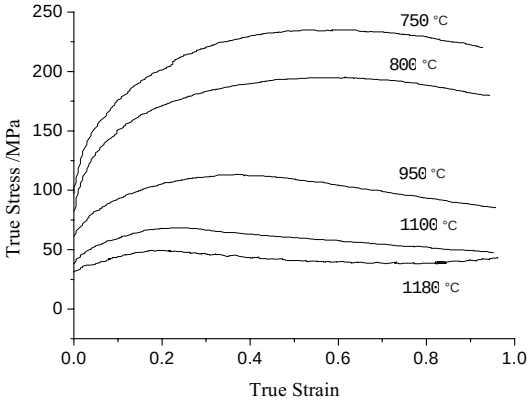

Fig.1. *Flow stress at a strain rate of 0.02/s at different temperatures*

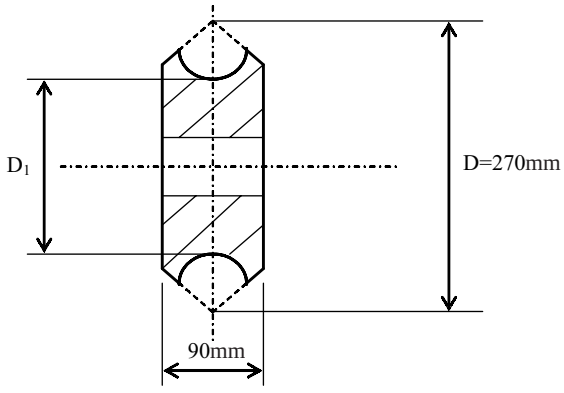

Fig. 2. *Schematic diagram of rolling roll*

stress curves are shown in Figure 1. The thermo-physical parameters including heat conductivity, specific heat capacity and thermal expanding coefficient at different temperature were directly input on the software windows, and the thermo-physical parameters at high temperature can be extrapolated based on Table 2 [6] and [7].

2 FINITE ELEMENT MODEL

Figure 2 shows a rolling roll of the three roll continuous hot rolling the machines of tube tension-reducing based on steel tube factory of wu-xi:

D_1 = D – (each pass tube diameters)

Making Φ60×5mm seamless tubes, every pass reducing size is about 3.4 %, the deformation temperature is 800°C to 860°C, the deformation rate is 0.02 s^{-1}.

Figure 3 shows a three-dimensional two-pass processing tube tension-reducing elasto-plastic FEM

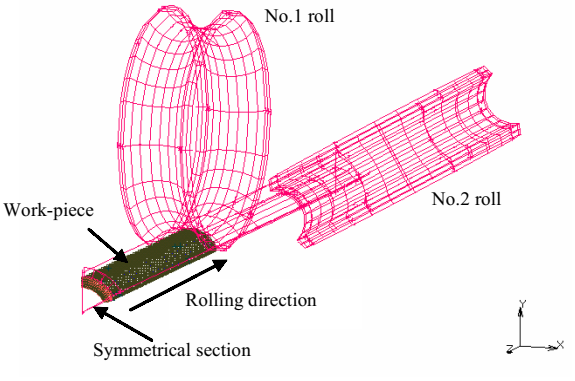

Fig. 3. *Three-dimensional elasto-plastic FEM model for two-pass processing tube tension-reducing*

model according to Figure 2. The distance between No.1 and No.2 rolls along rolling direction (-Z direction) is just set as 260 mm. The work-piece is a barren tube billet whose initial diameter and length are 64.4 mm and 380 mm, respectively. The maximum rolling speed of the first pass is 0.7 m/s

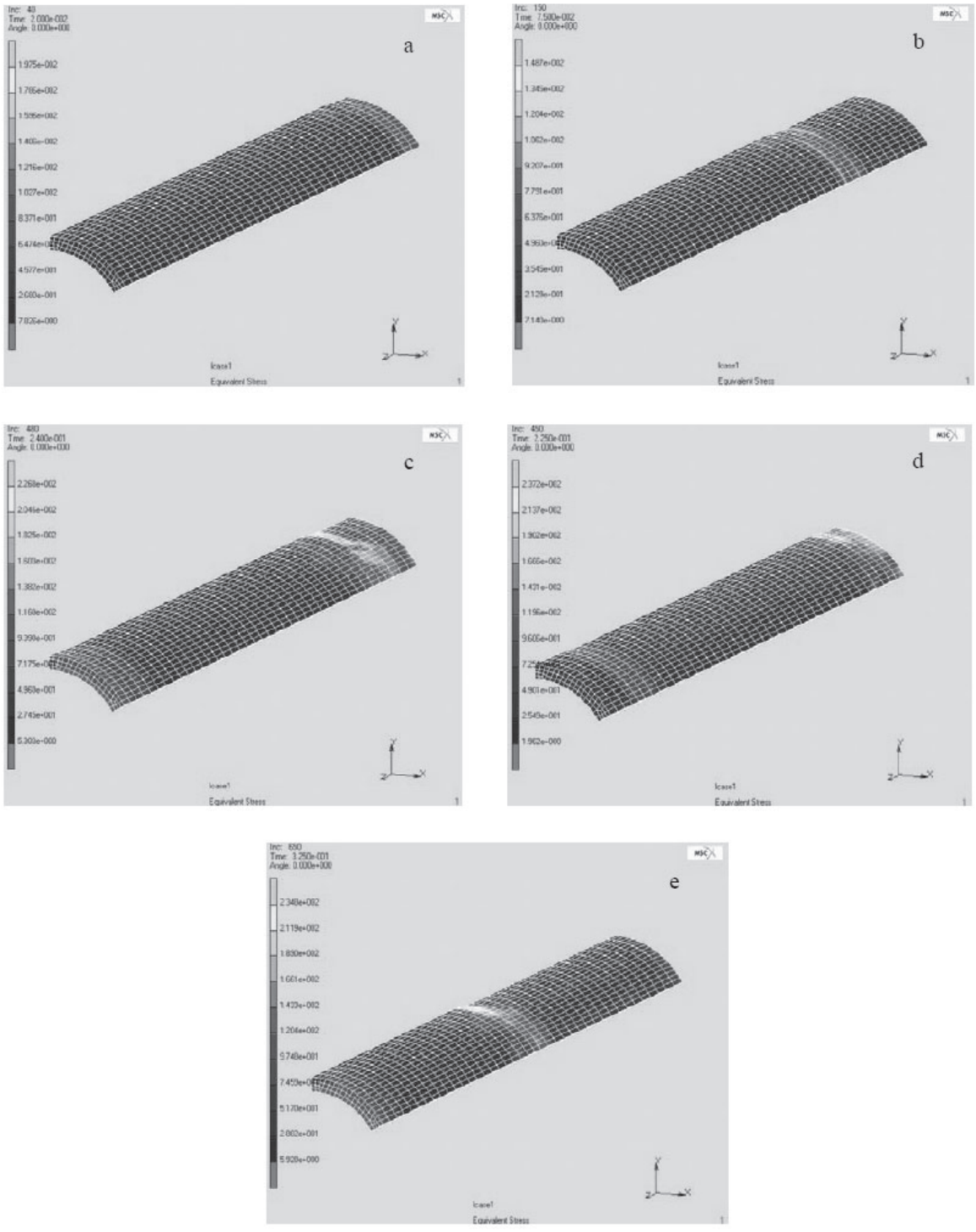

Fig. 4. *Metal flow and equivalent stress evolution on work-piece surface during two-pass processing tube tension-reducing. Initial deformation temperature: 860 °C; every pass reducing size = 3.4%; increment: (a) 40, (b) 150, (c) 450, (d) 480, (e) 650.*

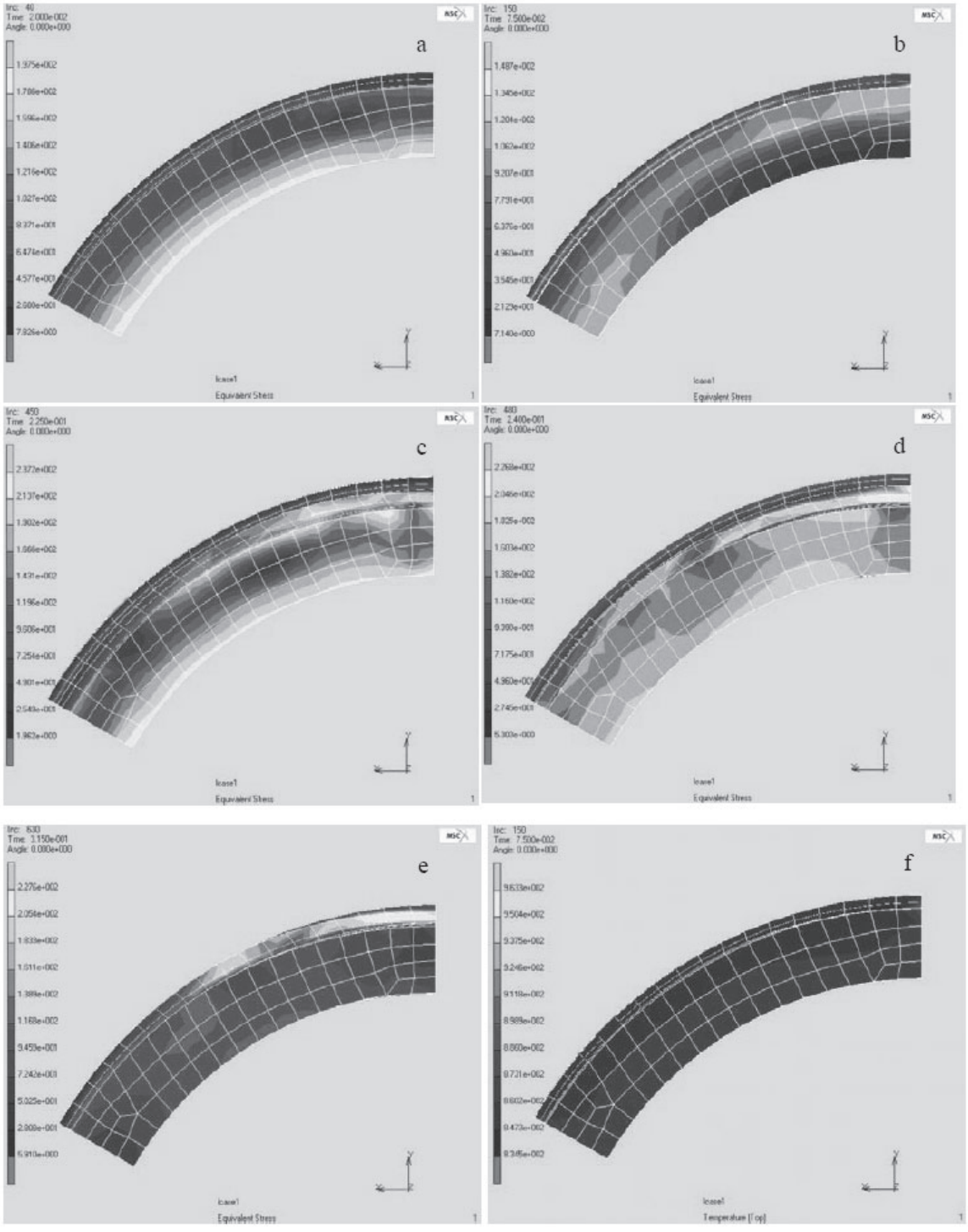

Fig. 5. *Distribution of equivalent stress and temperature on the cross section of the work-piece via the axis of No.1 roll. The initial deformation temperature: 860 °C; increment: (a) 40, (b) 150, (c) 450, (d) 480, (e) 650, (f) 150; reducing size = 3.4%. (a)~(e) equivalent stress, (f) temperature.*

and the second pass is 0.73 m/s. For its symmetry, just one sixth of the work-piece is taken as simulation object to further shorten computation time.

Eight-node hexahedral element type is taken, at the same time 2280 elements and 3239 nodes are obtained for the work-piece. The work-piece is assumed to be elasto-plastic and described by updated Lagrange method, i.e., it obeys the Mises yield criterion and Prandtl-Reuss flow rule, and its deformation is simulated in a step-by-step manner, updating the coordinates of material points and the property after each step. The rolls are assumed to be rigid and with heat-transfer, and they were analytically described.

The displacement of all nodes on symmetrical planes perpendicular to their corresponding symmetrical plane is zero. The friction between the work-piece and the roll contact surface keeps to shear law, and their friction coefficient is set as 0.7. The equivalent heat-transfer coefficient between the free surface of the work-piece and the ambience is set as 0.17 kW/(m^2 K). The contact heat-transfer coefficient between the work-piece and the roll is set as 23 kW/(m^2 K). The initial temperature of the work-piece, the ambient temperature and roll temperature is set as 860 °C, 20 °C and 200 °C, respectively. The conversion factor from plastic work to heat was set as 0.9 [8] and [9].

3 SIMULATION RESULTS AND DISCUSSION

3.1 Equivalent Stress Evolution on Work-Piece Surface

Figure 4 are charts of the new steel 33Mn2V for oil well tubes by MARC/AutoForge3.1 software. They show the equivalent stress evolution on the work-piece surface during two-pass processing tube tension-reducing. At increment 40, No.1 roll has already bitted the work-piece, and the rolling was still in a non-steady state; at increment 150, No.1 roll have already rolled the work-piece steadily; at increment 450, the rolling for No.1 roll was still in a steady state, and No.2 roll began to bite the work-piece and the rolling was still in a non-steady state; at increment 480, No.1 roll approached the end of the work-piece, which was non-steady-state rolling, but the rolling for No.2 roll has already been in a steady state; at increment 650, No.1 roll has completed the rolling, and the No.2 roll has been in steady state. Its maximum equivalent stress is about 211.9MPa near YZ plane after the rolling for No.2 roll is steady at increment step 650 and its minimum equivalent stress is about 102.7MPa after No.1 roll has already bitted the work-piece at increment step 40.

3.2 Distribution of Equivalent Stress and Temperature on Typical Cross Sections

We give an example to describe the distributions of equivalent stress and the temperature on typical cross sections. Fig.5 shows equivalent stress distribution and temperature distribution on the cross section of the work-piece via the axis of No.1 roll at different increment step. It can be seen from Fig.5 that they are very non-uniform, and their ranges are 26.8 to 205.4 MPa and 847 to 899 °C, respectively. Their non-uniform distributions attribute to equivalent strain, equivalent stress and temperature interaction. On the one hand, the distribution of strain or strain rate on the cross section is non-uniform of itself, therefore, the result in non-uniform stress distribution, and non-uniform temperature distribution appear as a result of plastic work and heat-transfer; on the other hand, non-uniform stress and temperature distributions have effect on the distribution of the strain and the strain rate.

4 CONCLUSIONS

We conclude this paper by physical simulation experiments and FEM simulation are performed to analyze the processing tube tension-reducing of the new steel 33Mn2V for oil well tubes. FEM simulation coupled with physical simulation vividly visualizes the metal flow and dynamic evolution of stress and temperature during processing tube tension-reducing of the new steel 33Mn2V for oil well tubes. Simulated results show that the non-uniform distribution of stress and temperature on the longitudinal and transverse sections and inside the work-piece is a distinct characteristic of processing tube tension-reducing. The prediction of the metal flow, the evolution of stress and temperature and their distributions on some special sections during processing tube tension-reducing can be used as basic data for improving tool and technics design, predicting and controlling the micro-structural evolution of

processing tube tension-reducing of the new steel 33Mn2V for oil well tubes.

Acknowledgement

We would like to acknowledge Huangjiankai for useful discussion and the Steel Tube Factory of Wuxi Jiangsu and the Tianjin Natural Science foundation of China No: 06YFJMJC0220 for supporting this study.

5 REFERENCES

[1] Jang, Y.S., Ko, D.C., Kim, B.M. Application of the finite element method to predict microstructure evolution in the hot forging of steel. *J. Mate. Process. Tech*, 101 (2000), p. 85-94.

[2] Aymone, J.L.F, Bittencourt, E., Creus, G.J. Simulation of 3-D metal-forming using an arbitrary Lagrangian-Eulerian finite element method. *J. Mate. Process. Tech*, 110 (2001), p. 218-232.

[3] Park, J.J., Oh, S.I. Application of three dimensional FEM analysis to shape rolling processes. *Journal of Engineering for Industry, Transactions of the ASME*, 112(1990), no.1, p. 36-45.

[4] Bittencout, E., Creus, G.J. Finite element analysis of three-dimensional contact and impact in large deformation problems. *Computers & Structures*, 69 (1998), p. 219-234.

[5] Laasraou, A., Jonas, J.J. Prediction of temperature distribution, flow stress and microstructure during the multi-pass hot rolling of steel plate and strip. *ISIJ International*, 31(1) (1991), p. 95-105.

[6] Laasraoui, A., Jonas, J.J. Prediction of steel flow stresses at high temperatures and strain rates. *Metallurgical transaction*, 22A (1991), p. 1545-1558.

[7] *Editing committee of mechanical engineering materials property data handbook: Mechanical engineering materials property data handbook*. China Machine Industry Publishing Company, (1995), p. 190.

[8] Wang, Y., Kang, Y., Yuan, D., et al. 3-D elastic-plastic FEM study on rolling square billet. *Iron & Steel*, 35(2000), No.2, p. 38-40. (in Chinese).

[9] Wertheimer, T.B. *Thermal mechanically coupled analysis in metal forming process, numerical methods in industrial forming processes*. Swanwea: Pineridge Press Ltd, 1982, p. 425.

Strojniški vestnik - Journal of Mechanical Engineering 54(2008)3, 225-231
UDC 676.056.73
Paper received: 27.3.2007
Paper accepted: 27.6.2007

Influence of Technological Factors on Physical and Mechanical Properties of Laminated Prints

Svetlana Havenko[1] - Aleksandr Bogorosh[2] - Marija Martynyuk[1] - Edmundas Kibirkštis*[,3] - Kęstutis Vaitasius[3]
[1]Ukrainian Academy of Printing, Lviv, Ukraine
[2]National Technical University of Ukraine, Kyiv, Ukraine
[3]Kaunas University of Technology, Kaunas, Lithuania

Research of qualitative parameters of lamination at different technological modes for different papers is carried out. Influence of temperature and speed of print lamination with an OPP film on the quality of laminates is considered. A mathematical model describing the strength and curling of a laminate depending on the regime factors of the process has been developed. Optimization of the technological process has been carried out.

Keywords: technological processes, lamination optimization, polypropylene films

0 INTRODUCTION

Finishing prints by means of pressing a transparent film gives a significant effect in mass production at low costs: it improves aesthetic and advertising qualities; gives ample opportunities of creative designing; provides the best protection of a surface against mechanical damages and the environmental impact [1].

In the world practice of polygraphic industry three basic ways of laying a polymeric material over paper are used:

1) Glueing the film on the paper by using varnish or glue (a glutinous way);
2) Pressing the duplicated film, one layer of which has considerably lower temperature of fusion than the other, and carries out thermoglue functions during pressing (a glueless way);
3) Coating paper with fusion polymer which acts as thermoglue during the coating process, and after cooling and hardening serves as protective coating (extrusion, co-extrusion).

When choosing a film for lamination, it is necessary to consider the purpose of the laminate, as well as its appearance. The most promising material for lamination is oriented polypropylene (OPP) as it is a strong, elastic, ageproof and rather inexpensive material. Other OPP advantages are high transparency, shine, low specific weight; therefore it represents special interest for lamination of polygraphic production [2].

Study on rough-surface biaxially oriented polypropylene film is presented in [3]. The influence of processing conditions on the roughness state of BOP was generally similar to that in the case of monolayer cast sheet.

Three different techniques for experimentally determining the bending stiffness of flexible films and laminates have been evaluated using a number of different packaging materials [4]. The calculations showed that layer modulus often is less important than layer thickness and that the position of the layer in the laminate can have a major influence on the overall stiffness.

Permanence and strength of digital prints on paper are show in [5]. Colour prints with a surface protection of polymer varnish or foil protection are very unstable, causing deterioration of colour, contrasts and colour balance.

With the big assortment of lamination films and a great variety of laminated materials, there is an urgent problem of defining optimum technological modes of lamination that would allow to reduce the duration of performance and to raise the quality of production [6].

The aim of this paper was to research qualitative parameters of lamination at different technological modes, as well as to develop the mathematical model of the lamination process for optimizing the mode parameters of the lamination process.

*Corr. Author's Address: Edmundas Kibirkštis, Kaunas University of Technology, Faculty of Design and Technology, Studentu str. 56-350, LT-51424 Kaunas, Lithuania, edmundas.kibirkstis@ktu.lt

1 METHODOLOGY OF RESEARCH

The mechanical properties of the films were investigated by a tensile machine: samples of a film 15×250 mm, distance between the clips of the tensile machine - 180 mm, speed of movement of the bottom clip - 100 mm/min. Measurements were taken in the longitudinal and cross-sectional directions of the film orientation. Strength at break σ_R (kPa) and lengthening at break ε_R (%) were also measured.

Contraction (%) (relative change of length of a film after its thermal processing and cooling to normal temperature):

$$S = \frac{L_0 - L_1}{L_0} 100\% \qquad (1),$$

where L_0 is the initial length, L_1 is the length after thermal processing and cooling.

Tests were carried out for two directions (longitudinal and cross-sectional), on samples of the size 100×100 mm at temperature 90 to 130 °C (depending on the kind of film) during 15 minutes. The accuracy of measurement was – 0.1 %.

Adhesive strength of laminating a duplicated OPP film to prints was defined by the method of stratification on the dynamometer. For this purpose samples of laminates were taken: strips in width of 15 mm and length 150 mm, which were not laminated on one side (so that there were ends in length of 20 mm for fixing in the dynamometer clamps). The maximum loading which caused tear of the film from the paper was fixed as the result of the tests. The parameters of strength of fastening a film to paper were taken as an arithmetic mean of three tests. Strength of lamination should make not less than 20 kPa [7].

An objective criterion of good adhesive interaction of glue with paper and a polymeric film is the factor of strengthening of the system:

$$K_{sh} = f_l / (f_p + f_f) \qquad (2),$$

where f_l, f_p, f_f are the breaking strength of the laminate and the initial materials: paper and polymeric film accordingly, kPa.

At the correct choice of lamination modes this factor $K_{sh} > 1$.

The quality of lamination was also investigated by means of Friction/Peel Tester 225-1. The value of the force necessary for detaching laminate from the basis and the character of its change were established.

For testing, 15 mm wide and 300 mm long samples from each laminated sheet of paper in the longitudinal and cross-sectional direction of lamination were prepared. The laminate was separated from the basis at an angle of 180 degrees with the speed of 50 mm/min.

Curl (deformation) of the sample is characterized by the size of rise of corners in relation to the horizontal surface, and also the ratio of the size of approximation of the sample edges to its middle all along the length of the sample, expressed in percentage. The lamination quality is considered good if the size of deformation of the sample does not exceed 5 % [8].

For determining the curling of laminates, samples were cut out from each sheet in the size of 100×100 mm and the height of rise of two opposite corners in relation to the plane of the table were measured. The exponent of twisting is the height of the edge rise of the sample in relation to the surface of the table in mm^{-1} [9].

The search of optimum parameter values for mathematical models of lamination process (dependence of strength of lamination and curling of laminates on temperature, speeds and weights of paper) was performed by applying the method of least squares [10] and [11].

Calculation of parameters of the obtained models and all following calculations were carried out by means of computer mathematical system Maple V [12].

2 RESEARCH OF TECHNOLOGICAL PARAMETERS OF LAMINATION PROCESS WITH OPP FILMS

Under certain technological conditions during lamination the polymeric film forms a new combined system with a print 'film-paper-film' whose properties are defined by the properties of a substratum, adhesive and modes of lamination. Factors which influence the quality of lamination can be divided into mode and technological ones. The process modes depend on technological factors and are selected according to the properties of the substratum, in view of the capabilities of the equipment.

The quality of laminated production is defined by three parameters: fastening strength of

the package 'film-paper-film', curling of laminates which testifies to the presence of internal pressure in the system, absence of outer defects (strips, morel, bubbles, etc.).

It is experimentally confirmed that adhesive strength of the system 'film-paper-film' depends on the character of initial materials and the mode of lamination. Besides, the temperatures and the total pressure, which intensify the penetration of the adhesive into the substratum pores, have the decisive effect on the results of lamination.

For revealing quality indicators and the optimum lamination mode, the basic physical-mechanical properties of prints and OPP films for lamination were determined.

The analysis of dependences of films 'lengthening-loading-lengthening' (Fig. 1) gives a more detailed understanding about their rheological (elastic-plastic) properties. An OPP film, 27 microns in the longitudinal direction, is easily extended at insignificant loading (dependence curve 1 sharply goes upwards). And on the contrary, in a cross-sectional direction at constant increase in loading the insignificant gradual increase in lengthening is observed (see curve 2). Such character of curves specifies the cross-sectional orientation of the film. Curve lengthenings 3 and 4 for a film of 80 microns are characteristic for nondirectional films, the strength of such a film is

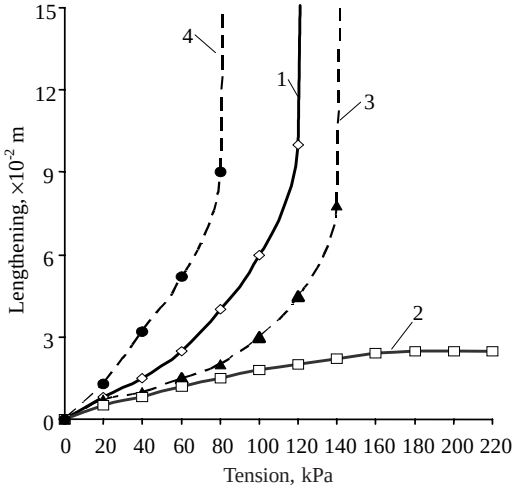

Fig. 1. *Dependence of relative lengthening upon loading for OPP films thickness 27 microns: 1 - longitudinal direction; 2 - cross-sectional direction; 80 microns: 3 - longitudinal direction; 4 - cross-sectional direction*

provided with significant thickness, instead of orderliness of molecular structures.

Anisotropism and high structure of an OPP film 27 microns thick in the cross-sectional direction also proves to be true by the diagram contraction (Fig. 2). In the longitudinal nondirectional direction the film has considerably smaller contraction than in the cross-sectional focused one. Films with 60 and 80 micron thickness are nondirectional and also have isotropic properties - their contraction makes up 0.4 % and 0.3 %, respectively, in both directions.

Investigation of quality indicators of lamination (strength of lamination and curling laminates) at different technological modes (the temperature of lamination and speed) for different papers is shown in graphic dependences Figures 3 and 5.

Figure 3 shows that the increase in the temperature of lamination leads to the increase in strength of fastening a film with paper, and the process is influenced essentially by the weight of a substratum. Thus, in order to obtain laminates with strength of adhesive fastening 20 kPa for the paper mass 80 g/m^2, the temperature of lamination should make 96 degrees; for the paper mass 120 g/m^2 - 110 degrees; for the paper mass 150 g/m^2 - 135 degrees.

With the increase of lamination speed (reduction of contact time of a package 'paper-film' with the heated surface of the shaft), the strength of lamination decreases (Fig. 3, b). So, at the lamination temperature of 110 degrees in order to obtain sufficient strength of an adhesive fastening (20 kPa), for the paper mass 80 g/m^2 lamination speed of 5 m/min is necessary; for paper 120 g/m^2 - 4 m/min., 150 g/m^2 - 3,2 m/min.

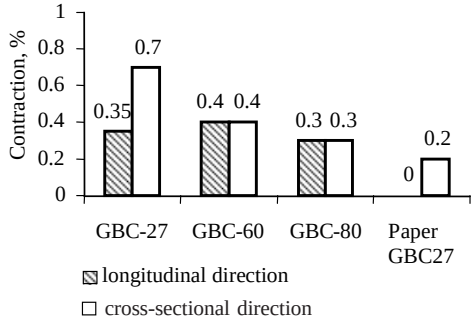

Fig. 2. *The diagram contraction of OPP films at temperature 100 degrees*

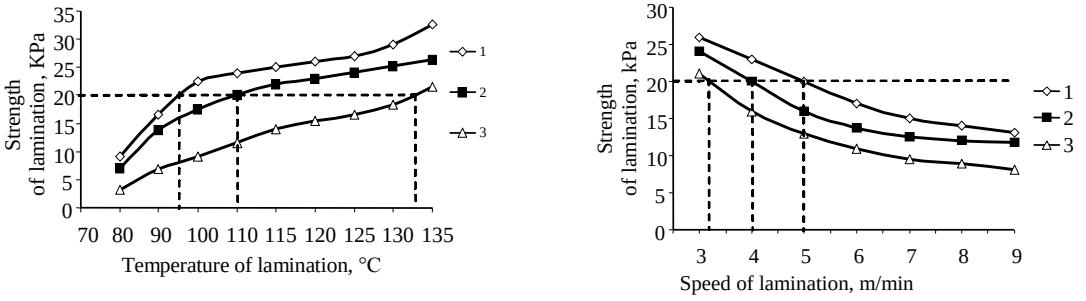

a) b)

Fig. 3. *Dependence of strength of lamination on temperature (a) and speed of lamination (b) for a paper in weight: 1 – 80 g/m²; 2 – 120 g/m²; 3 – 150 g/m²*

The analysis of the dispersion of the values of the laminate detachment force (see Fig. 4) indicates that it is small and does not exceed 4 % in the longitudinal direction (the greatest dispersion of sample 1 - up to 3.9 %). In the cross-sectional direction it is much higher (sample 2 up to 6.3 %). Dispersion of the values of the detachment force in sample 3 both in the longitudinal direction and in the cross-sectional direction is small (about 1 %) which testifies to high quality lamination.

Dependences in Figure 5, a show that with the increase in lamination temperature propensity of laminates to deformation rises and they start to curling. And the smaller the mass of the paper, the more it is deformed. So, at the lamination temperature of 100 degrees curling is observed in paper mass 80 g/m² on 7 mm, paper mass 120 g/m² - on 3 mm, and papers mass 150 g/m² - on 1.5 mm. With increasing speed of lamination (reduction of time of contact) deformation of laminates decreases (Fig. 5, b). So, if the process of lamination occurs at the speed of 6 m/min., the paper mass 80 g/m² is deformed on 8 mm, paper mass 120 g/m² - on 6 mm, mass 150 g/m² - on 4 mm.

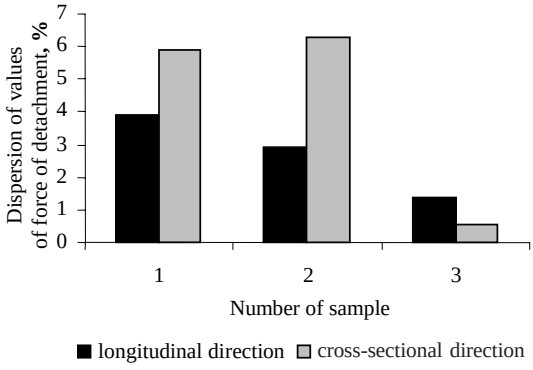

Fig. 4**.** *Dispersion of values of force of detachment of a laminate for the laminated prints: 1 – weight of papers 220 g/m², digital type of printing, thickness of a film 42 μm, temperature of lamination 200 °C, 2 – weight of papers 150 g/m², offset type of printing, thickness of a film 26.5 μm, temperature of lamination 115 °C, 3 – weight of papers 300 g/m², offset type of printing, thickness of a film 26.5 μm, temperature of lamination 230 °C*

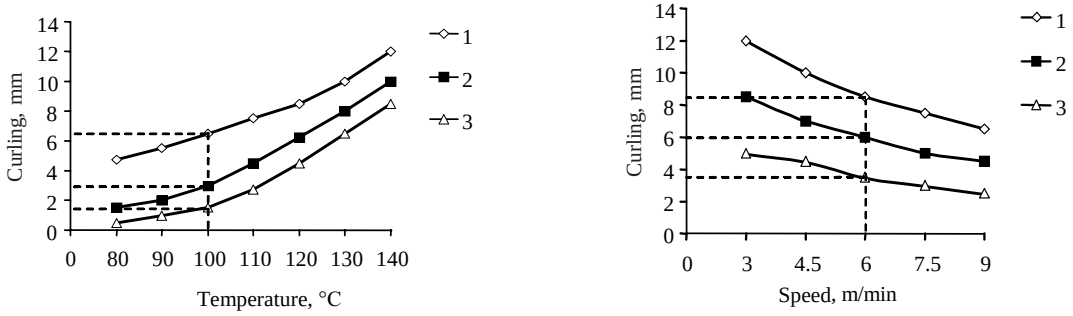

a) b)

Fig. 5. *Dependence of curl laminates on lamination temperature (a) and speeds of lamination (b) for papers in weight: 1 – 80 g/m², 2 – 120 g/m², 3 – 150 g/m²*

Thus, as regime and technology factors have an ambiguous influence on quality indicators of lamination (strength of lamination and curling of a laminate), for finding optimum parameters of the lamination process in each special case, it is necessary to carry out its mathematical modelling and optimization.

To obtain the mathematical model of strength of lamination, a great number of possible functional dependences have been checked, including the following:

$$Q_1(T,V,m) = a + b\cdot m + c\cdot T + d\cdot V \quad (3),$$

$$Q_2(T,V,m) = a + b\cdot \sqrt{m} + c\cdot T + d\cdot V \quad (4),$$

$$Q_3(T,V,m) = a + b\cdot m + c\cdot \sqrt{T} + d\cdot V \quad (5),$$

$$Q_4(T,V,m) = a + b\cdot m + c\cdot T + d\cdot \sqrt{V} \quad (6),$$

$$Q_5(T,V,m) = a + b\cdot \ln(m) + c\cdot T + d\cdot \sqrt{V} \quad (7),$$

$$Q_6(T,V,m) = a + b\cdot \ln(m) + c\cdot T + d\cdot \ln(V) \quad (8),$$

$$Q_7(T,V,m) = a + b\cdot m + c\cdot T + d\cdot \ln(V) \quad (9),$$

$$Q_8(T,V,m) = a + b\cdot m + c\cdot \ln(T) + d\cdot \ln(V) \quad (10).$$

The most suitable model for the description of the dependence of lamination strength on the paper weight, temperature and speed was the following expression:

$$\mathrm{Q}(\mathrm{T},\mathrm{V},\mathrm{m}) = 9.030779 - 0.1725819\cdot \mathrm{m} + 0.3603514\cdot \mathrm{T} - 8.4169\cdot \ln(\mathrm{V}) \quad (11).$$

The results of lamination strength obtained by this model provide the least values of root-mean-square deviations among all the considered, which makes 1.445.

The analysis of experimental data characterising the curl of laminates has been carried out under a similar scheme.

The following functional dependence describes most precisely the dependence of laminate curling on the weight of the paper and regime factors:

$$\mathrm{C}(\mathrm{T},V,m) = -0.6026537 - 0.08597808\cdot \mathrm{m} + 0.1602864\cdot \mathrm{T} - 0.5311999\cdot \mathrm{V} \quad (12).$$

The root-mean-square deviation of the values of deformation of laminates obtained by this model was the least from all considered and was equalled 0.979.

According to technological requirements, the strength of lamination is considered sufficient when it exceeds 20 kPa:

$$\mathrm{Q}(\mathrm{T},\mathrm{V},\mathrm{m}) > 20 \quad (13).$$

The inequality leads to a conclusion that for paper mass $\overline{m}$ at working speed $\overline{V}$, the temperature of lamination should satisfy the following inequality:

$$T > 27{,}66527 + 0{,}4789266\cdot \overline{\mathrm{m}} + 23{,}35748\cdot \ln(\overline{\mathrm{V}}) \quad (14).$$

As the admissible curling of paper at lamination should not exceed 5 mm:

$$\mathrm{C}(\mathrm{T},\mathrm{V},\mathrm{m})\ \mathrm{d} \le 5 \quad (15).$$

Hence, for paper mass at working speed the temperature of lamination should satisfy the inequality:

$$T \le 41{,}1928596 + 0{,}536403\cdot \overline{\mathrm{m}} + 3{,}314068\cdot \overline{\mathrm{V}} \quad (16).$$

So, according to conditions (14) and (16) for maintenance of qualitative lamination, the working temperature should satisfy the inequality:

$$T_{\min}(\overline{m},\overline{V}) < T < T_{\max}(\overline{m},\overline{V}) \quad (17),$$

where,

$T_{\min}(m,V) = 27.66527 + 0.478927\cdot m + 23.35748\cdot \ln(V)$,

$T_{\max}(m,V) = 41.19286 + 0.536403\cdot m + 3.314068\cdot V$.

According to this condition, to ensure qualitative lamination, the area of admissible values of temperatures depending on the weight of paper and working speed is limited to surfaces $T_{\min}(m,V)$ and $T_{\max}(m,V)$ with (Fig. 6). The figure shows that not at all speeds it is possible to reach qualitative lamination for paper of a certain weight. The possible admissible values of speeds are limited to a curve of section of surfaces and defined by the inequality:

$$T_{\min}(m,V) < T_{\max}(m,V) \quad (18).$$

So, using the mathematical models which describe strength of lamination (11) and twisting of a laminate (12), it is possible to define areas of admissible working speeds and temperatures which provide corresponding quality of laminate covers at the maximum productivity of technological process and the minimum power inputs.

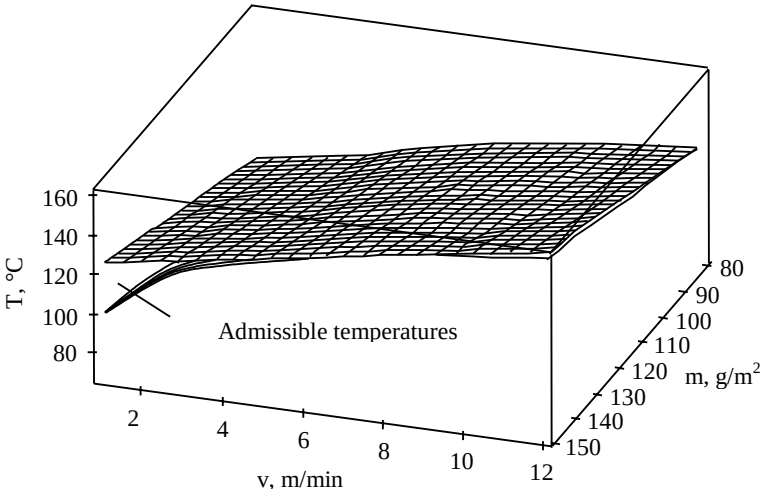

Fig. 6. *Dependence of admissible temperatures of lamination on speed of lamination and weight of paper*

Thus, as a result of the analysis of experimental data, models describing strength of lamination and twisting of laminates with sufficient accuracy, depending on the weight of paper and regime parameters, have been obtained. The obtained models have allowed us to establish conditions at which optimum temperature and speed of lamination for paper of a certain weight are defined. Programs for definition of optimum parameters of lamination are developed. The obtained results give a possibility to automate the process of adjustment of a laminator.

3 CONCLUSION

It has been determined that lamination quality is influenced by regime and technology factors as follows: at the increase in temperature the strength of lamination increases, and, the thicker the paper, the greater should be the temperature of lamination. At the increase in speed the strength of lamination decreases. The increase in lamination temperature increases the laminate curling, and the increase in speed decreases the curling.

The analysis of values of factor of strengthening for different 'film-paper' systems has shown that their strength is greater than the total strength of the materials the system is made of. Besides, for a film-paper system the factor of strengthening in the longitudinal direction is close to one, while in cross-sectional makes 2.81, which testifies strengthening the system in the cross-sectional direction almost three times.

On the basis of the analysis of experimental data models for the description of strength of lamination and curling laminates, depending on the weight of paper, working speed and temperature are obtained. By means of the obtained models, conditions at which admissible working speeds and temperatures of lamination are defined for paper of given weight are established. The obtained mathematical model of lamination allows to establish an optimum mode of lamination for certain initial conditions, to simplify the process of choice of lamination parameters and to ensure high quality production at the maximum productivity and the minimum power input.

Ackonwledgement

This research was funded by the grant of bilateral Lithuanian-Ukrainian international project of research and experimental development programme M/219-2005, N004SMM567/3 „Development of new technologies and printing materials for printed production, its qualitative evaluation, standardization and identification" from the Ministries of Education and Science, Lithuania and Ukraine.

5 REFERENCES

[1] Havenko, S. et al. *Finishing of a printed matter: technology, materials, equipment.* Kiev-Lviv, 2003. (In Ukrainian).

[2] Zamotaev, P.V. *Oriented polypropylene films*. Kiev, 1998. (In Russian).
[3] Fujiyama, M. et al. Study on rough-surface biaxially oriented polypropylene film. VI. Roughening by laminated cast sheet. *Journal of Applied Polymer Science*, vol. 36, 2003, p. 1049-1059.
[4] Wyser, Y., Pelletier, C., Lange, J. Predicting and determining the bending stiffness of thin films and laminates. *Packag. Technol. Sci*. vol. 14, 2001, p. 97-108.
[5] Cernic, M., Dolenc, J., Scheicher, L. Permanence and durability of digital prints on paper. *Applied physics a-materials science & processing.* vol 83, 2006, no. 4, p. 589-595.
[6] Martynyuk, M. *Research qualimetric parameters of lamination of book bindings*. Kvalilogija knigi, 2000, p. 144-149. (In Ukrainian).
[7] Volchek, V.L. Estimation of adhesive and deformation-durability properties of sheet production with pressing a film. *Prospects of development of printed and stitching-binding processes*, 1990, p. 124-129. (In Russian).
[8] Martynyuk, M. *Improvement of designs of book covers and optimization of their technology of manufacture*. Lviv, 2002. (In Ukrainian).
[9] Kalbina, E.L. et al. Application of an estimation method of the quality of polymeric film-paper pressing to the hardening factor. *Proceedings of Omsk Institute of Printing*. 1985, p. 45-47. (In Russian).
[10] Draper, N.R., Smit, H. Applied Regression Analysis. *Finance and statistics*, Moscow, 1986. (In Russian).
[11] Lobov, G.S. Methods of processing of polytypic experimental data. Moscow: *Science*, 1981. (In Russian).
[12] Popov, B.O. The decision of problems in the system of computer algebra Maple V. Kiev: ViP, 2001. (In Ukrainian).

Strojniški vestnik - Journal of Mechanical Engineering 54(2008)3, 232-244
UDC 662.756.3
Paper received: 4.10.2006
Paper accepted: 19.12.2007

Fuel Properties of Biodiesel Produced from Different Raw Materials in Croatia

Neven Voća*,[1] - Tajana Krička[1] - Vanja Janušić[1] - Željko Jukić[1] - Ana Matin[1] - Darko Kiš[2]
[1]University of Zagreb, Faculty of Agriculture, Croatia
[2]University of J.J. Strossmayer Osijek, Faculty of Agriculture, Croatia

During the past decade or even earlier almost all the EU countries, as well as most transition countries, launched the production of biodiesel fuel. Such a trend will continue in the future as it is indicated in the EU Directive (2003/30/EC) on alternative fuels for road transport and measures for promotion of the use of biodiesel. In Croatia, the production of biodiesel started only in 2005. It is based on raw materials which are available in the domestic environment: rapeseed oil and sunflower oil and waste edible oil. Methyl ester produced from rapeseed oil fully meets the EU standard under EN 14214, i.e., quality requirements for biodiesel fuel and may be used as pure (B100) or blended with mineral diesel fuels. Since methyl ester of sunflower oil and waste edible oil in some parameters do not meet the mentioned requirements, it is recommended to use them either as blended with rapeseed methyl ester or blended with mineral diesel fuel, which conforms to the recommendation of the European Union Strategy for biofuels production COM (2006).

Keywords: fuel production, Croatia, biodiesel, fuel properties

0 INTRODUCTION

Croatia, a country with limited natural resources, is a transitional country in the South-Eastern Europe and a candidate for joining the European Union. Energy consumption in 2004 in Croatia amounted to 412.04 PJ, which is an increase by about 4.1% comparing to 2003. However, in 2005 this value slightly decreased, by 0.1% and was 411.66 PJ. Total energy production in 2005 in Croatia amounted to 197.23 PJ, out of which 20.3% or 40.11 PJ of energy was produced from domestic crude oil sources. However, in the last 10 years we saw a dramatic downfall in domestic crude oil production. For example, in 1990 as much as 104.54 PJ of energy was produced from crude oil, which is approximately 62% more than in 2005. In contrast to this, energy import is constantly increasing, by almost 7.5% annually. The rise in liquid fuel consumption, decline of domestic oil sources and rising price of crude oil on the world market lead, at the end of the last century, to developing programs of more intensified use of renewable energy sources, especially of biodiesel fuel [1].

The energy utilization from biomass resources has received much attention since the mid-1990s. The energy of biomass (also referred to as biomass energy) from plants, animals (fed with plants or other animals) or wastes they produce originally comes from solar energy through the photosynthesis process. The energy supply from domestic waste is especially noted in that it not only enhances fuel diversification, but also eliminates the environmental pollution. Of the many energy productions from food wastes or food processing wastes, waste edible oils seems to be especially attractive based on bioresource sustainability, environmental protection and economic consideration.

The national strategy of the Government of Croatia recommends the adoption of an integrated approach to development covering different sectors: agriculture, energy, environment, tourism, etc. In the frame of this integrated approach and as part of the BIOEN national energy program, the efforts to introduce biodiesel production in Croatia started in 2000. The objective of introducing biodiesel industry is to reduce Croatian energy dependency, comply with the relevant EC Biofuels Directive, help improve the quality of the environment and diversify production and employment in the agriculture and industry sectors. The cultivation of energy/non food crops to produce

*Corr. Author's Address: University of Zagreb, Faculty of Agiculture, Svetošimunska 25, HR-10 000 Zagreb, Croatia, nvoca@agr.hr

biofuels should be an area of particular interest of the Croatian agricultural policy with the view of creating new economic resources and preserving employment in the rural communities. The production and use of biodiesel to replace fossil fuels in transport also contribute to meeting the signed commitment and targets resulting from the Kyoto Protocol to reduce greenhouse gas emission. Iz should also contribute to enhance the tourism industry by an emphasizing an environment friendly approach [2].

From the utilization perspective, biodiesel and its blends represent an excellent substitute for mineral diesel. Thus, biodiesel features should be benchmarked with mineral diesel features in all their aspects. While consumption features of biodiesel give, generally speaking, rather homogeneous results, its production features vary depending on the source of production. Namely, biodiesel can or could be obtained from various sources such as different vegetable oils, animal fats, recycled edible oil and, even, soapstocks. Consequently, biodiesel production process greatly depends on geographical and climate conditions as well as magnitude and organization of sectors related to use of edible oils, such as catering and households [3]. Here, the focus will be placed on biodiesel originated from the main raw material for biodiesel production in Croatia - rapeseed, sunflower and waste edible oil. They are produced in the first two biodiesel plants in Croatia which started operation in 2006.

Table 1. *Total energy supply during 1995 to 2005 in Croatia*

	PJ						
	1995	**2000**	**2001**	**2002**	**2003**	**2004**	**2005**
Overall energy consumption							
Coal and Coke	7.42	17.15	19.36	22.89	26.18	29.70	32.95
Fuel wood	13.52	15.64	12.24	12.39	15.96	15.88	14.77
Liquid Fuels	146.03	160.52	164.25	175.16	192.85	179.62	181.88
Natural Gas	82.77	94.98	98.87	101.10	100.45	104.66	101.06
Hydro Power	51.75	56.93	65.51	52.01	46.48	69.00	62.40
Electricity	12.59	14.40	11.36	12.68	14.01	13.19	18.41
Renewables	0.0	0.0	0.0	0.0	0.0	0.02	0.20
TOTAL	**314.08**	**359.62**	**371.58**	**376.23**	**395.93**	**412.04**	**411.66**
Primary energy production							
Coal	1.96	0.0	0.0	0.0	0.0	0.0	0.0
Fuel wood	13.52	15.64	12.24	12.39	15.96	15.86	14.77
Crude Oil	62.81	51.35	47.52	47.00	44.61	42.44	40.11
Natural Gas	69.12	59.40	70.86	74.53	76.83	77.08	79.76
Hydro Power	51.75	56.93	65.51	52.01	46.48	69.00	62.40
Renewables	0.0	0.0	0.0	0.0	0.0	0.02	0.2
TOTAL	**199.17**	**183.32**	**196.12**	**185.94**	**183.87**	**204.40**	**197.23**
Energy import							
Coal and Coke	6.76	20.89	18.49	25.13	27.54	33.73	31.51
Crude Oil	176.22	165.57	165.72	180.86	182.41	189.49	182.57
Petroleum products	10.88	9.31	20.11	34.07	31.08	40.01	43.34
Natural Gas	9.31	37.67	36.83	36.87	38.72	35.82	38.56
Electricity	15.77	15.79	13.48	14.14	16.12	19.07	31.49
TOTAL	**218.95**	**249.23**	**254.63**	**291.07**	**295.88**	**318.12**	327.47
Energy export							
Coal and Coke	0.04	0.26	0.10	1.28	1.95	1.28	1.08
Crude Oil	10.48	1.48	0.0	0.0	0.0	0.0	0.0
Petroleum products	90.94	73.01	71.14	68.49	73.06	86.71	79.00
Natural Gas	0.0	0.0	8.0	12.31	11.63	11.82	15.18
Electricity	3.19	1.39	2.12	1.46	2.11	5.88	13.08
TOTAL	**104.65**	**76.15**	**81.71**	**83.54**	**88.75**	**105.69**	**108.34**

Because of the growing crude oil prices, limited resources in fossil fuels and environmental concerns regarding air quality, the objectives of this paper will give a comprehensive review of biodiesel production from main raw materials in Croatia – rape seed oil, sunflower oil and waste edible oil. The main subjects dealt with in this paper are given in the following key elements:

- Current status of total energy supply, and diesel fuel supply and consumption;
- Status of oilseeds and edible oils supply;
- Generation and recycling of waste edible oils;
- Biodiesel production from main vegetable oils in Croatia – rapeseed, sunflower and waste edible oils.

1 CURRENT STATUS OF TOTAL ENERGY SUPPLY, AND DIESEL FUEL SUPPLY AND CONSUMPTION

1.1 Current Status of Total Energy Supply

Croatia is a country rich in renewable energy resources such as biomass, solar energy and wind energy. However, it has limited fossil energy resources such as crude oil and natural gas, which makes Croatia a high energy-importing country

Energy consumption per inhabitant is somewhat below the European average and amounts to 2,215 kgoe per inhabitant. As comparison, Island has the highest energy consumption per inhabitant or 15.638 kgoe, while at the bottom of the list there is Moldavia with only 700 kgoe per inhabitant. The future development of industry and transport sector in Croatia, the energy consumption is expected to rise, so it is necessary to ensure new, either domestic or imported energy sources. In Croatia, industry and transportation sector together use 52.6% of energy, while general sector makes for the remaining 47.4% of energy consume.

In 2005, the total primary energy supply decreases by 3.5% with respect to the previous year. The great fall was recorded in hydro power harnessing because the 2005 was less favorable in hydrological terms than the previous year.

As evident in Table 1, reliance on the imported crude oil of total energy import gradually decreased from 80.48% in 1995, 66.4% in 2000, 61.6% in 2003, and 59.6% in 2004, to 55.8% in 2005. Due to the national energy policy aimed to diversification of the imported energy sources, the second largest imported energy source in 2005 were petroleum products with a 13.2% share in total imported fuels. Other energy supply sources also include natural gas (11.8%), coal (9.6%) and electricity (9.6%) [1].

It is important to note that Croatia also exports a significant amount of energy (Table 1). The highest annual increase of energy export was recorded between 2003 and 2004, by 19.1%. The tendency of growing energy export was maintained and in 2005 it grew by another 2.5%. The most exported products were oil derivatives (73%), natural gas (14%) and electricity (12%).

By 2020, considerable portions of the energy demand will be met by natural gas/liquefied natural gas, hydro power and renewable energy (especially in wind energy and solar energy). This gradual increase in clean and green energy supply is the Croatia's response to the challenges to be by faced the economic, energy and environmental policies of sustainable development in the near future.

In the future, a gradual reduction in the production of fossil fuels and a rise in energy generation from renewable sources are expected. Renewables should play an increasingly important role in the energy supply. In the period until 2030 the share of fossil fuels will be gradually decreasing so that natural gas and crude oil together will have a share of approximately 25%. The remaining three quarters of primary energy production will consist of energy from renewable energy sources, where hydro power will make for 32%, fuel wood and biomass 19.6%, while other renewables will make for 23.6% (biodiesel included) [1].

1.2 Current Status of Diesel Fuel Supply and Consumption

It is well known that Croatia has its own sources of crude oil. In 2005 Croatia used 4,991,000 tons of crude oil, while its own production was 946,000 tons, which makes up 19% of total crude oil consumption. The remaining 81% of the total demand is met by imported crude oil. It is important to note that crude oil production is constantly falling, which is illustrated by the fact that in 1990 it amounted to nearly 2,496,800 tons.

The data by the Ministry of Economy, Labor and Entrepreneurship on diesel fuel supply and

Table 2. *Diesel fuel production and consumption during 1995 to 2005 in Croatia*

Diesel production and consumption	10^3 t						
	1995	**2000**	**2001**	**2002**	**2003**	**2004**	**2005**
Production	1,017.1	1,063.9	1,052.1	1,054.6	1,325.0	1,191.9	1,080.9
Final energy demand	**609.7**	**863.7**	**925.3**	**995.6**	**1,145.7**	**1,221.8**	**1,311.5**
Thermal power plants	4.8	0.0	0.0	0.0	0.0	0.0	0.0
Road transport	360.3	533.2	576.0	658.4	779.9	857.8	927.3
Other transport	80.6	77.8	78.9	81.1	82.9	85.1	85.1
Agriculture	120.1	186.6	202.4	189.5	189.0	183.1	183.0
Construction	43.6	65.4	67.7	76.4	93.9	95.8	110.6

consumption in Croatia are given in Table 2, as well as some important features relevant to diesel fuel supply and demand. The consumption of diesel fuel in Croatia in the last few years has been increasing significantly. Thus as far back as 1995 total consumption of diesel fuel was 609,700 tons, to rise up to 1,331,800 tons in 2005, out of which approximately 78% is consumed in the transportation sector and 14% in agricultural sector [1].

Recently it has been demonstrated that the diesel engines perform much better that gasoline engines in terms of oil saving and greenhouse gases (e.g. carbon dioxide) emission reduction. From the point of view of the global warming concerns and permanent high oil price levels, the diesel fuel consumption is expected to increase in the near future [4].

In the last decade or even earlier almost all the EU countries as well as most transition countries have started the production of biofuel: biodiesel and ethanol. Such a trend will continue in the future as it is shown in the EU Directive (2003/30/EC) concerning alternative fuels in road transport and measures for biofuel promotion. This document proposes the following measures, which, when accepted, will become an obligation for the EU candidate countries, which includes Croatia as well: by 2010 an amount of 5.75% of conventional fuels used for transport should be replaced by alternative ones; EU Member States have the right to apply differentiated tax rate on biofuels in order to encourage their use; by 2007 the share of biofuels in the European Union should amount to at least 3.5% [5].

It should be emphasized that these Directives are mandatory, which means that the projected fuel switch must be accomplished. These directives have been accepted by all EU Member States, but they must also be accepted by the future European Union members. This means that these obligations must be taken on by the Republic of Croatia as one of the future EU Member States.

2 STATUS OF OILSEEDS AND EDIBLE OILS SUPPLY FOR BIODIESEL PRODUCTION IN CROATIA

2.1 Status of Oilseeds Supply

The most significant plants for vegetable oil production in Croatia are sunflower, soy, and rapeseed [6]. Which raw material will be chosen for biodiesel production depends only on specific conditions of a country concerned (climate, populations' consumption patterns, standard agricultural plant production, etc). However, the most important raw materials for production of biodiesel fuel are rapeseed and sunflower. Unlike these, soy has higher protein content (ca 40%), and lower oil content (ca 20%), which makes it a very convenient source of animal feed. In addition, oilseed crop represent necessary cultures in the crops rotation plan and enable the optimum production of other crops [7].

The production of oilseed crops in Croatia is exercised at approximately 90,000 hectares and is focused on 3 plants: soybean, sunflower and rapeseed, with soybean dominating in acreage and yield. Table 3 shows the production and yield of the main oilseed crops as potential sources of biodiesel fuel in Croatia – rapeseed and sunflower [8].

Table 3. *Production and yield of rapeseed and sunflower in Croatia in the period 1995 to 2003*

Year	Production (t)		Area (ha)		Yield (t/ha)	
	Rapeseed	Sunflower	Rapeseed	Sunflower	Rapeseed	Sunflower
1995	24,472	10,982	19,385	37,066	2.23	1.91
2000	29,436	53,956	12,886	25,715	2.28	2.10
2001	22,456	42,985	10,319	25,336	2.18	1.70
2002	25,585	62,965	13,041	26,835	1.96	2.35
2003	28,596	69,253	15,530	28,165	1.84	2.45

It is clear that oilseed crops production in the Republic of Croatia is relatively low and that it varies significantly. It is interesting to note that the share of oilseed plant production in total arable crop production decreased. The factor that causes most concern is exceptionally low yield, ranging from 1.70 t/ha to 2.45 t/ha for rapeseed and 1.84 t/ha to 2.28 t/ha for sunflower (actual yield depending on the year of production). This emphasizes the importance of plant production technology in oilseed crop production. Low yields in rapeseed production are not surprising if we take into consideration that this crop is most often grown on poor and ill-cultivated soils where water supply and air properties are inadequate and sizeable depressions create water pools which lead to plant spacing reduction. Other reasons that rapeseed is grown on small areas and that crop yields and production give average result lie in obsolete and inadequate machinery, insufficient application of updated know-how, poor crop protection measures and modest skills and knowledge of family farm owners. Low interest of producers and low share of rapeseed in the crops mix on our fields are the result of the economic policy in the agricultural sector, in particular price policy, and from low interest shown by the processing industry.

Further expansion of the areas under the rapeseed, as a primary raw material for biodiesel fuel is possible only if such areas are significantly increased in the current narrow crop rotation plan and by re-cultivation of deserted and undeveloped land. This would provide new areas in a properly planned crop rotation. This is a realistic option for increasing rapeseed production and rising average yields up to 3.0 to 3.5 tons per hectare, which is feasible both in agro ecological and technological terms. In this way the production of rapeseed in the newly sown areas would increase by over 30% and ensure the raw material for biodiesel production.

2.2 Starting Materials for Biodiesel Production in Croatia

2.2.1 Rapeseed Oil

Rapeseed oil (*Brassica napus L. ssp oleifera*) was originally chosen for transesterification experiments by biodiesel pioneers because of its low price compared to other readily available vegetable oils. However, it soon became apparent that thanks to its high content of monounsaturated oleic acid and the low levels of both saturated and polyunsaturated acids, this oil is practically an ideal raw material by its combustion characteristics, oxidative stability and cold temperature behavior. Due to its favorable properties, rapeseed oil is still the feedstock of choice in most European countries, including the world's largest biofuel producers, Germany and France [9].

Rape seed contains 40 to 48% oil and 18 to 25% proteins. The rapeseed oil belongs to the group of semi-drying oils with iodine number 95 to 120, and is used for human nutrition (as refined oil) and for technical purposes (biodiesel fuel, detersive and soap production, etc). Intensive and efficient breeding activity created new rapeseed cultivars ("00"), improved quality of oil and crushed oilseed. In triglycerides of these cultivars, dominant is oleic acid (over 60%) instead of erucic acid. The linolenic acid content is reduced (below 10%), and the linoleic acid content is raised to 18 to 20%. This change in fatty acid content improved the consume value of rapeseed oil and it can match the best quality oils. Today, canola oil ("00" Canadian cultivars' oils) contains erucic acid only in traces, 5 to 8% saturated oils, 60 to 65% monosaturated oils and 30 to 35% polysaturated fats. Table 4 shows the normal content of fatty acids of rapeseed, with and without erucic acid. [7].

2.2.2 Sunflower Seed Oil

Sunflower (*Heliantus annuus. l. p.*) is an arable crop grown for its seed. In addition to oil and protein, the sunflower seed contains several important minerals and other substances. Hybrids grown at present contain mostly between 45 to 53% oil. The oil contains mainly fatty acids (80 to 90%) as well as linoleic (up to 60%) and oleic acid.

Helianthus species comprises many varieties, two of which are important for the production: common sunflower and Jerusalem Artichoke. Hybrids have been used in the Republic of Croatia since 1975. Vegetation period lasts from 2.5 to 5 months [10].

Sunflower seed oil (*Helianthus annuus*) comes second in the list of vegetable oil sources for biodiesel production in Europe. Undoubtedly recognized as a valuable oil source for human nutrition, its high content of linoleic acid puts limit to the use of sunflower seed oil for fuel production. According to the European biodiesel standard (EN 14214) pure sunflower oil methyl esters cannot be used as a fuel for diesel engines, as it exceeds the limit for iodine value set at ≤ 120 g I_2/100g. Moreover unadditivated sunflower oil fuels will also give poor ratings for oxidative stability. To solve this problem, cultivars enriched in oleic acid have been developed [9].

Table 4 shows the fatty acids content in sunflower. Unlike rapeseed oil with dominant oleic acid, sunflower mostly contains linoleic acid (71.5%), followed by oleic acid (15.9%).

2.3 Generation and Recycling of Waste Edible Oil

Waste edible oil is a very popular raw material for biodiesel fuel production, due to the fact that its treatment is both cost efficient and ecologically beneficial. Because of the fact that the refined waste edible oil has been sold at half price of crude rapeseed oil since as early as 1999, the use of this type of material in biodiesel fuel production contributed to it economic value, which lead to multiple growth in this type of production [9]. Today in Austria the waste edible oil is equal to rape seed oil as a raw material for production of biodiesel fuel. Biodiesel fuel produced from such oil was out at the market in 1992 and since 1994 it has been used as official fuel in the public transport in Graz. At the end 2005 city of Graz had over one hundred buses which use this type of fuel, making total mileage of over 6 million kilometers. So far no difficulties have been noted in using biodiesel fuel produced from waste edible oil.

Table 4 shows the fatty acid content in waste edible oil. It is evident that waste edible oils, in addition to higher oleic acid content (43 to 52%), have higher palmitic acid content as well (13 to 25%). Given the mentioned values, it can be assumed that in waste edible oils prevails palmitic

Table 4. *Normal fatty acids content in rapeseed oil (with high and low erucic acid content), in sunflower oil and waste edible oil*

Fatty acid	**Fatty acid content (% in oil)**			
	Rapeseed		**Sunflower**	**Waste edible oil**
	Withoout erucic acid	With erucic acid		
Palmitinic acid (C 16:0)	3.5	2.2	5.9	13 to 25
Stearinic acid (C 18:0)	1.5	1.5	5.2	5 to 12
Oleic acid (C 18:1)	60.2	11.2	15.9	43 to 52
Linolic acid (C 18:2)	21.3	13.6	71.5	7 to 22
Linolenic acid (C 18:3)	10.9	7.7	traces	0.5 to 3
Eicosenoic acid (C 20:1)	1.3	6.1	-	1.0
Erucic (C 22:1)	0.5	55.1	-	0.5
Nervonic acid (C 24:1)	traces	2.5	-	-

oil which is mostly used in catering industry for multiple uses in deep fryers [11].

The use of vegetable oils for frying results in substantial amounts of waste oils, which then cause the disposal problems. Therefore, the principle reason for using waste oils as raw material for biodiesel fuel production, in addition to lower price, is lies in fact that it solves the problem of its disposal. Acid catalyst processes in biodiesel fuel production from waste edible oil are competitive in economic terms to alkaline catalyst processes applied on crude vegetable oils. Waste edible oils in principle contain some decomposition products of vegetable oils and other substances. A potential problem in biodiesel fuel production from waste oil may arise from its poor physical and chemical performance in the low-temperature conditions due to higher level of saturated fatty acids. At present this is solved by applying additives and adjusting it for use during winter months [11].

Physical traits of methyl ester obtained from waste dibble oil slightly differ from those of methyl esters obtained from crude vegetable oils. The differences are noted at low temperatures, where methyl esters have weaker properties than methyl esters of crude vegetable oils. Due to this, in winter conditions biodiesel fuel from waste edible oil must be blended with mineral diesel fuel.

Biodiesel fuel production from waste edible oil is identical to that which uses animal fats raw material. However, the waste edible oil analysis determined very slight differences between used and unused oils, which can be solved by heating up and filtration of solid particles which are redundant for the foregoing transesterifications.

Although the fuels from edible oils cannot fully replace mineral diesel fuel, they play an important role as alternative fuel which may contribute to the main objective – energy self-reliance and security [9].

2.4 Biodiesel Production from Main Vegetables Oil in Croatia as a Raw Material – Rape Seed, Sunflower and Waste Edible Oils

Biodiesel and its blends represent an excellent substitute for mineral diesel which offers a variety of benefits, increased employment, development of rural areas, increased security of energy supply and a better overall trade balance. However, biodiesel is still not cost competitive with mineral diesel without subsidies or tax incentives except in cases where oil prices are extremely high and vegetable oil prices low [11].

Feedstock cost is the main factor affecting the competitiveness and profitability of biodiesel production, aside from its final cost on the market, and as such it is highly important to clearly identify and quantify current and potential feedstock (in terms of both availability and price), as well as to summarize factors that may impact the identified feedstock use for biodiesel fuel. To increase national rapeseed production, some measures from the Croatian government are necessary in the agricultural sector in order to encourage the rapeseed production. These measures would have to ensure, at least, the quantities of feedstock required for the planned production of biodiesel, increase the yield of rapeseed per hectare and regulate market channels for produced rapeseed and include financial incentives and continuous training and expert support for farmers as the most important components [2].

Many researchers have concluded that due to their low volatility and high cetane number vegetable oils and their derivatives carry more potential as alternative fuels for diesel engines rather than spark-ignited engines. However, the use of crude vegetable oils for diesel engines can cause numerous engine-related problems. The increased viscosity and low volatility of vegetable oils lead to severe engine deposits, injector coking, and piston ring sticking [12]. However, these effects can be reduced or eliminated through transesterification of the vegetable oil to form an alkyl ester [13]. The transesterification process removes glycerin from the triglycerides and replaces it with the alcohol used for the conversion process [14]. This process decreases the viscosity but maintains the cetane number and the heating value.

The energy obtained from waste edible oils is a form of renewable energy and, in principle, utilizing this energy does not add carbon dioxide, one of the major greenhouse gases, to the atmospheric environment, in contrast to fossil fuels [15]. Due to the extremely low contents of sulphur and nitrogen in the food waste, its direct utilization as fuel in the combustion utilities (e.g. internal combustion engine) generally generates less environmental pollution and health risks as compared to traditional fossil fuels.

By way of transesterification, the reaction of triglycerides with alcohol (e.g. methanol) under the caustic catalyst (e.g. potassium hydroxide) is processed to produce glycerol and monoalkyl esters, which are known as biodiesel and can be potentially used as alternative diesel fuels in compression-ignition (diesel) engines [16]. Biodiesel, as one of green fuels and/or clean energies, is compatible with traditional petroleum-based diesel and they both can be completely blended without any stratification. From the viewpoint of their chemical composition and properties, biodiesel fuels are biodegradable, low toxic, and release less air pollutants than hydrocarbon-based diesel. However, the use of biodiesel will be faced with the problem of high costs, when compared to petroleum-based oils, and some problems related to the decreased power output and torque force and to the increase in NOx emissions with increasing biodiesel content in the blends [17].

The catalytic conversion of waste edible oil by the transesterification process into biodiesel fuel has the advantage of both economic and environmental benefits. In this regard, the biodiesel fuel proved to be successfully produced from waste edible oils by an alkali-catalyzed transesterification process, and can be considered as alternative fuels for diesel engines and other utilities [18].

Table 5 shows the properties of biodiesel fuel produced in the lab-scale plant installed at the Faculty of Agriculture of the University of Zagreb, using three major raw materials available from domestic sources: rapeseed oil, sunflower oil, and waste edible oil. The analyses were carried out in the independent national laboratories for diesel fuel research in Croatia and Slovakia, and at the Faculty of Agriculture of the University of Zagreb. The methods applied in the analyses are also given in Table 5.

Biodiesel fuels generally display higher densities than mineral diesel, which is also reflected by the respective limits within the FAME standard (860 to 900 kg/m^3 at 15°C) and the EU fossil diesel norm EN 590 (820 to 845 kg/m^3 at 15°C). This difference has impacts on heating value and fuel consumption. Table 5 shows that investigated methyl esters remain within the limits laid down

Table 5. *Properties of biodiesel fuel produced from the lab-scale biodiesel plant*

Property		Unit	Rape seed ME	Sunflower ME	Waste edible oil ME	EN 14214	Tested method
Density at 15°C		kg/m^3	876.90	874.80	876.50	860 to 900	EN ISO 3675
Refraction index at 20°C		-	1.45722	1.45630	1.45581	≥1.490	ASTM D 1298
Sulphur content		mg/kg	≤10	≤10	≤10	≤10	EN ISO 20846
Kinematic viscosity at 40°C		mm^2/s	5.83	5.05	5.99	3.5 to 5.0	EN ISO 3104
Cloud point		°C	-1	0	-1	-	EN 23015
Pour point		°C	-7	-2	-5	-	ASTM D 97
CFFP		°C	-10	-2	-2	<0 (summer) <-15 (winter)	EN 116
Flash point		°C	157	149	126	≥120	EN ISO 3679
Calorific value		MJ/kg	38.3	38.2	37.5	≥35	DIN 51900-3
Cetane number		-	52	48	52	≥51.0	EN ISO 5165
Destillation	beginning	°C	181.6	181.7	179.5	-	-
	10%	°C	209.3	209.4	208.9	-	-
	20%	°C	224.1	224.1	224.0	-	-
	50%	°C	263.8	263.7	264.1	-	-
	90%	°C	334.1	333.9	337.9	-	-
	end	°C	375.3	375.1	378.5	≤385	-
Free fatty acid content		%	0.173	0.188	0.152	<3	AOAC (1999)
Acid value		mg KOH/g	0.346	0.376	0.304	≤0.5	pr EN 14104
Saponification number		mg KOH/g	184.70	183.40	189.90	185 to 190	AOAC (1999)
Iodine value		g I_2/100 g	111.00	128.40	98.30	<120	pr EN 14111

in EN 14214 and that the differences between them are not relevant.

The refractive index (or refraction index) of a medium is the inverse ratio of the phase velocity of a wave phenomenon such as light or sound and the phase velocity in a reference medium. Refraction index of biodiesel should be minimum ≥ 1.490 and from the Table 5 it is obvious that the investigated samples did not meet the requirements.

Fuels with high sulphur content have been associated with negative impacts on human health and on the environment, which is the reason for the current tightening of national limits. Sulphur is limited to a maximum content of 10 mg/kg in the European biodiesel standard. The analyzed methyl esters meet this requirement and they can be added to mineral diesel fuel as "sulphur free" additive.

Fuel viscosity is regulated by the standards at 40°C (Table 5). Viscosity temperature dependence is a very important characteristic of each fuel, because transportation means operate in a wide range of climatic conditions. The viscosity of vegetable oils is significantly higher than that of mineral diesel fuel and it is the main reason why they are not directly applied in diesel engines as fuel and the aim of transesterification is to lower the viscosity of vegetable oils. Kinematic viscosity of biodiesel at 40°C is 3.5 to 5.0 mm^2/s and it is twice as high as diesel fuel viscosity 2.4 to 2.6 mm^2/s. Viscosity, which is a measure of flow resistance of a liquid due to internal friction of one part of a fluid moving over another, affects the atomization of fuel upon injection into the combustion chamber and thereby, ultimately, the formation of engine deposits. The higher the viscosity, the greater the tendency of the fuel to cause such problems [14] Determination of kinematics viscosity values of selected vegetable oils and their respective methyl esters shows that there all fall within the same viscosity range. However, these values are somewhat above those laid down in EN 14214.

De Filippis et al [19] showed that the viscosity of a fuel sample might serve as an indication of its methyl ester content. Their study was based on the fact that the viscosities of other possible biodiesel components, such as free fatty acids, mono-, di-, triglycerides and glycerol, are higher than those of the methyl esters due to higher molecular weights or stronger intermolecular forces. Thus, after calibration with samples for which the methyl ester contents have been determined via capillary gas chromatography, a single determination of viscosity allows the estimation of the methyl ester content within 3% error.

The behavior of fuels under low environment temperature is an important quality measure. Partial solidification in cold weather may cause blockages of fuel lines and filters, leading to fuel starvation and problems during the engine start-up. In order to assess biodiesel fuel performance in cold-temperature various parameters have been suggested, including cloud point (CP), pour point (PP) and cold-filter plugging point (CFPP). Cloud point, denoting the temperature at which first visible crystals are formed within a fuel sample when it cooled, whereas pour point, standing for the lowest temperature to which the sample may be cooled while still retaining its fluidity. Neither of these parameters is considered as a reliable tool for predicting actual engine operability limits and they are not included in biodiesel norm [20] and [21].

Flash point is a measure of the flammability of fuels and thus an important parameter of assessing hazards during fuel transport and storage. As reflected by the limit within the respective standards (≥ 120°C for FAME as opposed to >55°C for mineral diesel), flash points of diesel samples are only about half the values of those for biodiesel. The highest flash point was determined in methyl ester obtained from rapeseed oil (157°C), whereas the lowest one was found in methyl ester obtained from waste edible oil (126°C).

Calorific value is the quantity of heat energy, discharged by fuel at the time of combustion under the set conditions of the experiment. Lower calorific value is applied to internal combustion engines which evaluate the heat losses for water vaporization which occurs because of the oxidation of hydrogen of the fuel. This heat can be discharged only at the time of condensation of vapors in exhaust gases following the limits of a diesel engine. Calorific value is directly related to elemental composition of fuel [22]. This parameter is not included in diesel fuel standard, but it is a limited parameter within the standard for methyl esters used as heating fuels (EN 14214), requiring a minimum of 35 MJ/kg for heating value [9]. It is evident that all investigated methyl esters meet the

mentioned requirement so, in addition to their normal use as a fuel they can also be used for thermal energy generation.

Cetane number is a characteristics of fuel which shows the ability of self ignition in the cylinder of a diesel engine. It is determined through experiments in a standard single-cylinder engine. Cetane number depends on fuel composition and influences the start of a diesel, the beginning of the combustion process, equal operation of a diesel and the emission of exhaust gases. Cetane number of biodiesel is higher than that of diesel fuel [22]. Generally, the cetane number is a dimensionless descriptor of the ignition quality for diesel fuel. Both EN 14214 and EN 590 standards require a minimum cetane number of 51. As shown in Table 5, all investigated methyl esters display higher cetane number than fossil diesel, which is considered to be a significant advantage in terms of engine performance and emission [23]. However, a significantly lower cetane number value was determined in methyl ester of sunflower oil, which is below required standard under the norm EN 14214.

Limits for the respective proportions of condensates recovered by atmospheric distillation of fuel samples at specified temperatures are included in the European fossil diesel standard. It is evident from Table 5 that in investigated samples the determined value is within the range set out by te norm EN 14214. These values give hints at the presence of extremely high-boiling compounds, which are associated with the formation of engine deposits, or low-boiling substances, which negatively affect flash point. Whereas distillation characteristics are considered as important quality parameters in fossil diesel fuels, they are only minor relevance in biodiesel. Most biodiesel fuels mainly consist of methyl esters of C_{16} and C_{18} fatty acids, which have almost identical boiling points, whereas fossil diesel are complex mixtures of aliphatic and aromatic hydrocarbons whose boiling points widely diverge [9].

The free fatty acid is a key parameter for determining the viability of the vegetable oil transesterification process [24]. In order to carry out the base catalyzed reaction to completion, a free fatty acid (FFA) value lower than 3% is needed, which was at the same time established in all investigated samples. The higher the acidity of the oil, the smaller is the conversion efficiency. The excessive, as well as insufficient amount of catalyst may cause soap formation.

Acid value or neutralization number is a measure of mineral acid and free fatty acids contained in fuel sample. This parameter also mirrors the degree of fuel aging during storage, as it gradually increases due to hydrolytic cleavage of ester bonds. The obtained methyl esters fully meet the requirements of the norm EN 14214 of ≤ 0.5 mg KOH/g.

Saponification value is the number of milligrams of potassium hydroxide or sodium hydroxide required to saponify 1g of fat under the conditions specified. It is a measure of the average molecular weight (or chain length) of all the fatty acids present. Saponification itself is the hydrolysis of an ester under basic conditions to form an alcohol and the salt of a carboxylic acid. Saponification value should be within the range of 185 to 190 mg KOH/g, which was found only in the methyl ester of waste edible oil.

Iodine value is a measure of total instauration within a mixture of fatty materials, regardless of the relative shares of mono-, di-, tri- and polyunsaturated compounds. The high iodine value shows the unsaturation of fuel which leads to the formation of sediments and can cause the problem of stability of fuel [22]. Under the European biodiesel norm it is limited to ≤ 120 g I_2/100 g. Moreover, EN 14214 also sets out the maximum content of linolenic acid methyl ester and polyunsaturated fatty acid methyl ester to 12% and 1% (m/m), respectively. Engine manufactures have long argued that, when heated, fuels with high iodine value tend to polymerize and form deposits on injector nozzles, piston rings and piston rings grooves [9]. The limit of 120 g I_2/100 g required by the European biodiesel norm excludes several potential oil sources – such as sunflower seed oil, unless the resulting ester are blended with suitable biodiesel types or fossil diesel fuel.

In addition to the standardized procedure for the determination of fatty acid methyl ester contents in biodiesel fuel, several other methods have also been suggested, mainly serving as simple and fast means of process control. Samples directly drawn from the transesterification reaction mixture can be subjected to thin-layer chromatography, which allows a rough assessment of the degree of conversion and therefore facilitates the optimization of reaction parameters.

Table 6. *Composition of fatty acids in methyl esters obtained from rapeseed oil, sunflower oil and waste edible oil*

Measured value	Unit	Rape seed ME	Sunflower ME	Waste edible oil ME	Required value
C 18:1 trans	%	0.70	0.00	3.80	-
C 18:2 trans	%	0.10	0.00	1.20	-
C 18:3 trans	%	1.10	1.20	0.90	-
Total trans isomers	%	1.90	0.00	5.90	-
C 12:0 Lauric acid	%	0.00	0.00	0.20	-
C 14:0 Myristic acid	%	0.10	0.00	0.30	-
C 16:0 Palmitic acid	%	5.00	4.20	11.40	3.3 to 6.0
C 16:1 Palmitoleic acid	%	0.00	0.00	0.40	0.1 to 0.6
C 17:0 Heptadecanoic acid	%	0.00	0.00	0.10	-
C 17:1 Heptadecenoic acid	%	0.00	0.00	0.10	-
C 18:0 Stearic acid	%	1.60	1.50	4.40	1.1 to 2.5
C 18:1 Oleic acid	%	63.40	65.60	52.40	52.0 to 66.9
C 18:2 Linoleic acid	%	19.70	18.70	26.20	16.1 to 24.8
C 18:3 Linolenic acid	%	8.30	8.40	2.70	6.4 to 14.1
C 20:0 Arachidic acid	%	0.40	0.40	0.40	0.2 to 0.8
C 20:1 Eicosenoic acid	%	1.10	1.00	0.70	0.1 to 3.4
C 20:2 Eicosedienoic acid	%	0.00	0.00	0.00	0.0 to 0.1
C 22:0 Behenic acid	%	0.20	0.20	0.40	0.0 to 0.5
C 22:1 Erucic acid	%	0.00	0.00	0.10	0.0 to 2.0
C 22:2 Docosadienoic acid	%	0.10	0.00	0.10	-
C 24:0 Lignoceric acid	%	0.00	0.00	0.00	0.0 to 0.2
C 24:1 Nervonic acid	%	0.00	0.00	0.00	0.0 to 0.04

It is evident from Table 6 that the composition of methyl esters of rapeseed and sunflower oil is within the limits found in references sources [11]. It shows that in investigated methyl esters oleic fatty acid is dominant, followed by linoleic acid. In methyl ester obtained from waste edible oil the concentration of palmitolec, stearic and linoleic acids are above set out levels, while the concentration of linolenic acid is below the required levels. It can be established that the composition of fatty acids of waste edible oil demonstrated poorer qualities than methyl ester obtained from rapeseed and sunflower oil.

3 CONCLUSION

In the past decade, the relation between energy consumption and environmental pollution as well as diversification of energy supply have been in the focus of environmental protection and economic activities aimed at achieving sustainable development and creating renewable energy in the Republic of Croatia. Because of the limited oil reserves and growing environmental concerns, alternative fuels from agricultural resources will become increasingly important in the near future.

Moreover, it can be concluded that the Republic of Croatia has the capacities for production of oil crops as the most important raw materials for the production of biodiesel fuel. Since the Republic of Croatia today has approximately 300,000 hectares of uncultivated land, the production of oil crops for biodiesel fuel is more than necessary. From the viewpoint of resource recycling and use of energy, biodiesel fuel from waste edible oil for diesel engines can be considered as one of green energies.

In case that methyl ester is used for blending with mineral diesel fuel it can be used regardless of whether it is produced from rapeseed, sunflower or waste edible oil. Blending up to 5 % of methyl ester obtained in this way (in conformity to the European quality standard for mineral diesel fuel EN 590) positive effects are achieved in terms of quality of exhaust gases and mineral diesel fuel combustion in the engine.

However, if biodiesel fuel is used in its pure form (B100), it is allowed to use methyl ester

produced from rapeseed oil, which is, unlike methyl ester from sunflower oil and waste edible oil, fully conform to the European standard for biodiesel fuel quality EN 14214. Methyl ester of sunflower and waste edible oil can be used in its neat form (B100) with added methyl ester from rapeseed oil which improves its combustion properties in conformity to the mentioned standard. The same recommendation is given by the EU Strategy for biofuels production COM (2006) [25]. It recommends blending the rapeseed oil methyl ester with methyl esters of lower quality.

Acknowledgements

This research was supported by the Ministry of Science, Education and Sports of Republic of Croatia through project 178-1780703-0698.

4 REFERENCES

[1] *Energy in Croatia 2005*, Annual Energy Report. Zagreb: Ministry of Economy, Labour and Entrepreneurship of Republic of Croatia, 2006.

[2] *BIOEN, Programme of using energy from biomass and waste.* Zagreb: Energetic Institute "Hrvoje Požar", 1998. (In Croatian)

[3] Koo-Oshima, S., Hahr, N., Van Gerspen, J. *Compressive health and environmental effects of biodiesel as an alternative fuel*. Biodiesel Industries, 1999.

[4] Canakci, M., Van Gerpen, J. A pilot plant to produce biodiesel from high free fatty acid feedstocks. *Transactions of the American Society of Agricultural Engineers* 46 (4), 2003, p. 945-954.

[5] *EC 2003/30/EC, Directive on the promotion of the use of biofuels or other renewable fuels for transport*, Official Journal of the European Union, 2003.

[6] Mustapić, Z., Pospišil, M., Kunšten, B. Possibile utilization of rapeseed meal of novel "00" cultivars in livestock feed. *Poljoprivredne aktualnosti (Agricultural Actualities)*, vol. 30, 1994. (In Croatian)

[7] Mustapić, Z., Pospišil, M. Oil and rapeseed meal quality of "00" cultivars. *Sjemenarstvo (Seed Science)*, vol. 14, 1995. (In Croatian)

[8] *Statistical yearbook*. Zagreb: Central Bureau of Statistics, 2004.

[9] Mitelbach, M., Remschmidt, C. *Biodiesel: the comprehensive handbook*, Boersedruck Ges.m.b.H., Vienna, Austria, 2005.

[10] Gagro, M. *Industrial crops and forage*. Zagreb: HAD, 1998. (In Croatian)

[11] Erhan, S.Z. *Industrial uses of vegetable oils*. AOCS Publishing, 2005.

[12] Perkins, L.A., Peterson, C.L. Durability testing of transesteri Wed winter rape oil (Brassica napus L.) as fuel in small bore, multi-cylinder, DI, CI engines. *SAE Paper 911764*, 1991.

[13] Zhang, Q., Feldman, M., Peterson, C. Diesel engine durability when fueled with methyl ester of winter rapeseed oil. A*SAE Paper 88-1562*, 1988.

[14] Knothe, G. *Viscosity of Biodiesel*, In: The Biodiesel Handbook, Illinois, USA, 2005, p. 81-82.

[15] Bishop, P.L. *Pollution prevention: fundamentals and practice*. Boston, MA: McGraw-Hill, 2002.

[16] Srivastava, A., Prasad, R. Triglycerides-based diesel fuels. *Renew Sustain Energy Rev*., 2000, 4:111-133.

[17] Carraretto, C., Macor, A., Mirandola A., Stoppato, A., Tonon, S. Biodiesel as alternative fuel: experimental analysis and energetic evaluations. *Energy*, 2004, 29:2195-211.

[18] Murayama T. Evaluating vegetable oils as a diesel fuel. *INFORM*, 1994, 5:1138-45.

[19] De Filippis, P., Giavarini, C., Scarsella, Sorrentino, M. Transesterification process for vegetable oils: A simple control method of methyl ester content. *Journal of the American Oil Chemists Society*, 72 (11), 1995, p. 351-354.

[20] Knothe, G., Dunn, R.O. Recent results from biodiesel research at the National Center for Agricultural Utilization Research. *Landbauforschung Volkenrode*, Sonderheft 190, 1998, p. 69-78.

[21] Dunn R.O. *Cold weather properties and performance of biodiesel*, In: The Biodiesel Handbook, Illinois, USA, 2005, p. 83-122.

[22] Lebedevas, S., Vaicekauskas, A. Research into the application of biodiesel in the transport sector of Lithuania. *Transport* 11(2), 2006, p. 80-87.

[23] Knothe, G., Matheaus, A.C., Ryan, T.W.

Cetane numbers of branched and straight-chain fetty esters determined in an ignition quality tester, Fuel 82, 2003, p. 971-975.
[24] Meher, L.C., Vidya Sagar, D., Naik, S.N. Technical aspects of biodiesel production by transesterification: a review. *Renew. Sustain. Energy Rev.* 10(3), 2006, p. 248-268.
[25] *A EU strategy for biofuels*. Commission of the European Communities, COM (2006) 34 final, SEC (2006), Brussels.

Instructions for Authors

From 2008 the Journal of Mechanical Engineering is to be published in English only, but with separate Slovene abstracts. The authors are entirely responsible for the correctness of the language. If a reviewer indicates that the language in the paper is poor, the editor will require the author to correct the text with the help of a native English speaker before the paper is reviewed again.

Papers can be submitted electronically to the journal's e-mail address (info@sv-jme.eu) or by post.

Papers submitted for publication should comprise the following:

- Title, Abstract, Keywords,
- Main body of text,
- Tables and Figures (graphs, drawings or photographs) with captions,
- List of References,
- Information about the authors, the corresponding author and a full set of addresses.

For papers from abroad (in the case that none of the authors is a Slovene) the editor will obtain a Slovenian translation of the Abstract.

Papers should be short, about 8 to 12 pages of A4 format, or at most, 7000 words. Longer papers will be accepted if there is a special reason, which should be stated by the author in the accompanying letter. Short papers should be limited to less than 3000 words.

THE FORMAT OF THE PAPER

The paper should be written in the following format:

- A Title, which adequately describes the content of the paper.
- An Abstract, which should not exceed 250 words. The Abstract should state the principal objectives and the scope of the investigation, the methodology employed, summarize the results and state the principal conclusions.
- An Introduction, which should provide a review of recent literature and sufficient background information to allow the results of the paper to be understood and evaluated.
- A Theory and the experimental methods used.
- An Experimental section, which should provide details of the experimental set-up and the methods used for obtaining the results.
- A Results section, which should clearly and concisely present the data using figures and tables where appropriate.
- A Discussion section, which should describe the relationships and generalisations shown by the results and discuss the significance of the results, making comparisons with previously published work.
- Because of the nature of some studies it may be appropriate to combine the Results and Discussion sections into a single section to improve the clarity and make it easier for the reader.
- Conclusions, which should present one or more conclusions that have been drawn from the results and subsequent discussion and do not duplicate the Abstract.
- References, which must be numbered consecutively in the text using square brackets [1] and collected together in a reference list at the end of the paper.

THE LAYOUT OF THE TEXT

Texts should be written in Microsoft Word format. The paper must be submitted in an electronic version, by e-mail or by post on a CD.

Do not use a LaTeX text editor, since this is not compatible with the publishing procedure of the Journal of Mechanical Engineering.

Equations should be on a separate line in the main body of the text and marked on the right-hand side of the page with numbers in round brackets.

Units and abbreviations

Only standard SI symbols and abbreviations should be used in the text, tables and figures. Symbols for physical quantities in the text should be written in italics (e.g., *v, T, n,* etc.). Symbols for units that consist of letters should be in plain text (e.g. m/s, K, min, mm, etc.).

All abbreviations should be spelt out in full on first appearance, e.g., variable time geometry (VTG).

The meaning of symbols and units belonging to symbols should be explained in each

case or quoted in special table at the end of the paper before the References.

Figures

Figures must be cited in consecutive numerical order in the text and referred to in both the text and the caption as Fig. 1, Fig. 2, etc. Pictures should be saved in a resolution good enough for printing, and in any common format, e.g., BMP, GIF or JPG. However, graphs and line drawings should be prepared as vector images, e.g., CDR, AI.

All Figures should be prepared in black and white, without borders and on a white background. All the figures should be sent separately in their original formats.

When labeling axes, physical quantities, e.g., *t, v, m,* etc., should be used whenever possible. Multi-curve graphs should have the individual curves marked with a symbol. The meaning of the symbol should be explained in the figure caption.

In the case that the author wishes, for whatever reason, to publish Figures in colour, the author must pay the resulting costs.

Tables

Tables must be cited in consecutive numerical order in the text and referred to in both the text and the caption as Table 1, Table 2, etc. In addition to the physical quantity, e.g., *t* (in italics), units (normal text), should be added in square brackets. Each column should have the title line. Tables should not duplicate information that is already noted anywhere in the paper.

Acknowledgement

An acknowledgement for cooperation or help can be included before the References. The author should state the name of the research (co)financer.

The list of references

All references should be collected at the end of the paper in the following styles for journals, proceedings and books, respectively:

[1] Wagner, A., Bajsić, I., Fajdiga, M. Measurement of the surface-temperature field in a fog lamp using resistance-based temperature detectors. *Strojniški vestnik – Journal of Mechanical Engineering*, February 2004, vol. 50, no. 2, p. 72-79.

[2] Boguslawski L. Influence of pressure fluctuations distribution on local heat transfer on flat surface impinged by turbulent free jet. *Proceedings of International Thermal Science Seminar II*, Bled, June 13.-16., 2004.

[3] Muhs, D., et al. *Roloff/Matek mechanical parts*, 16th ed. Wiesbaden: Vieweg Verlag, 2003. 791 p. (In German). ISBN 3-528-07028-5

ACCEPTANCE OF PAPERS AND COPYRIGHT

The Editorial Board reserves the right to decide whether a paper is acceptable for publication, obtain professional reviews for submitted papers, and if necessary, require changes to the content, length or language.

The corresponding author must, in the name of all authors, also enclose a written statement that the paper is original unpublished work, and not under consideration for publication elsewhere.

On publication, copyright of the paper shall pass to the Journal of Mechanical Engineering. The JME must be stated as a source in all later publications.

Submitted materials will not be returned to the author. Unpublished materials are not preserved and will not be sent anywhere without the author's consent.

The paper, prepared for publication, will be sent to the author in PDF format. The author should check for any necessary corrections, which should be the minimum required. With this the author confirms that the paper is ready for publication.

PUBLICATION FEE

For all papers the authors will be asked to pay a publication fee prior to the paper appearing in the journal. However, this fee only needs to be paid after the paper is accepted for publication by the Editorial Board. The fee is €180.00 (for all papers with a maximum of 6 pages), €220.00 (for all papers with a maximum of 10 pages) and €20.00 for each additional page. The publication fee includes 25 off-prints of each paper, which will be sent to the corresponding author.

Vsebina

Strojniški vestnik - Journal of Mechanical Engineering
letnik 54, (2008), številka 3
Ljubljana, marec 2008
ISSN 0039-2480

Izhaja mesečno

Uvodnik

Moja prednost je spisati to stran, ki uvaja 3. številko Strojniškega vestnika v letu 2008. Pri tem ne bom povzemal vsebino in druge značilnosti posameznih prispevkov, pač pa se bom dotaknil občutljivega področja Bolonjske reforme študija strojništva. Ta v Mariboru poteka že od jeseni 2007, v Ljubljani pa nekoliko zaostaja in bo pričela delovati v jeseni 2008. Preteklo leto sem predlagal prodekanoma obeh fakultet, da podata opise podrobnosti svojih novih programov, vendar teh doslej v uredništvo nismo prejeli. Zaradi tega naj na tem mestu opišem svoje lastne izkušnje s študenti prvega letnika po Bolonjskem programu v Mariboru, posebej pri predmetu Mehanika v jesenskem semestru (od konca novembra 2007 do januarja 2008).

Mariborski študenti so imeli 8 tednov stičnih predavanj in vaj, opravili pa so tudi seminarske domače naloge. Te so vsebovale tri primere, prvega o določevanju težišč in vztrajnostnih momentov prerezov z uporabo poligonskih obrazcev, drugega o sosrednjih valjih s steno večje debeline, tretjega pa o določitvi sil in pomikov v paličju. Domače naloge so predstavljale 20 možnih točk v končnih ocenah.

Dodatno so pisali dva pisna testa, ki sta omogočala 40 ocenjevalnih točk. Nato je sledil še ustni izpit, ki je pravtako dal do 40 ocenjevalnih točk. Celotna ocena preko 90 točk pomeni odlično oceno (10), medtem ko skupna ocena preko 60 točk predstavlja zadostno oceno (6). Dejansko je doslej le 1 (eden) študent dosegel 20+40+25 = 85 točk (tj. 9) in odličen ni bil nihče.

Spodnja preglednica daje pregled izidov (samo za prvi in drugi del, saj tretji del večina študentov še ni opravljala). Od 27 sodelujočih študentov, so izidi trenutno naslednji:

Pisni del
- 76 do 100% = 2 študenta,
- 51 do 75% = 11 študentov,
- 26 do 50% = 10 študentov,
- ter do 25% = 4 študenti.

Domače delo
- 51 do 100% = 24 študentov
- in do 50% = 3 študenti.

Zaključna ocena (februar do maj 2008)
- 9 = 1 študent,
- 8 = 1 študent,
- 7 = 4 študenti,
- 6 = 6 študentov.

Naslednji pisni in ustni izpitni roki bodo junija in septembra 2008.

Iz gornjih podatkov lahko izluščimo nekaj izkušenj, ki bi pomagale pri naslednji generaciji 1. letnika 2008/2009. Predvsem 8 ur predavanj tedensko v 8 tednih, bi bilo smotrno spremeniti v 4 ure predavanj skozi celoten zimski semester (od oktobra do januarja), kot je to bilo v prejšnjih študijskih letih. Poleg tega bi domače delo spremenili v vodeno skupinsko delo v prostorih fakultete, ob enakih pogojih za vse udeležence.

Prof. dr. Andro Alujevič, urednik

Strojniški vestnik - Journal of Mechanical Engineering 54(2008)3, SI 29
UDK 533.662.3
Prejeto: 25.5.2007
Sprejeto: 28.9.2007

Vpliv deformacije lopatice na integralno karakteristiko aksialnega ventilatorja

Matjaž Eberlinc*,[1] - Matevž Dular[1] - Brane Širok[1] - Bojan Lapanja[2]
[1]Univerza v Ljubljani, Fakulteta za strojništvo
[2]Hidria Inštitut Klima, Godovič

Lopatice turbinskega stroja se zaradi sil, ki delujejo nanje, deformirajo. Postavlja se vprašanje vpliva deformacij lopatic na integralne in lokalne aerodinamske značilke ventilatorjev. V prispevku je predstavljena študija vpliva deformacij lopatic na primeru aksialnega ventilatorja. Delo je usmerjeno v merjenje deformacij lopatic pri znanih celovitih obratovalnih pogojih. Rezultati - deformacije temenskega dela ventilatorske lopatice so uporabljeni v numerični študiji vpliva spremenjene oblike lopatice na aerodinamske značilke ventilatorja. Integralne značilke ventilatorja so bile izmerjene v skladu s standardom ISO-DIS 5801:1997 na vetrovniku Inštituta KGH Godovič, merjenje deformacij lopatice pa je bilo opravljeno na merilni postaji na Fakulteti za strojništvo Univerze v Ljubljani s pomočjo računalniško podprte vizualizacije. Deformacije so bile merjene v treh obratovalnih režimih, ki so bili določeni s celovitimi parametri ventilatorja.

Rezultati meritev so bili uporabljeni pri določitvi spremenjene oblike lopatice, ki je bila v nadaljevanju uporabljena pri numeričnem modeliranju za iste celovite obratovalne parametre ventilatorja. Izvedena je bila študija vpliva deformacij, ki je temeljila na numerični simulaciji.

Ključne besede: aksialni ventilatorji, lopatice, deformacije, vizualizacija

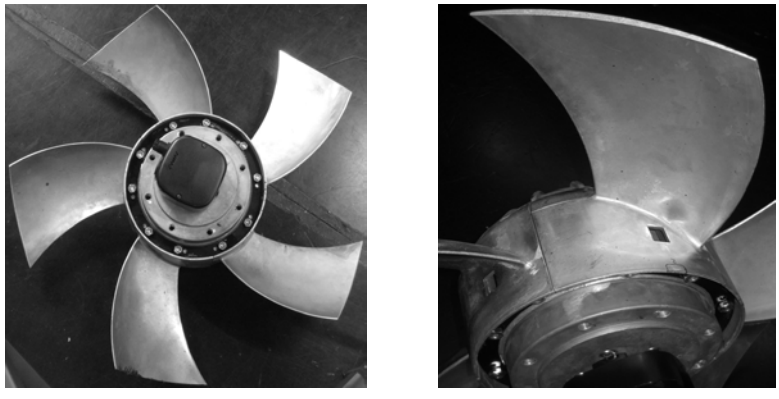

Sl. 1. *Aksialni ventilator ∅630 mm s petimi profiliranimi lopaticami [1]*

*Naslov odgovornega avtorja: Univerza v Ljubljani, Fakulteta za strojništvo, Aškerčeva 6, 1000 Ljubljana, matjaz.eberlinc@fs.uni-lj.si

Strojniški vestnik - Journal of Mechanical Engineering 54(2008)3, SI 30
UDK 533.661
Prejeto: 23.3.2007
Sprejeto: 19.12.2007

Izboljšan postopek reševanja aerodinamičnih obremenitev lopatice rotorja helikopterja pri letenju naprej

Aleksandar Bengin[1] - Časlav Mitrović[1] - Dragan Cvetković*[,2] - Dragoljub Bekrić[1] - Slavko Pešić[1]
[1]Univerza v Beogradu, Fakulteta za strojništvo, Srbija
[2]Univerza "Singidunum" Beograd, Fakulteta za poslovno informatiko, Srbija

V prispevku je predstavljen numerični model, razvit za izračun aerodinamičnih obremenitev lopatice rotorja. Model je nestacionarnega in popolnoma trirazsežen. Predpostavili smo, da je lopatica rotorja toga, njeno gibanje med vrtenjem pa smo modelirali za primer modela rotorja helikopterja "Gazela" Aerospatiale SA 341 (lopatica je pritrjena v središče z loputo in tečaji). Tokovno polje okrog lopatice smo opazovali v sosledju večih azimutnih leg. Tokovno polje okrog rotorja helikopterja smo modelirali kot popolnoma trirazsežnega, neustaljenega in potencialnega. Aerodinamiko lopatic smo modelirali z uporabo dvižnega površinskega modela. Vrtinec rotorja se sestoji iz premih elementov s stalno vrtilnostjo, ki izhaja iz roba pri stalnih kotih azimuta. Ti vrtinci predstavljajo tako vlečne kot tudi sled zagonske komponente in se lahko prosto prenašajo vzdolž krajevnih vektorjev hitrosti. Vrtinec smo modelirali kot neodvisnega, njegovo obliko pa lahko v določenih trenutkih izračunamo iz enostavnih kinematičnih zakonov, uporabljenih na kolokacijskih točkah vrtinca. Zmaličenje vrtinca smo izračunali le v polju blizu rotorja, tj. pri končnem številu vrtljajev rotorja. Elemente vrtinca smo modelirali z jedrom vrtinca. Predpostavili smo, da je jedro vrtinca neodvisno od časa ter da je odvisno od spremembe kroženja v točki, v kateri se element vrtinca odlepi od lopatice.

Ključne besede: neustaljena aerodinamika, helikopterji, lopatice rotorjev, potencialni tok, dvižne površine

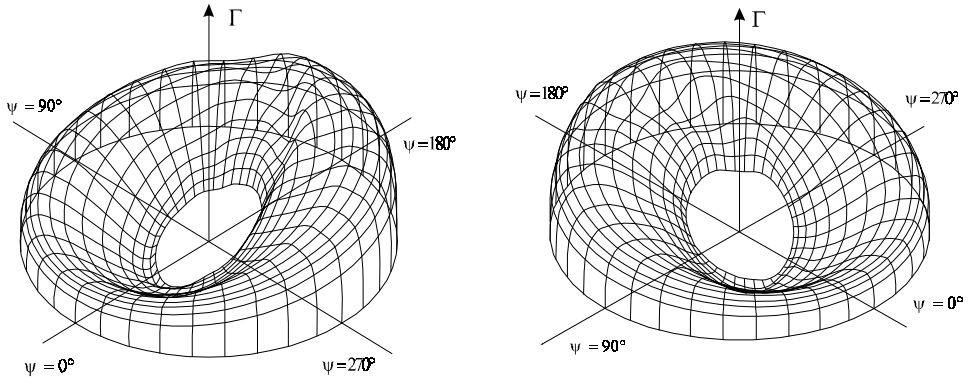

Sl. 9. *Porazdelitev kroženja na rotorju; m =0,35 (različna pogleda)*

*Naslov odgovornega avtorja: Univerza "Singidunum", Fakulteta za poslovno informatiko, Danijelova 32, 11000 Beograd, Srbija, dcvetkovic@singidunum.ac.yu

Strojniški vestnik - Journal of Mechanical Engineering 54(2008)3, SI 31
UDK 681.5
Prejeto: 10.5.2007
Sprejeto: 19.12.2007

Uporaba nevronskih mrež pri vrednotenju tehnološkega časa

Goran Šimunović* - Tomislav Šarić - Roberto Lujić
Univerza v Osijeku, Fakulteta za strojništvo v Slavonskem Brodu, Hrvaška

Običajni pristop k načrtovanju postopkov, ki večinoma temelji na izkušnjah tehnologov, zahteva veliko zbranega znanja, je neprilagodljiv in časovno zamuden. Uporaba metod umetne inteligence lahko pomaga in močno izboljša tak pristop. V prispevku opisujemo rezultate, ki smo jih dobili z raziskavo uporabe nevronskih mrež pri vrednotenju proizvodnih parametrov in posredno tudi tehnološkega časa poliranja cevne zveze. Analizirali smo različne sestave povratnih nevronski mrež ter izbrali optimalno z najmanjšo napako koren srednjih kvadratov (RMS - Root Mean Square). Dobljeni model smo vključili v sistem ERP (Enterprise Resource Planning system) proivodnega podjetja. Z bolj natančnim vrednotenjem tehnološkega časa, dobljenega z modelom sistema ERP smo zaključili predhodno določena proizvodna opravila in oblikovali osnovo za načrtovanje proizvodnje ter časov nadzora dobave. Delo tehnologov je tako eostavnejše, prav tako pa je krajši tehnološki čas priprave proizvodnje.

Ključne besede: načrtovanje postopkov, umetna inteligenca, nevronske mreže

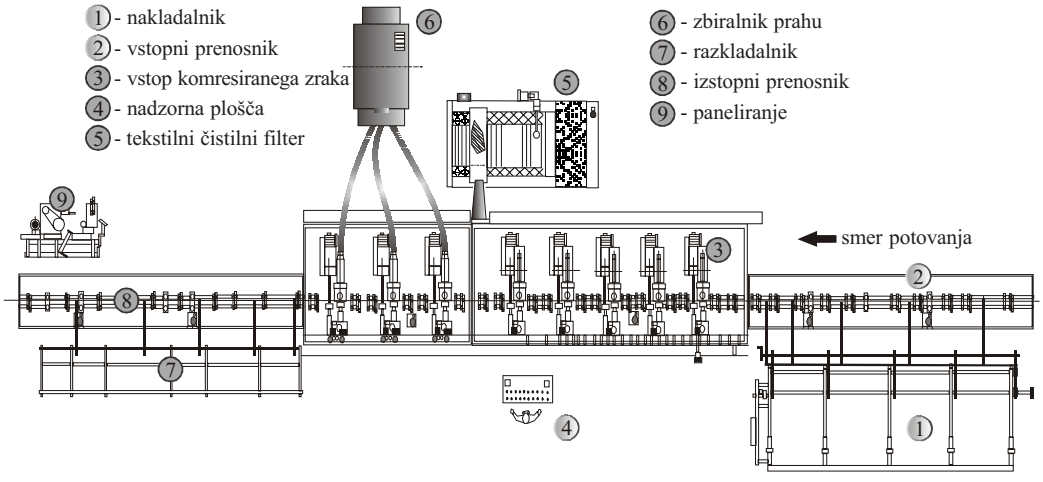

Sl. 1. *Shema polirne in brusilne linije*

*Naslov odgovornega avtorja: Univerza v Osijeku, Fakulteta za strojništvo v Slavonskem Brodu, Trg I. Brlić-Mažuranić 2, HR-35000 Slavonski Brod, Hrvaška, goran.simunovic@sfsb.hr

Strojniški vestnik - Journal of Mechanical Engineering 54(2008)3, SI 32
UDK 621.8
Prejeto: 5.2.2008
Sprejeto: 12.3.2008

Pregled učinkovitosti in mehanizmov trdih prevlek iz diamantu podobnega ogljika (DLC) v stikih z jeklom pri mejnem mazanju

Igor Velkavrh - Mitjan Kalin* - Jožef Vižintin
Univerza v Ljubljani, Fakulteta za strojništvo

Pomembnost trdih prevlek v različnih strojnih uporabah skokovito narašča že več kot 20 let. Razvoj novih materialov kot npr. sodobne keramike, diamantu podobnega ogljika ter nano-kompozitnih prevlek je vzpodbudil intenzivne znanstvene raziskave na področju tribologije in inženiringa površin, ter hkrati usmeril pozornosti v področje mikro/nano tehnologij. Prevleke iz diamantu podobnega ogljika - DLC - so trenutno ena izmed najbolj perspektivnih vrst trdih prevlek. Njihove glavne prednosti so majhno trenje, dobre proti-obrabne lastnosti, adhezijska zaščita, in druge. Vendar pa je zaradi nizke površinske energije DLC prevlek njihova reaktivnost s konvencionalnimi olji in aditivi slabša. Za kakovosten preskok, ki bi izboljšal delovanje in omogočil učinkovito optimizacijo ter izboljšano "konstrukcijo" mejno mazanih DLC stikov za različne mehanske sisteme, je potrebno razumeti zakaj, kako, pod katerimi pogoji in s katerimi vrstami DLC prevlek ter mazivi je njihovo mejno mazanje sploh mogoče. V desetletju raziskav tega področja je bilo objavljenih že precej rezultatov, vendar so le-ti zaradi različnih tipov prevlek, maziv in aditivov v posameznih študijah pogosto neprimerljivi in včasih tudi nasprotujoči. Veliko povečanje zanimanja za uporabo DLC prevlek v mazanih sistemih v različnih vejah industrije pa zahteva poglobljeno razumevanje mehanizmov mazanja in celostnega delovanja teh prevlek. Ravno zato je, za skokovit napredek na tem področju, potreben pregled trenutnega stanja in sinteza precej razpršenih rezultatov dosedanjih raziskav mazanih DLC-stikov. V predstavljenem prispevku je podana analiza triboloških lastnosti stikov DLC/jeklo in predpostavljenih mehanizmov mazanja iz do sedaj objavljenih študij. Povzeli smo temeljne ugotovitve in trenutno razumevanje mejnega mazanja kontaktov DLC/jeklo, s čimer dopolnjujemo našo podobno analizo opravljeno za stike DLC/DLC.

Ključne besede: DLC prevleke, mejno mazanje, olja, aditivi, nanotribologija

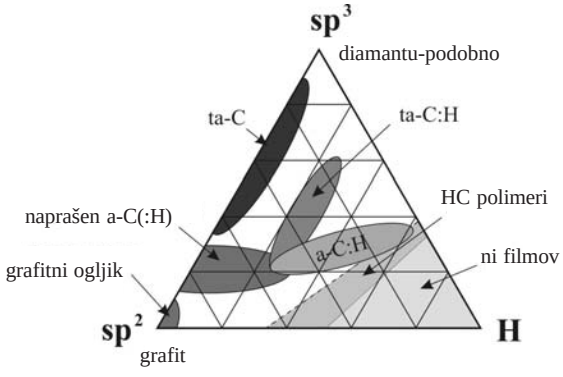

Sl. 1. *Fazni diagram količin sp2- in sp3-vezanega ogljika ter vodika v različnih oblikah diamantu-podobnega ogljika (DLC)*

*Naslov odgovornega avtorja: Univerza v Ljubljani, Fakulteta za strojništvo, Aškerčeva 6, 1000 Ljubljana, mitjan.kalin@ctd.uni-lj.si

Strojniški vestnik - Journal of Mechanical Engineering 54(2008)3, SI 33
UDK 658.5
Prejeto: 22.8.2007
Sprejeto: 19.12.2007

Kakovost in stroški v postopku vodenja proizvodnje

Magdalena Rosu*[,1] - Cristian Doicin[1] - Mirko Soković[2] - Janez Kopač[2]
[1]Politehnična univerza v Bukarešti, Romunija
[2]Univerza v Ljubljani, Fakulteta za strojništvo

Prispevek podaja pregled pristopov, ki se običajno uporabljajo v proizvodnji, še posebej pri planiranju in krmiljenju. Namen je dopolniti "veliko sliko" metod in tehnik, ki jih pogosto srečujemo v celotnem postopku proizvodnje, vključno z fazami planiranja in krmiljenja.

Zato so na kratko opisani nekateri pomembni koncepti in tehnike kot Šest sigma, Sočasno osvajanje izdelka (CE), Razvoj funkcij kakovosti (QFD), Planiranje virov podjetij (ERP) in Vzvratni inženiring (RE), skupaj z tehnikami in metodami za skrajševanje pretočnega časa.

Opis je podprt z diagrami, ki kažejo potek dejavnosti vključenih v posamezno metodo.

Ključne besede: proizvodni procesi, vodenje proizvodnje, vodenje kakovosti, stroški, zmanjševanje vodilnih časov

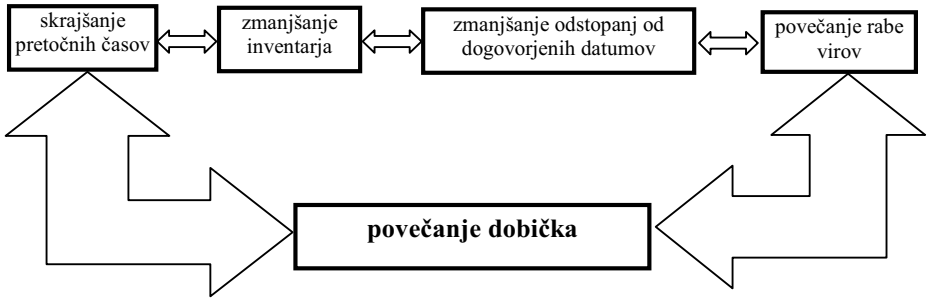

Sl. 2. *Cilji ekonomične proizvodnje*

*Naslov odgovornega avtorja: Politehnična univerza v Bukarešti, Splaiul Independentei 313, 060032 Bukarešta, Romunija, magdalenarosu@yahoo.com

Strojniški vestnik - Journal of Mechanical Engineering 54(2008)3, SI 34
UDK 620.17:62-462.2
Prejeto: 18.4.2007
Sprejeto: 27.6.2007

Analiza primerjalne napetosti za zmanjševanje napetosti cevi za naftne vrtine iz 33Mn2V jekla

Fuzhong Wang*[,1] - Lu Lu[1,2] - Huichun Zhang[1] - Lina Zhao[2] - Guoquan Liu[3] - Jiahe Ai[3]
[1]Politehnična univerza Tianjin, Oddelek za fiziko, Kitajska
[2]Univerza Bo Hai, Center za znanstvene in tehnične preizkuse, Kitajska
[3]Univerza za znanost in tehnologijo v Pekingu, Šola za naravoslovje, Kitajska

Za simulacijo zmanjševanje napetosti cevi za naftne vrtine iz novega jekla 33Mn2V smo uporabili metodo končnih elementov. Simulirani rezultati predstavljajo dinamični razvoj primerjalne napetosti, še posebno znotraj obdelovanca. Razvidno je, da je spremenljiva porazdelitev primerjalne napetosti po vzdolžnem in prečnem prerezu izrazita značilka zmanjševanja napetosti naftnih cevi, kar lahko uporabimo kot osnovni parameter za izboljšanje orodja in tehnike, napovedovanje in regulacijo mikro-strukturnega razvoja za proizvodnjo cevi za rtine

Ključne besede: cevi za naftne vrtine, jeklo 33Mn2V, metode končnih elementov, zmanjševanje napetosti, primerjalne napetosti

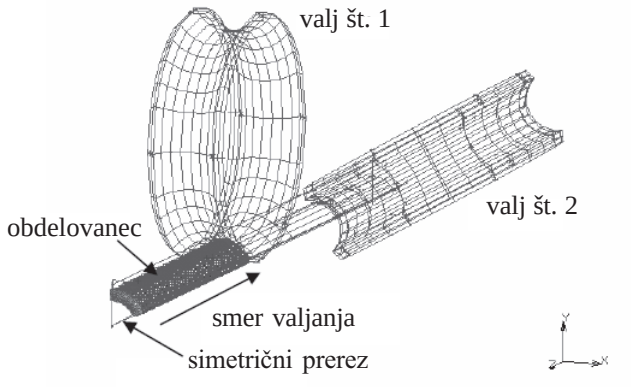

Sl. 3. *Trirazsežni elasto-plastični model končnih elementov za zmanjševanje napetosti naftnih cevi*

*Naslov odgovornega avtorja: Politehnična univerza Tianjin, Oddelek za fiziko, Tianjin 300160, Kitajska, wangfuzhong@163.com

Strojniški vestnik - Journal of Mechanical Engineering 54(2008)3, SI 35
UDK 676.056.73
Prejeto: 27.3.2007
Sprejeto: 27.6.2007

Vpliv tehnoloških faktorjev na fizikalne in mehanske lastnosti z nanašanjem tiska

Svetlana Havenko[1] - Aleksandr Bogorosh[2] - Marija Martynyuk[1] - Edmundas Kibirkštis*[,3] - Kęstutis Vaitasius[3]
[1]Ukrajinska akademija za tisk, Lvov, Ukrajina
[2]Državna tehnična univerza Ukrajine, Kijev, Ukrajina
[3]Tehnična univerza v Kaunasu, Kaunas, Litva

Izvedli smo raziskavo parametrov kakovosti nanašanja različnih vrstah tehnologij za različne papirje. Upoštevali smo vpliv temperature in hitrosti tiskarskega nanašanja s polipropilenskimi filmi na kakovost nanosa. Razvili smo matematični model, ki opisuje trdnost in vihanje nanosa v odvisnosti od faktorjev ureditve postopka. Izvedli smo tudi optimizacijo tehnološkega postopka.

Ključne besede: tehnološki postopki, optimiranje laminiranja, polipropilenski filmi

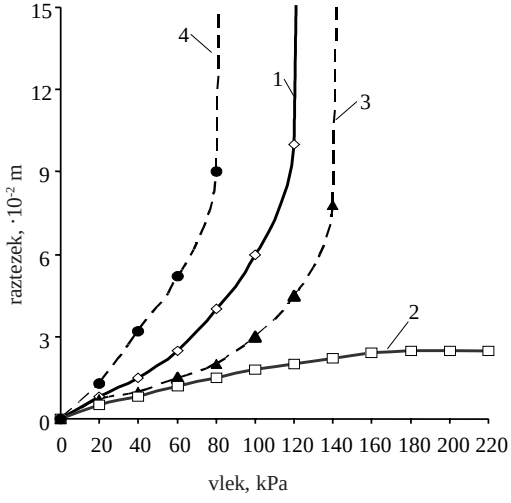

Sl. 1. *Odvisnost relativnega podaljšanja od obremenitve za polipropilenske filme debeline 27 μm: 1 - vzdolžna smer; 2 - prečna smer; 80 μm: 3 - vzdolžna smer; 4 - prečna smer*

*Naslov odgovornega avtorja: Tehnična univerza v Kaunasu, Fakulteta za načrtovanje in tehnologijo, Studentu str. 56-350, LT-51424 Kaunas, Litva, edmundas.kibirkstis@ktu.lt

Strojniški vestnik - Journal of Mechanical Engineering 54(2008)3, SI 36
UDK 662.756.3
Prejeto: 9.5.2007
Sprejeto: 19.12.2007

Gorivne lastnosti biodizla iz različnih surovin, pridelanih na Hrvaškem

Neven Voća*[,1] - Tajana Krička[1] - Vanja Janušić[1] - Željko Jukić[1] - Ana Matin[1] - Darko Kiš[2]
[1]Univerza v Zagrebu, Fakulteta za agronomijo, Hrvaška
[2]Univerza J.J. Strossmayer v Osijeku, Fakulteta za agronomijo, Hrvaška

V zadnjem desetletju in celo že prej so v vseh državah Evropske zveze, prav tako pa tudi v tranzicijskih državah, pričeli s proizvodnjo biodizelskega goriva. Kot je navedeno v Evropski smernici (2003/30/EC) o alternativnih gorivih za cestni transport in ukrepih za pospeševanje rabe biodizla, se bo ta trend nadaljeval. Na Hrvaškem smo s proizvodnjo biodizla pričeli šele leta 2005. Temelji na surovinah, ki so pridelane v domačem okolju: olje iz repičnega semena, sončnično olje in odpadno jedilno olje. Metilester, pridobljen iz repičnega olja popolnoma ustreza evropskemu standardu EN 14214, tj. zahtevam za kakovost biodizelskih goriv, in ga lahko uporabljamo čistega (B100) ali mešanega z mineralnimi dizelskimi gorivi. Ker metilseter iz sončničnega olja in odpadnega jedilnega olja v določenih parametrih ne ustrezata omenjenim zahtevam, je priporočljivo, da se uporabljata mešana z repičnim metilestrom ali z mineralnimi dizelskimi gorivi, ter se ga tako prilagodi priporočilom Strategije evropske zveze za proizvodnjo biogoriv COM (2006).

Ključne besede: proizvodnja goriv, Hrvaška, biodizli, lastnosti goriv

Proizvodnja dizelskega goriva in njegova poraba v letih od 1995 do 2005 na Hrvaškem

Proizvodnja in poraba dizelskega goriva	**10^3 t**						
	1995	**2000**	**2001**	**2002**	**2003**	**2004**	**2005**
proizvodnja	1.017,1	1.063,9	1.052,1	1.054,6	1.325,0	1.191,9	1.080,9
potreba po končni energiji	**609,7**	**863.7**	**925,3**	**995,6**	**1.145,7**	**1.221,8**	**1.311,5**
termoelektrarne	4,8	0,0	0,0	0,0	0,0	0,0	0,0
cestni transport	360,3	533,2	576,0	658,4	779,9	857,8	927,3
ostali transport	80,6	77,8	78,9	81,1	82,9	85,1	85,1
kmetijstvo	120,1	186,6	202,4	189,5	189,0	183,1	183,0
gradbeništvo	43,6	65,4	67,7	76,4	93,9	95,8	110,6

*Naslov odgovornega avtorja: Univerza v Zagrebu, Fakulteta za agronomijo, Svetošimunska 25, HR-10 000 Zagreb, Hrvaška, nvoca@agr.hr

Osebne vesti

Magisterija in diplome

MAGISTERIJA

Na Fakulteti za strojništvo Univerze v Mariboru sta z uspehom zagovarjala svoji magistrski deli:

dne *12. februarja 2008*: **Matjaž Kamnik**, z naslovom: "Uporaba vida v prilagodljivih obdelovalnih sistemih" (mentorja: prof. dr. Jože Balič in prof. dr. Miran Brezočnik);

dne *28. februarja 2008*: **Albin Leskovar**, z naslovom: "Analiza dinamike procesorsko vodene hidravlične stiskalnice v proizvodnji aluminija" (mentor: prof. dr. Edvard Kiker).

DIPLOMIRALI SO

Na Fakulteti za strojništvo Univerze v Ljubljani so pridobili naziv univerzitetni diplomirani inženir strojništva:

dne *1. februarja 2008*: Marko BENJE, Sebastjan BOGATAJ, Simon PAVLIN, Marko RUTAR;

dne *29. februarja 2008*: Rok APAT, Grega BERTONCELJ, Anže ČELIK, Miran JELEN, Jaka KLEMENC, Dalibor ŠEGA.

Na Fakulteti za strojništvo Univerze v Mariboru sta pridobila naziv univerzitetni diplomirani inženir strojništva:

dne *28. februarja 2008*: Aleksander PESJAK, Peter VAUH.

*

Na Fakulteti za strojništvo Univerze v Ljubljani so pridobili naziv diplomirani inženir strojništva:

dne *15. februarja 2008*: Damijan BIZJAK, Gregor LIPOVŠEK, Jure ŠTRUCL, Tim TONEJC.

Na Fakulteti za strojništvo Univerze v Mariboru sta pridobila naziv diplomirani inženir strojništva:

dne *28. februarja 2008*: Ciril KERN, Benjamin KRUŠIČ, Ivan PUŠAVER, Andrej ROJKO, Andrej VAUPOTIČ, Peter VILTUŽNIK.

Popravek

V Strojniškem vestniku 2/08 je v rubriki Osebne vesti prišlo do napake pri zapisu magisterija. Pravilen zapis se glasi:

Na Fakulteti za strojništvo Univerze v Mariboru je z uspehom zagovarjal svoje magistrsko delo:

dne *22. januarja 2008*: **Jasmin Kaljun**, z naslovom: "Ergonomski in estetski vidiki razvoja izdelkov" (mentor: prof. dr. Bojan Dolšak).